PROACTIVE TOPOLOGY OPTIMIZATION AND SERVICE RESTORATION FOR IMPROVED DISTRIBUTION SYSTEM OUTAGE MANAGEMENT

by

Tumininu Ayotunde Mbanisi

A dissertation submitted to the faculty of
The University of North Carolina at Charlotte
in partial fulfillment of the requirements
for the degree of Doctor of Philosophy in
Electrical Engineering

Charlotte

2023

Approved by:

_____
Dr. Valentina Cecchi

_____
Dr. Badrul Chowdhury

_____
Dr. Tao Hong

_____
Dr. Zachary Wartell

ABSTRACT

TUMININU AYOTUNDE MBANISI. Proactive topology optimization and service restoration for improved distribution system outage management. (Under the direction of DR. VALENTINA CECCHI)

It is estimated that close to 90% of outages in the electric power grid originate in the distribution system. Although the use of advanced metering infrastructure has increased situational awareness in the distribution system, current approaches to outage management are often reactive and do not fully leverage insights from outage prediction models for the service restoration process. Hence, this work aims to provide a holistic strategy for combining outage prediction and service restoration in the outage management process.

First, a detailed analysis of an outage dataset is conducted in order to gain insights into the frequency and duration of outages in a distribution system. Two machine learning techniques, random forest and gradient boosting, are used to rank outage features, including outage causes, climate descriptions, and failed equipment, to determine which outage features have the greatest impact on average outage duration in a distribution system.

Following that, this dissertation proposes a proactive topology optimization and service restoration framework that leverages forecasts from outage prediction models to mitigate the impacts of predicted outages in the distribution system. The proposed framework is formulated as a mixed integer linear programming (MILP) problem with the objectives of minimizing the load lost prior to the outage and maximizing the restorable load when the outage occurs at the predicted locations. The MILP model was simulated using the Python Optimization Modeling Objects (Pyomo) package, an open-source tool, and solved using the CPLEX solver. Using modified versions of the IEEE 13-node and 123-node test feeders, the framework considers three optimization cases: single outage, multiple outage, and weighted multiple outage. In addition, a

sensitivity analysis based on the weighted multiple outage case is presented in order to determine the optimal topology to operate in given a range of probabilities for the possible outage locations in the distribution system.

Furthermore, the MILP model used in this work is validated by comparing its power flow results with those obtained from OpenDSS, an open-source simulation tool for electric power distribution systems. The results show that the MILP model provides a reasonable approximation of the nonlinear power flow model.

Overall, this dissertation provides a method for improving situational awareness within the distribution system. Using the proposed approach, distribution system operators can determine what topology to operate in ahead of predicted outages, thereby reducing the loads left out of service.

DEDICATION

To the Almighty God, my Source of wisdom and help

ACKNOWLEDGEMENTS

As I reflect on my PhD journey at the University of North Carolina at Charlotte, I am humbled and immensely grateful for the support I received along the way. Indeed, I had a village of people, too many to name, who supported me throughout my graduate school career.

I would especially like to acknowledge the tremendous support and guidance I received from my research advisor, Dr. Valentina Cecchi. As her student, I learned to persevere through the rigors of research. On the days when I found my research discouraging, her patient confidence in my abilities provided the needed motivation. Thank you so much Dr. Cecchi.

Also, I appreciate the members of my dissertation committee, Dr. Badrul Chowdhury, Dr. Tao Hong and Dr. Zachary Wartell, who reviewed and provided valuable comments and recommendations on my dissertation. Furthermore, I would like to acknowledge the valuable contributions of my research collaborators, Dr Isaac Cho, Dongyun Han and Vinayak Sharma.

My decision to pursue a PhD in Electrical Engineering at UNC Charlotte began with a conversation with Dr. Aba Ebong, who was the Graduate Program Director of the ECE department when I joined UNC Charlotte as a Masters student. Thank you so much Dr. Ebong for encouraging me to pursue this path. It was long and at times challenging, but it was also rewarding.

I am grateful to the UNC Charlotte Graduate School for the various funding opportunities it provided me to complete my studies at UNC Charlotte. These included the Graduate Assistant Support Plan (GASP), 2020 Proposal Development Summer Fellowship and the 2021 Graduate School Summer Fellowship Program. Special thanks to Dr. Lisa Russell-Pinson for the valuable support she provided me and other graduate students through the Dissertation Writing Group. Being part of the Dissertation Writing Group helped me make much needed progress on my proposal and

dissertation.

In addition, I am grateful for the support provided by the Energy Production and Infrastructure Center (EPIC), the Department of Electrical and Computer Engineering, and the William States Lee College of Engineering throughout my time at UNC Charlotte through graduate and teaching assistantships and conference travel grants.

Moreover, I would like to thank my former UNC Charlotte colleagues, Dr. Saeed Mohajeryami, Dr. Masoud Davoudi, Dr. Mahbubur Rahman, Dr. Roozbeh Karandeh, and Dr. Bilkis Banu, for their support and collaboration. Thanks Saeed for showing me the ropes and for the tools you introduced to me as a new graduate student.

Thanks to Dr. Victor Emenike for his mentorship from my time as an undergraduate and during my PhD studies. Thanks for your comments and encouragement after I was faced with my first paper rejection. Thanks to Adedoyin Inaolaji, who has been my go-to person for MILP and power systems optimization questions. I greatly appreciate you.

To my brothers and sisters at Grace Presbyterian Church and my friends, Dr. Adeola Sorinolu, Chiamaka Fatoki, Aanuoluwapo Uduebor, Oluwatosin Folorunsho, Chidimma Okoli, Dr. Pelumi and Dr. Deborah Oluwasanya, Ogechi Ogazi, Samuel and Oyinwunmi Iyiola, Dr. Bayode Fagbohungbe and Adunola Fashogbon, thank you so much for being a wonderful community I could lean on at several points in my PhD journey. Thank you so much for your prayers and encouragement.

Additionally, I am grateful for the support and love I receive from my parents and siblings. To my parents, thank you so much for investing in me and my academic endeavors. You have consistently urged me to do my best and have celebrated my accomplishments along the way. Thank you especially to my mother who came to help my husband and me when we welcomed our baby so I could progress on my dissertation.

I am especially grateful for the kindness of the Ogunros and Olatosis who welcomed

me into their homes. My gratitude for your love, support and delicious meals during my time at UNC Charlotte is beyond words. Thanks to my friends at Bridges International for being a home away from home for me and several international students during our studies at UNC Charlotte.

To my dear husband, thank you for being a pillar of support and blessing to me; words fail to truly express my gratitude for your tremendous love, help and encouragement throughout this journey. To my dear son, it has been a blessing to watch you grow over the past year. I love you both very much!

And to the Almighty God who provided me with the wisdom, help, health, grace, strength and so much more than I needed to complete this PhD journey, I give You all the glory!

TABLE OF CONTENTS

LIST OF TABLES

LIST OF FIGURES

LIST OF ABBREVIATIONS

AMI	Advanced Metering Infrastructure
CAIDI	Customer Average Interruption Duration Index
CAIFI	Customer Average Interruption Frequency Index
CLPU	Cold Load Pickup
CVR	Conservation Voltage Reduction
DER	Distributed Energy Resource
DG	Distributed Generation
DMS	Distribution Management System
EPRI	Electric Power Research Institute
FLISR	Fault Location, Isolation And Service Restoration
GIS	Geographical Information Systems
MILP	Mixed Integer Linear Programming
MINLP	Mixed Integer Non-linear Programming
MIQP	Mixed Integer Quadratic Programming
MISOCP	Mixed Integer Second-order Cone Programming
OMS	Outage Management Systems
OPM	Outage Prediction Model
POL	Predicted Outage Location
SAIDI	System Average Interruption Duration Index
SAIFI	System Average Interruption Frequency Index

SCADA	Supervisory Control And Data Acquisition
SR	Service Restoration

CHAPTER 1: INTRODUCTION

1.1 Overview

Around 90% of all outages in the electric power system can be traced to the distribution network [1, 2]. The increase in severe weather events leading to widespread and long-duration outages to customers is a source of concern for electric utilities. Other factors such as aging infrastructure and cyberphysical attacks also result in outages in the distribution system. The impacts of outages in the grid could range from mild inconveniences to losses in millions of dollars, or even loss of life. For example, the economic losses due to the February 2021 North American winter storm were estimated at around $130 billion in Texas alone [3, 4]. Hence, there is a need to develop strategies that help prevent outages or mitigate the impacts of outages and improve the resilience of the power system.

This dissertation examines the need to improve situational awareness given the increase in the frequency of outages in the distribution system and proposes a method for managing outages in a more proactive manner.

The following are discussed in subsequent sections of this chapter:

- Background and motivation for this work
- Objectives of this work
- A summary of the contributions
- The dissertation organization

1.2 Background and Motivation

In September 2000, the National Academy of Engineering named the electric power grid as the greatest engineering achievement of the twentieth century [5, 6]. The electric power grid, which has also been described as the most complex machine ever invented, comprises of a network that transports power from generation through transmission and down to the distribution system, where electricity is delivered to the final customers.

There is a need for high reliability in the distribution system due to its proximity to customers. However, the reliability and resilience of the distribution system is often threatened by several factors including severe weather events, aging infrastructure and cyberphysical attacks which could cause outages and damages in the distribution system [7].

In the past, electric utilities had no way of detecting outages automatically, and had to depend primarily on phone calls from customers [8, 9]. Upon receiving these calls, utilities used paper maps to pinpoint the location of affected customers, and possibly, the exact location of the fault, after which repair crews were dispatched to the outage locations [10]. Once on site, the crew had to investigate the source of the fault, and isolate the fault. To isolate the fault, network reconfiguration could be implemented to restore power to some affected customers [11]. After repairs, service restoration was considered complete. One problem with this traditional approach is that it was highly reactive in nature—the outage occurs, and then the utility responds. Other issues stemmed from the fact that utilities did not have complete network connectivity information such as phase connectivity and meter-to-transformer connectivity in the network [12, 13].

This changed with the introduction of smart electricity meters which led to increased monitoring and visibility at the distribution level. Electric utilities now have access to huge amounts of data from smart meters, distribution system sensors as well

as other systems including distribution management and outage management systems. As of 2019, close to 95 million smart meters have been deployed in the United States [14], and this has increased the amount of data processed by electric utilities by at least three thousand times [15]. These data have opened up opportunities for more advanced functions such as volt/var optimization, distribution automation, and demand response in the distribution system. Hence, utilities consider the use of advanced metering infrastructure (AMI) data for improved outage management and service reliability of utmost importance [16, 17]. AMI comprises sensors, devices and communication networks that enable bidirectional communication between meters/devices and electric utilities, allowing for increased monitoring and management of the grid.

For outage management purposes, AMI data is often integrated with information such as customer calls and notes from repair crews from outage management systems (OMS). Similarly, utilities have created online outage maps by integrating AMI data with OMS and geographical information systems (GIS). Some benefits of using AMI data for outage management include faster outage isolation, reduced trips by outage crews, and faster power restoration [18]. Smart meters could be pinged to verify outages caused by momentary events, and to verify actual outage location [11]. Using the last gasp feature of smart meters [16, 19], outages can be detected even before customers call in, thus reducing outage duration, and improving reliability indices and customer satisfaction. After outage response by field crews or remotely, smart meters can be used to verify service restoration to customers [11]. Nonetheless, this approach is still reactive: the outage occurs before the utility responds [9].

Nevertheless, AMI data, coupled with improvements in data analysis and forecasting methods, provide utilities the opportunity to move from managing outages reactively to managing them proactively. This paradigm shift adds a new layer to the traditional outage management process—outage prediction. The field of data an-

alytics makes it possible to analyze patterns and detect anomalies in the distribution system using large datasets, including historical outage and weather data. Thus, it is possible to predict the failure of a piece of distribution system equipment before it happens, or detect weather or vegetation patterns that could lead to outages using outage prediction models (OPMs) [20–23].

In addition to outage prediction, the service restoration process could be improved by leveraging distribution system data through a combination of prescriptive and predictive analytics. While predictive analytics focuses on analyzing historical outages and predicting future outages before they occur, the focus of prescriptive analytics is on leveraging outage forecasts to optimize the service restoration process.

1.3 Research Objectives

This dissertation proposes a proactive topology optimization and service restoration framework that leverages forecasts from OPMs to prevent or mitigate the effects of predicted outages in the distribution system. The result is a holistic and more proactive approach to outage management in the distribution system. The objectives of this work are as follows:

1. To analyze outage frequency and duration in a distribution network by applying machine learning techniques to an OMS dataset.

2. To propose a two-stage proactive topology optimization and service restoration framework that prescribes a set of switching actions and an optimal network topology that minimizes the impact of outages at predicted outage locations. The objectives of the framework are as follows:

    - The objective of the first stage is to optimize the network topology by minimizing the power flowing through the predicted outage locations. The results show that by minimizing the power flowing through the predicted

outage locations the out-of-service (or unserved) load is minimized when the outage occurs as predicted.

- The objective of the second stage is to maximize the amount of loads left in service after the outage occurs at the predicted locations.
- Both objectives are achieved by changing the status of switchable lines in the distribution network.

1.4 Summary of Contributions

The contributions of this work are summarized as follows:

1. The frequency and duration of power system outages in a distribution system are analyzed based on several features in an outage management dataset including outage cause, climatic description, and voltage level of the affected circuit. The impact of these features are ranked using two machine learning techniques: random forests and gradient boosting regression.

2. A topology optimization and service restoration framework is proposed for proactive outage management in the distribution system. This framework is formulated as a two-stage mixed integer linear programming (MILP) problem with the following objectives:

   - In the first stage, the objective is to minimize the power flowing through the predicted outage locations. By minimizing the power flowing through the predicted outage locations, the unserved load is minimized when the outage occurs as predicted.
   - In the second stage, the amount of loads left in service after the outage occurs at the predicted locations is maximized by changing the status of the operational switchable lines.

3. In addition, three cases are proposed for implementing the proactive topology optimization and service restoration framework as follows:

    - Single outage case
    - Multiple outage case
    - Weighted multiple outage case

1.5 Dissertation Organization

The rest of this dissertation is organized as follows:

- Chapter 2 presents a review of literature on outage management in distribution systems including current approaches to service restoration.
- In Chapter 3, the gap in current approaches to outage management in the distribution system are identified, and the problem statement is presented and discussed in further detail.
- Chapter 4 presents an analysis of frequency and duration of outages in the distribution network using outage data from a utility in southeastern United States.
- In Chapter 5, the proposed topology optimization and service restoration framework is presented and described in detail. The framework is formulated using an MILP model and applied to three optimization cases.
- In Chapter 6, the proposed topology optimization and service restoration formulation is demonstrated using modified versions of the IEEE 13-bus and 123-bus feedesr. Results of the three optimization cases discussed in the previous chapter are presented to demonstrate the validity of the proposed framework.
- The conclusion, summary of contributions as well as recommendations for future work are presented in Chapter 7.

CHAPTER 2: LITERATURE REVIEW

2.1 Overview

Outages in the distribution system impact system reliability and customer satisfaction. Effects of outages could range from minor inconveniences and stress to customers, safety hazards at road intersections due to traffic lights losing power, to economic losses in thousands or even millions of dollars. Moreover, the average cost per event for a momentary outage in the United States is estimated to range from around $3.90 for residential customers to as high as $12,952 for medium and large commercial and industrial customers [24]. This cost increases with the duration of the outage. In 2017, it was estimated that Delta Air Lines lost up to $50 million during an 11-hour outage at the Hartsfield-Jackson Atlanta International Airport [25,26]. Hence, this chapter presents a review of literature on distribution system outage management including the state-of-the-art on outage analysis and prediction as well as current approaches to distribution system service restoration.

2.2 Distribution System Outage Management

Outage management encompasses activities undertaken by an electric utility to predict, prevent, identify and locate outages, and promptly restore power to its customers, thereby reducing the time customers are left without power. Fig. 2.1 displays a summary of the traditional approach to outage management in distribution systems as described in Section 1.2.

Significant research has been conducted in the area of outage management dating back to the 1990s. However, considerable interest in outage management increased significantly in the 2000s due to the advent of smart meters and the consequent explo-

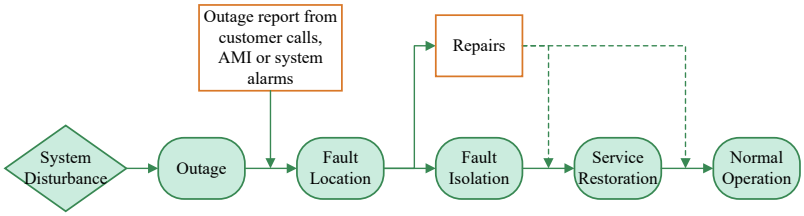

Figure 2.1: Traditional outage management approach

sion of data in the distribution system. These studies can be broadly categorized into the following themes: outage analysis and detection, outage prediction and modeling and service restoration. Some studies have also focused on the application of machine learning/data analytics to the afpremention areas.

2.2.1 Outage Analysis and Prediction

Most of the literature have approached the subject of outage management by analyzing or predicting the causes of outages in the distribution system using historical data. Fig. 2.2 shows the top causes of power outages in different regions of the United States. Common causes of distribution system outages include: vegetation, weather, animals, equipment failure and planned maintenance and repairs; a large percentage of literature focuses on analyzing outages based on the first three cause categories. It is important to note that sometimes the cause of an outage may be unknown [27].

Early studies on outage analysis and prediction focused on analyzing and predicting

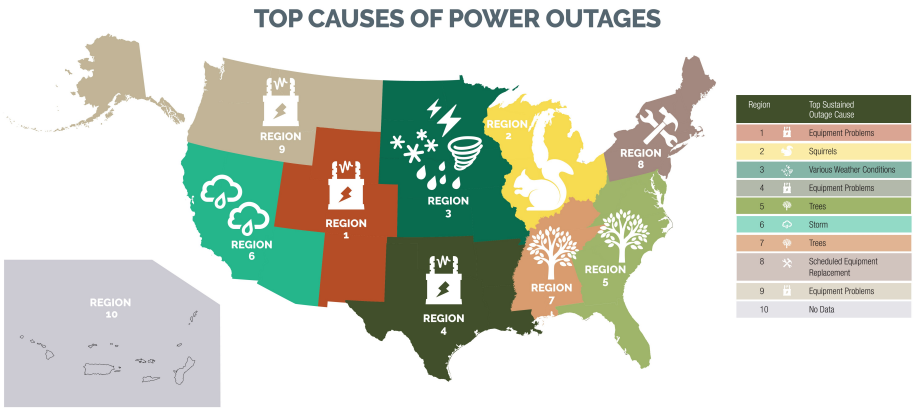

Figure 2.2: Top causes of power outages in the United States [28]

outages due to various causes including trees and animals simultaneously [29–32]. A drawback of this approach is that factors affecting each outage cause could be different. For example, some outage causes are affected more by weather-related factors than others, and there could be seasonal variations in outages due to different causes. Hence, more recent studies have emerged that focus on outages due to a single cause category. Most of these studies are focused on outages due to trees or vegetation, animals, lightning and weather.

Outages attributed to vegetation could be growth-related (that is, growth of tree branches to make contact with distribution lines and equipment) or weather-related (weather-related factors causing vegetation to make contact with distribution lines and equipment). The study in [33] used time series and nonlinear machine learning models to categorize outages due to vegetation as growth-related or weather-related, and predict the number of monthly-related outages in a distribution network. This study revealed a seasonal pattern in growth-related outages while weather-related vegetation outages showed no apparent trend over time. Other studies such as [34] and [35] focused on predicting the failure risk or rate of vegetation-related outages in the distribution system. In [35], a spatiotemporal prediction model was used to develop an optimal dynamic tree trimming scheduler which reduces the risk of vegetation-related outages by more than 30%.

Over 70% of power outages in the US can be traced directly or indirectly to weather-related causes [36], hence a considerable amount of literature has also been published on outages directly caused by weather phenomena such as wind, hurricanes, thunderstorms and ice. This may be attributed to an increase in adverse weather events affecting the US power grid. The studies in [21, 37–40] proposed outage prediction models (OPMs) to analyze and predict outages caused by severe weather such as thunderstorms, ice storms and hurricanes. Tree-based machine learning models were used in [21, 39, 40] while [37] and [38] used generalized linear mixed models and negative

binomial regression, respectively. These studies, along with others in literature investigating weather-related outages typically leverage historical and forecasted weather data along with historical outage records.

With respect to outages caused by animals, studies have shown that most animal-related outages are caused by squirrels [41, 42]. These studies showed that weather and season play significant roles in animal-related outages with most of the outages occurring in the spring and fall seasons in the locations under study. A range of methods have been used for predicting these outages including dynamic regression [41], neural networks [43–45] and Bayesian network models [22, 42, 44]. In addition, some studies applied wavelet techniques [46] and boosting algorithms [43] to improve the performance of neural network models used to predict animal-related outages.

Studies focused on outage analysis or prediction often use historical outage records from outage management systems (OMS) as well as weather data. The studies in [41] and [43, 44] used five years and ten years worth of historical outage records in the Carolinas and in the state of Kansas, respectively. The date-time information from historical outage records is often decomposed to create new variables such as season, day of week, time of day, and month of year. Commonly used weather variables include temperature, wind speed, humidity, and precipitation.

With respect to distribution system reliability, it is important to know the frequency and duration of outages occurring in the distribution network; hence reliability indices measure how outage frequency and duration impact the system as well as the customers. Commonly used distribution reliability indices include: system average interruption frequency index (SAIFI), customer average interruption frequency index (CAIFI), system average interruption duration index (SAIDI) and customer average interruption duration index (CAIDI) [47].

Consequently, several papers in literature focused on analyzing and predicting outage frequency and duration, with a larger proportion focusing on estimating outage

frequency or number of outage events. Furthermore, a number of studies investigated the impact of different variables on outage duration. Variables considered in these studies include: outage cause, action taken by repair crew to resolve the outage and calendar variables such as month, day of week, and hour of day. Outage cause was found to have the most impact on outage duration in [48] and [49]. In [50], outage duration was predicted in real-time using recursive neural networks to analyze weather information, outage reports and repair logs. Natural language processing was used to identify the outage cause from outage reports.

Furthermore, several machine learning or data-driven techniques have been applied to predict and analyze power outages. Some of these techniques include regression models [41, 51–53], artificial neural networks [43–45], tree-based approaches [20], and support vector machines [54]. Specifically, [52] and [53] investigated and compared the performance of several regression-based models for analyzing outages caused by wind and lightning. Other studies formulated outage analyses as classification problems with the goal of identifying the cause of outages in distribution systems. The study in [20] compared the performance of three classification methods—decision tree, logistic regression and naive Bayesian classifier—in identifying equipment failure outages in distribution systems. The study used outage data and weather data for five years, and outages due to equipment failure were analyzed based on twelve variables including weather conditions, clearing device activated and time of day. The results showed that the decision tree classifier outperformed the other two classifiers. The study in [55] proposed a method that used a supervised topic model for outage detection and location using information from Twitter. On the other hand, [51] used logistic regression to predict outages of grid devices during severe weather events such as hurricanes.

Overall, these studies revealed the value of data and machine learning techniques in drawing actionable insights that could help utilities better manage and predict

outages in the distribution system.

2.2.2 Distribution System Service Restoration

Following an outage, it is important to restore service to affected customers as quickly as possible. Distribution service restoration is the last step in the fault location, isolation and service restoration (FLISR) process that involves restoring power to customers affected by an outage. The primary objective of service restoration is to restore service to as many customers as possible and it typically involves reconfiguring the distribution network [56] subject to various constraints.

The service restoration (SR) problem is complex and often involves multiple objectives. A survey of nineteen papers focused on distribution system restoration presented in [57] highlights two primary objectives of service restoration: restoring power to as many affected customers as possible and restoring power as quickly as possible. The SR problem has been formulated using different methods including heuristics [58–60], expert systems [61], combinatorial optimization, and evolutionary programming such as genetic algorithms [62, 63].

With regards to combinatorial optimization (specifically mathematical programming), the SR problem is often formulated using methods such as mixed integer linear programming (MILP) [64, 65], mixed integer second-order cone programming (MISOCP) [66–68], mixed integer quadratic programming (MIQP) [69,70], and mixed integer nonlinear programming (MINLP) [71, 72]. Some objectives considered in literature include minimizing total restoration time [73, 74], minimizing the duration of customer interruption [73], minimizing the number of switching operations [75–78], minimizing the number of customers without supply, maximizing the total restored energy [64], minimizing lines losses [77, 79] as well as feeder load balancing [60, 80]. Constraints considered in the formulations include: feeder loading limits, voltage magnitude limits, transformer and line capacity limits, switching time, network radiality [62, 69, 75–77, 81, 82]. For MILP models, the linear DistFlow equations in-

troduced in [80] are often used to linearize the power flow equations. Some other considerations in these formulations include cold load pickup (CLPU) conditions, integration and dispatch of renewable energy resources, energy storage systems and microgrids [65, 73, 74, 82].

Some studies have included distributed generation (DG) in the service restoration process to increase the amount of load restored, reduce losses in the network and to deal with load uncertainties due to CLPU. [82] proposes an approach that uses distributed generation for service restoration and conserves load diversity in the system, hence mitigating the CLPU problem. The study considers both utility-owned and non-utility owned DGs in the restoration process. [66] presents a two-stage stochastic optimization model that considers the uncertainty of load demand and distributed generation in the service restoration process. Some studies considered the effects of DG output uncertainty on the SR problem using stochastic models [66, 81, 83]. Other studies [69, 84, 85] considered microgrids in the service restoration formulation; this involved leveraging power support from local microgrids or sectionalizing the distribution network into microgrids to maximize the loads restored or minimize load shedding during the SR process. [69] leveraged power support from local microgrids to restore power to de-energized loads in the network.

The study in [64] presented a multi-time step service restoration methodology that considers distributed generators (DGs) and energy storage systems connected in the network. The study considered cold load pickup in the SR process. The proposed methodology generated a sequence of control actions for controllable switches, dispatchable DGs and energy storage systems. The SR problem was formulated using an MILP model with the objective of maximizing the total restored energy. The proposed methodology was validated using the IEEE 13-node and 123-node test feeders, and in each case, the test systems were restored in several time steps ensuring that operation constraints were not violated. One limitation of this study is that it

assumed that the system was completely de-energized at the start of the restoration process. However, most outages do not lead to a complete de-energization of the distribution network; typically, only some parts of the distribution network are de-energized during outage events. Hence, it is necessary to consider outage scenarios in which only some sections of the distribution system are affected. The study also assumes the same line impedance for each line in the test systems.

2.3 Summary

In conclusion, this chapter presented a survey of current literature on distribution system outage management, with a focus on outage analysis and prediction as well as service restoration.

In the area of outage analysis and prediction, studies focusing on different outage causes were discussed, and several machine learning and statistical methods used for outage analysis and prediction were presented. With regards to service restoration (SR), different approaches to the SR problem in literature, including heuristics and mathematical programming, were examined. Common objectives, constraints as well as considerations such as CLPU and the use of distributed energy resources in the SR problem were discussed.

CHAPTER 3: PROBLEM STATEMENT

3.1 Overview

In the previous chapters, background and motivation for a more proactive approach to outage management were presented. Current approaches to distribution system outage management in the literature were also discussed. Specifically, a survey of the literature on outage analysis and prediction as well as on service restoration approaches was presented. This chapter begins with a synthesis of the gaps in literature, followed by a presentation of the problem statement and the specific contributions of this work.

3.1.1 Gaps in Literature

Based on the literature survey presented in Chapter 2, it is clear that the outage management and service restoration problems in distribution systems have been widely researched and are well-understood. However, in the area of outage analysis and prediction, most of the literature focuses on analyzing historical outages and predicting outage cause or location, by using descriptive and predictive analytics methods. These studies typically do not propose actions to prevent these predicted outages or to mitigate their impacts on the distribution network. In the area of service restoration, studies in literature often propose the next course of action after the outages have occurred instead of prescribing actions to be taken before the outage occurs.

In addition, existing studies often focus on either outage analysis and prediction or service restoration without making a vital connection between these two processes that comprise the overall outage management framework. This results in an outage

management approach that is largely reactive and somewhat disjointed. Although outage prediction models (OPMs) provide valuable insights to distribution system operators, it is important to go a step further by prescribing specific actions that allow system operators to manage outages proactively [86]. Hence, there is a need for a prescriptive approach that leverages insights gleaned from outage prediction in the service restoration process, by recommending actions to be taken to reduce the impact of predicted outages on customers in the distribution system.

3.2 Problem Statement

The research questions addressed in this dissertation are as follows: Given a set of predicted possible outage scenarios,

1. Can proactive actions be prescribed and implemented in the distribution network that would prevent predicted outages from even occurring?

2. If the predicted outage cannot be prevented, can actions be implemented before the outage in the distribution system (in real-time) that would result in the shortest outage duration or the least number of affected customers affected?

To address these questions, this work proposes a prescriptive approach to service restoration that leverages outage forecasts with a goal of reducing the impact of outages in the distribution system. This is done using a two-stage framework comprising topology optimization and service restoration. In this approach, topology optimization and service restoration are achieved by performing switching operations in the distribution network. Asides switching, methods that have been proposed in literature include line hardening, installing backup generators, upgrading distribution poles and vegetation management [87, 88]. Although these methods have been proven to improve resilience in distribution networks, they require medium-term to long-term planning or investment in distribution system equipment to be implemented. On

the other hand, the proposed topology optimization and service restoration framework can be implemented in the short-term using already available switches in the distribution system.

In the first stage, proactive topology optimization is carried out. The impact of predicted outages is first evaluated by estimating the total unserved load (or total load not served) in kilowatts (or megawatts) in the event of the predicted outages. The predicted outage locations (POL) are assumed to be outputs of a probabilistic OPM that leverages historical outage and weather records for the distribution network in question. Then, topology optimization is carried out by prescribing a set of switching actions that result in an optimal topology with the least amount of load lost in the event of the predicted outage.

In the second stage, service restoration is carried out with a goal of maximizing the amount of load restored in the event of the outage. This may result in a new operating topology for the distribution network.

The two-stage topology optimization and service restoration problem is formulated using mixed integer linear programming (MILP). The objective of the topology optimization stage is to reconfigure the distribution network by changing the status of switchable lines such that the minimum kW amount of loads would be lost if an outage occurs at the predicted locations. This is achieved by minimizing the power flowing through the predicted outage locations as shown in (3.1) below:

$$OF_1 : \min \sum |P_{ij}^{BR}| \qquad (i,j) \in \mathcal{B}_F \tag{3.1}$$

where P_{ij}^{BR} is the power flowing through line ij and $\mathcal{B}_F$ represents the set of predicted outage locations. The predicted outage locations are assumed to be lines in the distribution network.

In other words, the goal of the first stage is to reconfigure the distribution network,

by solving for the status of switchable lines in the network that optimize the above objective function.

The objective of the second stage is to reconfigure the distribution network by changing the status of switchable lines such that the maximum kW amount of loads is restored after an outage occurs at the predicted locations. This is represented in (3.2) as follows:

$$OF_2 : \max \sum_{i=1}^{n} x_i^L P_i^L \qquad i \in \mathcal{N} \tag{3.2}$$

where x_i^L is the status of the load demand at the ith bus, P_i^L is the load demand in kW on the ith bus, n is the number of energized buses in the system, and $\mathcal{N}$ represents the set of nodes in the distribution network.

The above objectives are subject to a number of constraints including the linear DistFlow constraints, load limits, transformer and line loading limits, voltage limits, switching limits, radiality constraints as well as a number of connectivity constraints. A detailed formulation of the optimization problem will be presented in Chapter 5.

Three cases of the proposed proactive topology optimization and service restoration framework are considered as follows:

- Single outage case: In this case, the impact of a single outage case on the distribution network is evaluated and the proposed topology optimization and service restoration framework is implemented. The goal is to optimize the network topology for a single scenario of predicted outage(s). An outage scenario may comprise a single or multiple predicted outage locations.

- Multiple outage case: In this case, multiple outage scenarios are considered and the proposed topology optimization and service restoration framework is applied to minimize the impact of outages across the multiple scenarios.

- Weighted multiple outage case: The weighted multiple outage case extends the multiple outage case by assigning weights to each outage scenario based on its

probability or likelihood of occurrence.

3.3 Summary of Contributions

The contributions of this work are summarized as follows:

1. A proactive approach to service restoration that leverages outage forecasts is proposed with a goal of reducing the impact of outages in the distribution system. This is achieved through a proactive topology optimization and service restoration framework formulated as a two-stage MILP. The objectives of the MILP are to minimize the load lost prior to an outage and maximize the restorable load if the outage occurs at the predicted location(s). The MILP formulation is validated using test feeders applied to the following three optimization cases:

    - Single outage case
    - Multiple outage case
    - Weighted multiple outage case

2. A sensitivity analysis is presented to assist distribution system operators in making decisions about the topology to operate in given a range of possible outage locations in the distribution network along with their probabilities of occurrence. The optimal topologies are generated by assigning weights to predicted outage locations and implementing the weighted multiple outage case using the proposed topology optimization and service restoration framework.

3. The frequency and duration of power system outages in a distribution system are analyzed based on several features in an outage dataset. The impacts of the features, including outage cause, climatic description, and voltage level of the affected circuit, are ranked using two machine learning techniques: random forest and gradient boosting regression.

CHAPTER 4: ANALYSIS OF OUTAGE FREQUENCY AND DURATION IN DISTRIBUTION SYSTEMS USING MACHINE LEARNING*

4.1 Overview

Outage frequency and duration impact system reliability and customer satisfaction. With regards to outages, customers are most concerned about the duration of outages [50]. Hence, there is a need to study factors that significantly impact the duration of outages in a distribution system. In this chapter, the impact of several features on outage frequency and duration in a distribution network is analyzed using the frameworks presented in [90] and [91]; the features considered in this analysis include: outage cause, interrupted phase, voltage level of the affected circuit, climatic description, and calendar variables. The impact of these features are ranked using random forest and gradient boosting regression.

4.2 Introduction

Outage frequency and duration impact system reliability and customer satisfaction. With regards to outages, customers are most concerned about the duration of outages [50]. A major priority of utilities is to reduce the amount of time that customers are left without power. The impact of outages on customers can range from inconvenience and stress (for residential customers) to loss of revenue and man-hours (for commercial and industrial customers). The study in [24], which was conducted in 2015, estimates that the average cost per event for a momentary outage in the United States ranges from around $4 for residential customers to as high as $12,952 for medium and large

*This chapter is based on the following paper: T. Lawanson, V. Sharma, V. Cecchi, T. Hong, "Analysis of Outage Frequency and Duration in Distribution Systems using Machine Learning," *2020 52nd North American Power Symposium (NAPS)*, 2021, pp. 1-6. doi: 10.1109/NAPS50074.2021.9449708 [89]

commercial and industrial customers. Results from the same study show that the average cost per event rises as the outage duration increases. Hence, there is a need to study factors that significantly impact the duration of an outage.

Much of the current literature pays attention to analyzing outages based on their frequency and causes; typically these studies focus on using machine learning techniques to predict the cause of outages or to analyze outages based on a particular outage cause (typically, trees and animals) [41, 46, 52, 92, 93].

Conversely, fewer studies have analyzed factors that impact outage duration. Reliability indices can be improved by reducing not only outage frequency, but also outage duration. One of the most common distribution system reliability indices, Customer Average Interruption Index (CAIDI), represents the average time to restore service after an outage. Authors in [90] investigate the impact of several variables on time of outage restoration (TOR) in distribution systems using statistical methods and measures such as the chi-square approximation to Kruskal-Wallis test and the coefficient of determination (R^2). The variables considered in the analysis were categorized under time (hour of day, day of week and month), consequence (number of phases affected and protection device activated) and external factors (weather condition and outage cause). Similarly, [91] presents an analysis to assess the impacts of different features on outage duration in a distribution network. Some features considered in the study include outage cause, action taken by repair crew, weather conditions, clearing device, number of customers and calendar variables such as year, month, and hour of day. On the other hand, [50] uses recursive neural networks (RNN) to predict the duration of distribution system outages in real-time. Data used in this study include weather information, outage reports and repair logs. Outage causes are identified by applying natural language processing to utility outage reports.

In the following sections, the impact of several features on outage frequency and duration in a distribution network is analyzed using random forest and gradient boosting

regression. The analysis uses the frameworks presented in [90] and [91]; the outage features considered in this analysis include: outage cause, interrupted phase, voltage level of the affected circuit, climatic description, and calendar variables. The impact of these features are ranked using random forest and gradient boosting regression.

4.3 Outage Data Description

This study uses outage data obtained from an electric power utility in southeastern United States. The dataset, which comprises over 20,000 entries, includes outage information from 2016 to 2018 for an electric power distribution network. Prior to analyzing the data, data cleansing is performed by removing duplicates and missing entries from the dataset.

Features in the dataset include: climatic description during the outage, voltage level of the circuit affected by the outage, outage cause, outage duration, interrupted phase and failed equipment. In addition to the features in the original dataset, the date of the outage is decomposed into new features: year, month, day of the week and season. Table 4.1 presents a summary of the features from the outage dataset along with their respective classes. The failed equipment feature (not listed in Table 4.1) comprises over 20 classes, some of which include: transformer, switchgear, regulator, meter, and conductor.

This study also uses weather information for the distribution network location, sourced from OpenWeatherMap, an online weather data service [94]. The weather variables considered are: temperature (Fahrenheit), wind speed (miles/hour) and humidity (%). Table 4.2 presents a statistical summary of the daily average of the three weather variables.

4.4 Data Analysis

This section presents results from exploratory analysis of the outage data. The features listed in the previous section are analyzed based on outage frequency and

Table 4.1: Summary of features in outage dataset © 2021 IEEE

Features	***Classes/Description***
Climatic Description	Calm, Precipitation-Rain, Thunderstorm, Wind & Precipitation
Day of Week	Mon, Tue, Wed, Thu, Fri, Sat, Sun
Interrupted Phase	A, AB, ABC, AC, B, BC, C
Month	Jan, Feb, Mar, Apr, May, Jun Jul, Aug, Sep, Oct, Nov, Dec
Outage Cause	Animal, Equipment Failure Event Response, Lightning, Other, Third Party, Tree, Unknown
Season	Fall, Spring, Summer, Winter
Voltage Level	4 kV, 12 kV, 46 kV, 161 kV
Year	2016, 2017, 2018

Table 4.2: Summary statistics for weather variables

Statistics	***Temperature (°F)***	***Humidity (%)***	***Wind Speed (mph)***
Mean	66.48	70.10	6.68
Standard Deviation	13.04	11.95	2.72
Minimum	17.04	31.25	1.87
25th Percentile	57.80	62.08	4.73
Median	71.06	71.79	6.09
75th Percentile	77.01	78.17	7.82
Maximum	85.43	96.04	15.63

average outage duration (in minutes).

4.4.1 Number of Outages/Outage Frequency

Fig. 4.1 shows a breakdown of the outage events by cause. Outages due to trees are the most frequent and account for 38.5% of the outages, while outages caused by a third party are the least frequent, and account for 3.4% of the outages. Outages attributed to *Third party* include outages caused by vehicle accidents and contractor dig-ins. It is interesting to note that the cause of nearly 7% of the outages is categorized as Unknown. Outages categorized under *Event response* refer to outages caused

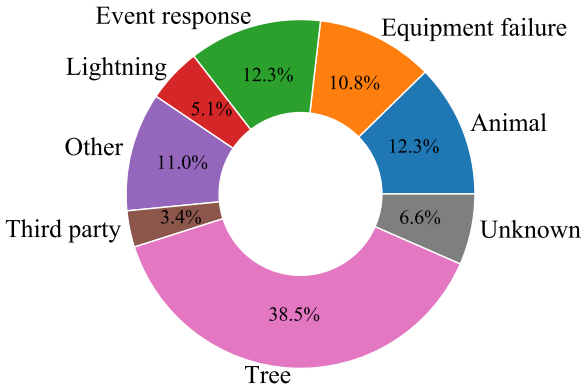

Figure 4.1: Distribution of outage frequency by cause © 2021 IEEE

by opening a protection device for repair purposes, whereas outages categorized as *Other* include outages that do not fall into any of the other cause categories shown.

Fig. 4.2 presents plots of outage frequency with respect to each feature in the outage dataset listed in Table 4.1.

Fig. 4.2(a) shows the number of outages categorized by the climatic condition at the time of the outage. The climatic description feature has four classes: calm, wind and precipitation, precipitation-rain, and thunderstorm. About 75% of the outages occur in calm weather, while 18% of the outages occur during thunderstorms. The precipitation-rain class has the lowest number of outages.

Fig. 4.2(b) presents the number of outages categorized by each day of the week. This is done to identify any patterns that might be present due to changing load profiles for different days of the week. Monday has the highest number of outages, followed by Saturday, while Friday and Sunday have the least outages. Thursday, Tuesday and Wednesday have very similar number of outages.

Fig. 4.2(c) presents the number of outages by the interrupted phase, that is, the phase affected by the outage. 75% of the outages affect only a single phase (A, B, or C) with phase C having the most outages. This is not surprising as single-phase faults are the most common faults in distribution systems [95]. 18% of the outages affect all three phases (ABC) simultaneously. On the other hand, less than 5% of the

outages affect only two phases (AB, AC or BC) at the same time.

Similarly, Fig. 4.2(d) presents the number of outages categorized by the months of the year. The month of June stands out with the maximum number of outages, nearly 15% of the total. It can be observed that in the initial months of year, i.e.

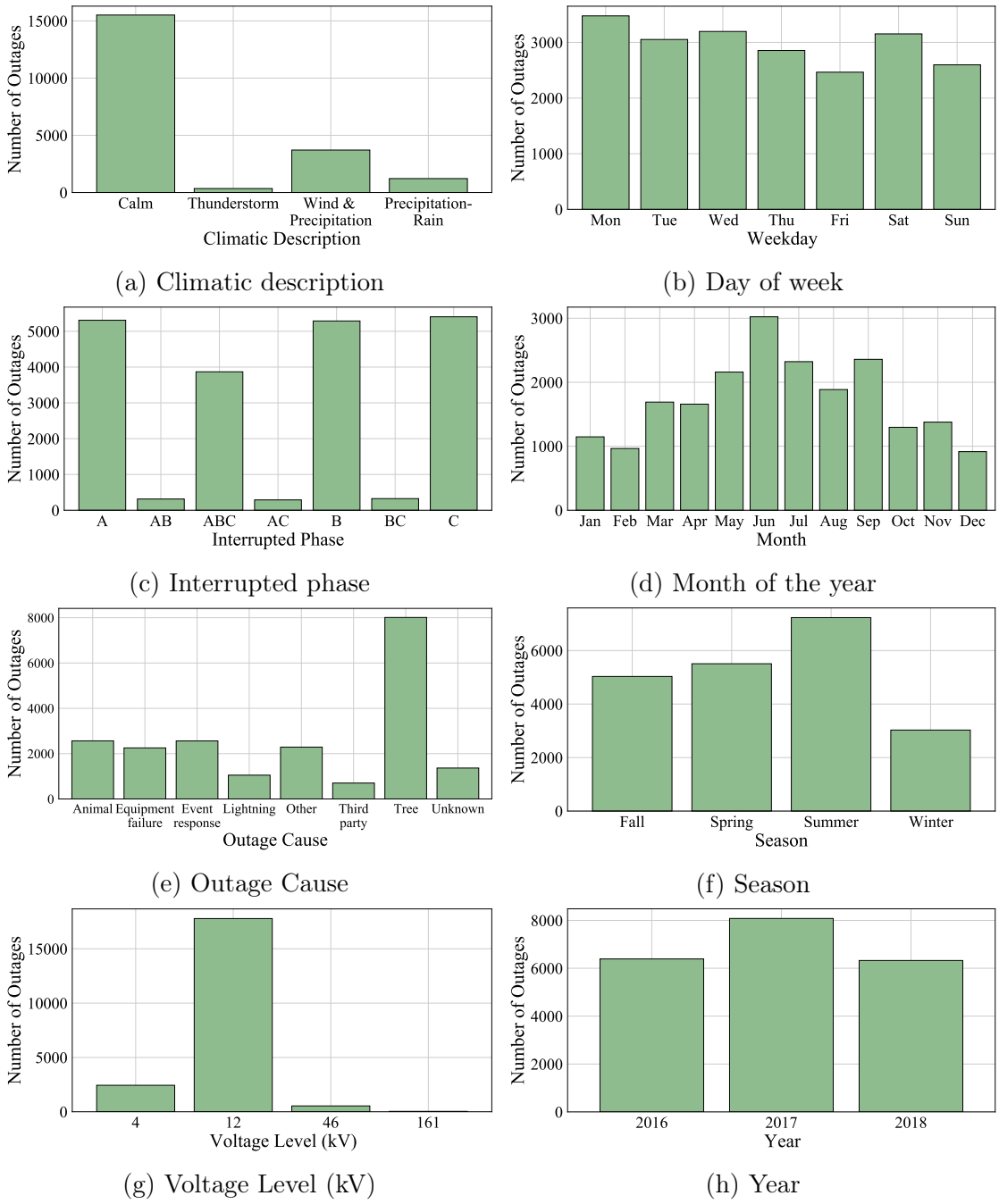

(a) Climatic description

(b) Day of week

(c) Interrupted phase

(d) Month of the year

(e) Outage Cause

(f) Season

(g) Voltage Level (kV)

(h) Year

Figure 4.2: Outage frequency with respect to categorical features in outage data set

January, February and March, the outages are low. The outages begin to rise in the months of April, May, peaking in June. After June, the number of outages begin to decrease until September, which has higher number of outages and then the number of outages decrease till December.

Fig. 4.3 shows the distribution of outages by climatic description and by month of the year. The highest number of outages during thunderstorm occurs in June. It is worth noting that September is the only month that has all four climatic description classes present. Further investigation revealed that the highest frequency of outages during wind and precipitation occurred in September 2017, and this coincides with the period Hurricane Irma struck the US. On the other hand, June and July account for the most outages during thunderstorms, while August accounts for the most outages during calm weather.

Outage frequency by cause categories is presented in Fig. 4.2(e). As previously stated, outages caused by trees are the most frequent, while outages caused by a third party are the least frequent.

Fig. 4.2(f) shows the number of outages by season. The months of the year are categorized into four seasons as follows: Spring (March to May), Summer (June to August), Fall (September to November), and Winter (December to February). As was

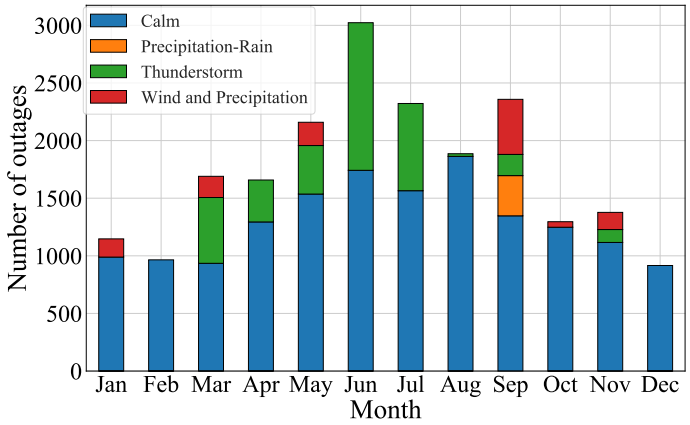

Figure 4.3: Outage frequency by month of the year and climatic description © 2021 IEEE

observed from the monthly plot, outages are most frequent are in the summer months and least frequent in winter. The lower number of outages during the winter could be attributed to the location of the the distribution network location, which typically experiences mild winters. However, this location experiences a significant number of tornadoes, hurricanes and thunderstorms, in the other three seasons. Hence, the number of outages in each of these seasons are at least 1.5 times as much as the number of outages in the winter.

Fig. 4.2(g) shows the number of outages by voltage level (kV) of the affected circuit. The most number of outages occur in the 12 kV circuits. Most of the circuits in the distribution network in this study operate at the 12 kV level.

Fig. 4.2(h) shows the number of outages per year. 2017 has the highest number of outages.

Fig. 4.4 presents plots of outage frequency with respect to temperature (°F), humidity (%) and wind speed (mph).

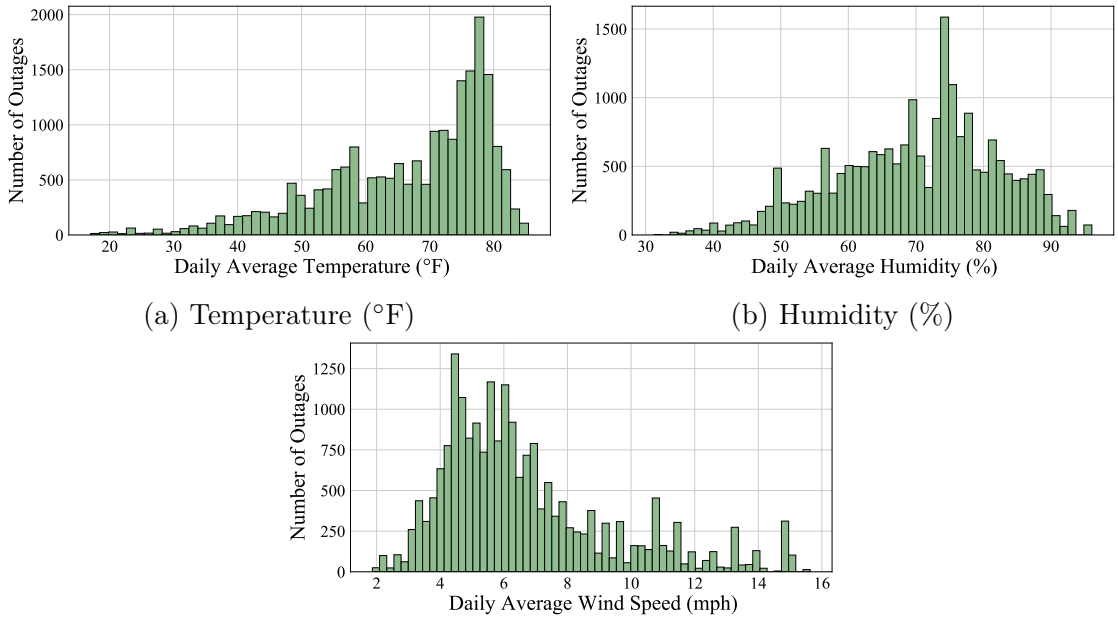

(a) Temperature (°F)

(b) Humidity (%)

(c) Wind Speed (mph)

Figure 4.4: Outage frequency with respect to weather variables

4.4.2 Average Outage Duration

This section presents a visual analysis for the average outage duration in minutes by each category in the outage dataset. The histogram in Fig. 4.5 shows the distribution of outage duration (in minutes) of outages in this analysis. As seen in the histogram, most of the outages last between 38 to 76 minutes. The shortest outages lasted for only 1 second, while the longest outage lasted for about 2 days. It is interesting to note that close to half of the outages lasted at least 2 hours or more. The average duration of all the outages in the dataset (indicated with a dashed line in Fig. 4.5) is around 3.5 hours (213 minutes to be precise).

Fig. 4.6(a) shows the average outage duration by climatic description. Although calm weather had maximum number of outages, the average duration of the outages during calm weather is the lowest. The maximum average outage duration is during wind & precipitation and thunderstorm. This could be due to the amount and severity of damage caused by severe weather events, hence leading to longer repair times and outage duration compared to outages that occur in calm weather.

Fig. 4.6(b) shows the average outage duration per weekday. Maximum average outage duration occurs on Saturday while the minimum occurs on Friday.

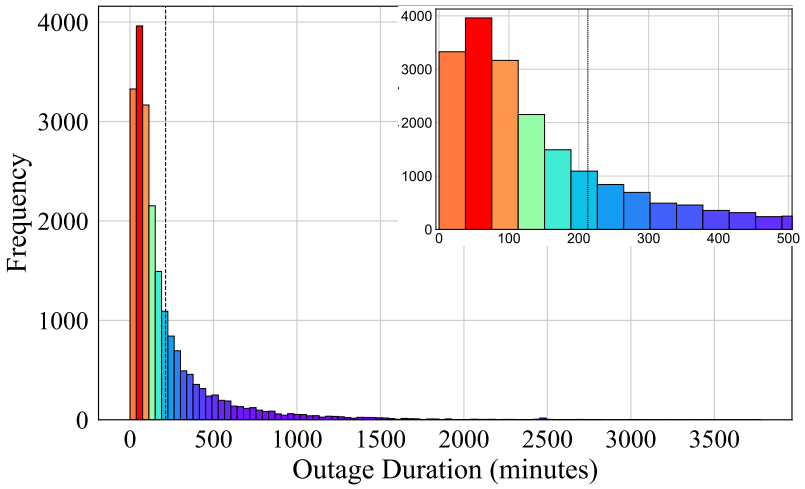

Figure 4.5: Histogram of outage duration (minutes) © 2021 IEEE

Fig. 4.6(c) categorizes the average outage duration by the interrupted phase. Although outages affecting two phases simultaneously (AB, AC, BC) accounted for the lowest number of outages, they result in higher average outage durations as shown.

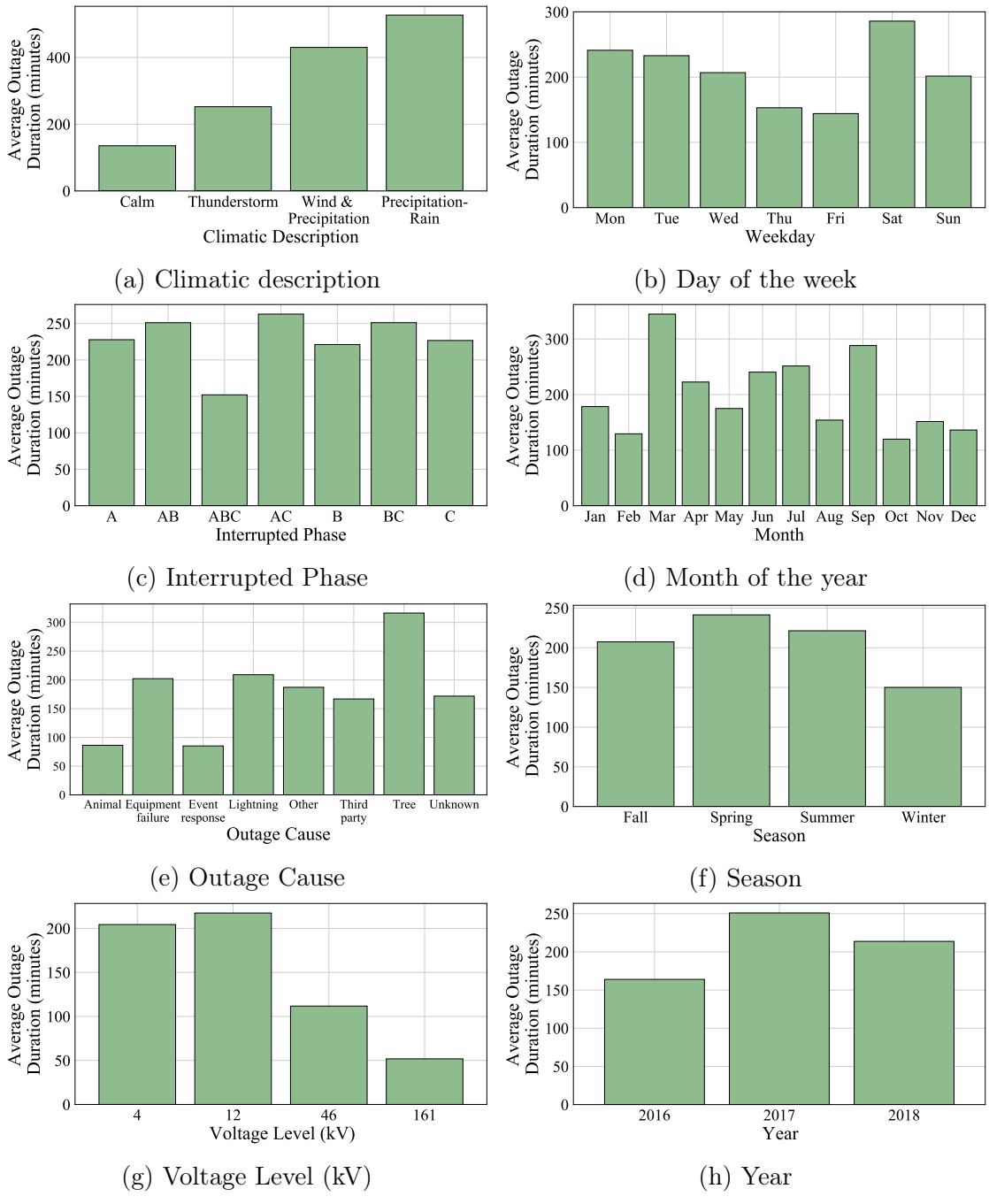

(a) Climatic description

(b) Day of the week

(c) Interrupted Phase

(d) Month of the year

(e) Outage Cause

(f) Season

(g) Voltage Level (kV)

(h) Year

Figure 4.6: Average outage duration (minutes) with respect to features in outage data set

On the other hand, outages affecting all three phases (ABC) account for the lowest outage duration.

Fig. 4.6(d) shows the average outage duration per month of the year. March has the highest average outage duration whereas October has the least average outage duration. It is interesting to note that although the month of March ranked 6th in the frequency of outages, it has the highest average outage duration. Further investigation reveals that this is due to long duration outages occuring during thunderstorms as well as wind and precipitation in March as shown in Fig. 4.7. The distribution of average outage duration by climatic description and by month of the year is presented in Fig. 4.7. September has the highest average outage duration during wind and precipitation.

Fig. 4.6(e) shows the average outage duration per outage cause. Outages caused by trees have the highest average outage duration, followed by outages caused by lightning and equipment failure.

Fig. 4.6(f) shows the average outage duration for each season. Spring and summer have higher average outage durations than the fall and winter.

Fig. 4.6(g) shows the average outage duration by voltage level in kV. It can be observed that average outage duration is higher for the 12 kV and 4 kV circuits

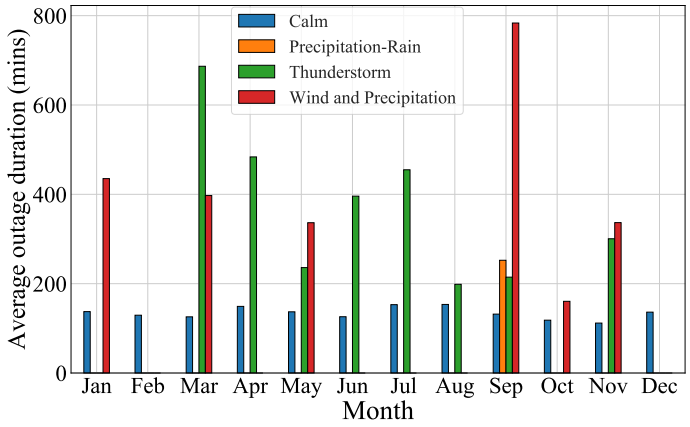

Figure 4.7: Average outage duration by month of the year and climatic description

compared to the 46 kV and 161 kV circuits.

Fig. 4.6(h) shows the average outage duration by year. 2017 has the highest average outage duration.

Table 4.3 presents a summary comparison of outage frequency and average outage duration for the features considered in this analysis. The results in the table show that the class with the most number of outages does not automatically account for the highest average outage duration. For example, with respect to the month of the year, the highest number of outages occurred in June, but March had the highest average outage duration. On the other hand, with respect to interrupted phase, outages affecting phases A and C simultaneously accounted for the least number of outages, but had the longest average outage duration.

4.5 Feature Importance

In addition to exploring outage frequency and average outage duration, this study seeks to determine the features or variables in the dataset that affect average outage duration. To rank the importance of each variable, two machine learning-based approaches are used: Random Forest Regressor and Gradient Boosting. Both techniques are implemented using Python's Scikit-Learn library [96]. Feature importance is estimated by calculating the ratio of the number of samples that get through to

Table 4.3: Outage frequency and duration for outage features © 2021 IEEE

	Number of Outages		***Average Outage Duration***	
Features	***Highest***	***Least***	***Longest***	***Shortest***
Voltage Level	12 kV	161 kV	12 kV	161 kV
Climatic Description	Calm	Precipitation (Rain)	Wind and Precipitation	Calm
Weekday	Monday	Friday	Saturday	Friday
Interrupted Phase	C	AC	AC	ABC
Month	June	December	March	October
Outage Cause	Tree	Third Party	Tree	Event Response
Season	Summer	Winter	Spring	Winter

a node to the total number of samples [97]. The more important the feature, the greater the value of its feature importance score.

4.5.1 Random Forest Regressor

Random Forest is a tree-based supervised learning algorithm introduced in [98]. The random forest algorithm is a bagging-based algorithm that takes the ensemble of randomly sampled trees [99]. A random Forest regressor-based model is used to rank the various features based on their importance. The random forecast model is trained using the entire outage dataset and the importance of each feature is estimated. The random forest model is modeled with 150 trees. The number of trees was selected by performing a grid search, varying the trees from 30 to 300 trees and comparing their prediction score.

Fig. 4.8(a) shows the feature importance as estimated by the random forest algorithm. It is observed that climatic description has the maximum importance followed by failed equipment and wind speed. Interrupted phase, outage cause and temperature are moderately important while humidity, month, weekday, voltage level, year and season have very low importance. In general, calendar variables like year, month, season and weekday have very less importance, showing that there is no significant seasonal pattern in the dataset used in this study.

4.5.2 Gradient Boosting Regressor

Gradient boosting regressor is a supervised learning algorithm introduced in [100]. As the name suggests, gradient boosting is a boosting-based approach that uses decision trees and selects the best trees using a gradient loss function [101]. The gradient boosting model is trained using the entire outage dataset and the importance of each feature is estimated. The gradient boosting model is modeled with 100 trees. The number of trees was selected by performing a grid search, varying the trees from 30 to 300 trees and comparing their prediction score.

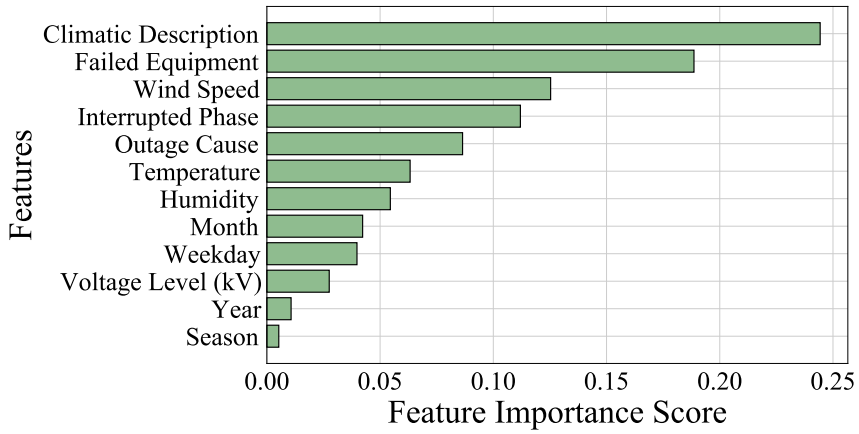

(a) Feature importance using random forest regressor

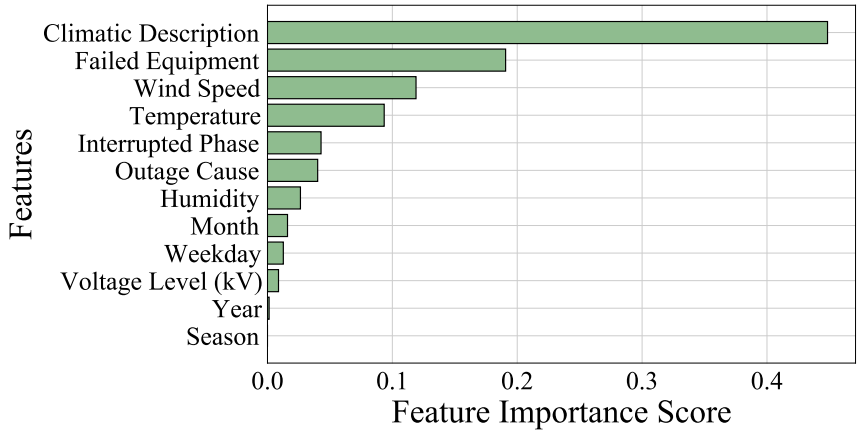

(b) Feature importance using gradient boosting regressor

Figure 4.8: Feature ranking using random forest and gradient boosting regressors

Fig. 4.8(b) shows the feature importance according to the gradient boosting algorithm. Consistent with results from the random forest model, climatic description has the highest importance, however the magnitude of importance is more, followed by failed equipment and wind speed. Temperature ranks higher than interrupted phase and outage cause; this is different from the results of the random forest model. Season, year, voltage level and weekday are the features with the least importance. Again, this shows that there is no significant seasonal pattern in the outage dataset used in this study.

4.6 Conclusion

This chapter presented an analysis of the frequency and average duration of outages in a distribution network using the frameworks presented in [90] and [91]. Also, random forests and gradient boosting regression are used to rank the importance of several features in predicting outage duration. The results from both regressors show that climatic description is the most significant feature for explaining the variability of outage duration for the distribution network considered in this study. Other significant features include: failed equipment, wind speed and interrupted phase. Future work will focus on data-driven probabilistic outage prediction using weather data.

CHAPTER 5: PROPOSED PROACTIVE TOPOLOGY OPTIMIZATION AND SERVICE RESTORATION FRAMEWORK

5.1 Overview

This chapter begins with a brief background on distribution system optimization, followed by a detailed presentation of the proposed topology optimization and service restoration scheme which leverages outage forecasts. By applying the proposed scheme, distribution system operators can minimize the loads left out of service due to predicted outages. This scheme is formulated as a MILP problem consisting of two stages: pre-outage proactive topology optimization and post-outage service restoration. A detailed mixed integer linear programming (MILP) formulation for these two stages is presented, after which three outage optimization cases are considered to implement the proposed scheme as follows: single outage, multiple outage, and weighted multiple outage.

5.2 Distribution System Optimization

Distribution system optimization entails finding the most efficient way to operate the distribution system in order to achieve a certain objective or set of objectives within specific constraints. In [102], distribution system optimization problems were broadly categorized into operations and planning problems. Distribution system operations problems include: network reconfiguration, optimal power flow, volt-var optimization, demand side management and electric vehicle charging. On the other hand, distribution system planning problems include: distribution network planning, capacitor placement, meter placement, and distributed generation (DG) planning.

Distribution system optimization problems primarily consist of an objective func-

tion, $f(X)$ (which is minimized or maximized), as well as a set of decision variables, X, and constraints. They are typically formulated as follows:

$$\min / \max \ f(X) \tag{5.1a}$$

$$\text{s.t. } g(X) \ = \ 0 \tag{5.1b}$$

$$h(X) \ \leq \ 0 \tag{5.1c}$$

where $f(X)$ represents the objective function, $g(X)$ represents the set of equality constraints, $h(X)$ represents the set of inequality constraints, and X represents the set of decision variables, $\{x_1, x_2, \ldots, x_n\}$ which optimize the objective function while satisfying the given constraints.

Common objectives in distribution system optimization problems include minimizing power losses, load unbalance, capacitor costs, voltage deviation, fuel costs or investment costs. Similarly, the objective could be maximizing the total load served or savings from reduced energy and peak power losses in the distribution network. Some problems may have more than one objective, which would result in a multi-objective optimization problem. In the case of service restoration, for example, the objectives may be to minimize power losses, out-of-service loads, and the number of switching operations [77].

Decision variables in distribution optimization problems may vary depending on the problem: they may be continuous variables or discrete variables. In network reconfiguration and service restoration problems, for example, real and reactive line flows are normally continuous variables, whereas switch status is typically modeled as a binary variable, $x \in \{0, 1\}$. In addition to the line flows and switch status, other decision variables include the location to place capacitors, DG or meters in the network as well as the size of the capacitors or DGs to install in the network.

Furthermore, distribution system optimization problems require the solution of

power flow equations, which are represented as equality and inequality constraints in the formulation. Equations relating to power flow, such as the real and reactive power balance, are incorporated as equality constraints. Operational limits such as voltage limits, current limits or generator real and reactive power limits are represented as inequality constraints. Inequality constraints can also represent resource constraints (such as the number of capacitors or meters available for installation in capacitor or meter placement problems) in the optimization problem.

Equations (5.2) to (5.3) present commonly used equality and inequality constraints derived from a simple mathematical formulation of a distribution system optimization problem presented in [79].

$$P_i^G + \sum_{h=1}^{n} P_{hi} = \sum_{j=1}^{n} P_{ij} + \sum_{j=1}^{n} P_{ij}^{losses} + P_i^L \tag{5.2a}$$

$$Q_i^G + \sum_{h=1}^{n} Q_{hi} = \sum_{j=1}^{n} Q_{ij} + \sum_{j=1}^{n} Q_{ij}^{losses} + Q_i^L \tag{5.2b}$$

$$|V_j|^2 - |V_i|^2 = 2(R_{ij}P_{ij} + X_{ij}Q_{ij}) - (R_{ij}^2 + X_{ij}^2)|I_{ij}|^2 \tag{5.2c}$$

$$V_i^{min} \leq V_i \leq V_i^{max} \tag{5.3a}$$

$$|I_{ij}| \leq |I_{ij}^{max}| \tag{5.3b}$$

Equations (5.2a) and (5.2b) represent real and reactive power balance equations for each bus in the network, and (5.2c) represents the voltage drop along each branch ij of the network. P_i^G and Q_i^G are the real and reactive powers generated at bus i. P_i^L and Q_i^L are the real and reactive load demand at bus i, respectively. P_{ij} and Q_{ij} are the real and reactive power flows through line ij. P_{ij}^{losses} and Q_{ij}^{losses} are the real and reactive power losses in line ij. $|V_i|$ represents the voltage magnitude at bus i, R_{ij} and X_{ij} represent the resistance and reactance of branch ij, respectively,

and $|I_{ij}|$ is the magnitude of current flowing through branch ij. Equations (5.3a) and (5.3b) represent constraints on the bus voltages and line currents, respectively. During normal operation, bus voltages are usually limited between 0.95p.u. and 1.05p.u, that is, $V_i^{min} = 0.95p.u.$ and $V_i^{max} = 1.05p.u.$ [103] while line current or power is limited by the capacity of the line or transformer.

Radiality constraints are often used in distribution system optimization problems since distribution networks are typically operated in radial configurations to ensure effective protection coordination [104]. A significant amount of critical attention has been focused on modeling of radiality in distribution systems, particularly in network reconfiguration and service restoration problems. Radiality is further complicated by the increase in DGs and microgrids, which could result in bidirectional power flow in the distribution network. To enforce radiality, several methods have been applied, including heuristics, metaheuristics, and mathematical models. Additionally, graph theory has been used to enforce radiality, since the distribution network can be viewed as a graph, $G(\mathcal{V}, \mathcal{E})$ consisting of vertices (or nodes), $\mathcal{V}$ and edges (or branches), $\mathcal{E}$. Several works in literature have incorporated the radiality constraint into mathematical models using only (5.4) as follows:

$$\mathcal{N}_{\mathcal{E}} = \mathcal{N}_{\mathcal{V}} - \mathcal{N}_{\mathcal{S}} \tag{5.4}$$

where $\mathcal{N}_{\mathcal{E}}$ represents the number of active edges/lines in the network, $\mathcal{N}_{\mathcal{V}}$ is the number of vertices/nodes in the network and $\mathcal{N}_{\mathcal{S}}$ is the number of substations.

Recent studies have demonstrated that while (5.4) is a necessary condition for radiality in a distribution network, it is insufficient for enforcing radiality. Using only (5.4) could still result in a disconnected system with loops. Hence, additional constraints are required to ensure radiality in the distribution network as illustrated in [104–107]. [106] summarizes some methods for expressing radiality constraints in network reconfiguration problems; it also proposes a method for enforcing radiality

using graph theory concepts.

Several methods have been proposed and applied to solving distribution system optimization problems. Among these methods are heuristics (such as the branch exchange method presented in [80]), metaheuristics (such as genetic algorithm, simulated annealing and particle swarm optimization), hybrid methods and mathematical programming. Some mathematical programming models used include: mixed integer linear programming (MILP), mixed integer non-linear programming (MINLP), mixed integer second-order cone programming (MISOCP), and mixed integer quadratic programming (MIQP).

In distribution optimization problems, it is necessary to solve the power flow equations. However, due to its complexity, nonconvexity and nonlinearity, the AC power flow formulation requires a high level of computational effort. Moreover, the distribution system is inherently unbalanced, which necessitates three-phase modeling; this further complicates the computation of AC power flow. To approximate the nonlinearity of AC power flow in distribution systems, linear power flow formulations have been developed; these models reduce the computational burden of the nonlinear power flow model and can be efficiently solved with commercial solvers such as CPLEX and Gurobi [108] or open-source solvers such as SCIP [109] and CBC [110].

Several linear formulations including the DC power flow model have been proposed in literature for solving power flow in distribution system optimization methods [111,112]. MILP models often use the linearized version of the DistFlow equations (popularly known as LinDistFlow model) introduced by Baran and Wu in [80, 113]. In the LinDistFlow formulation, the loss terms in (5.2) are ignored since they are much smaller than the branch power terms. Hence, (5.2) is modified as follows:

$$P_i^G + \sum_{h=1}^{n} P_{hi} \;=\; \sum_{j=1}^{n} P_{ij} + P_i^L \tag{5.5a}$$

$$Q_i^G + \sum_{h=1}^{n} Q_{hi} \;=\; \sum_{j=1}^{n} Q_{ij} + Q_i^L \tag{5.5b}$$

$$U_j - U_i \;=\; 2(R_{ij}P_{ij} + X_{ij}Q_{ij}) \tag{5.5c}$$

where U_i and U_j represent the square of the voltage magnitude at buses i and j respectively. The LinDistFlow equations are used in the MILP formulation of the proposed proactive topology optimization and service restoration scheme presented in Section 5.3.2.

5.3 Proactive Topology Optimization and Service Restoration Framework

Chapter 2 discussed the need for a proactive approach to service restoration that harnesses insights from outage prediction models (OPMs) to enhance resilience in the distribution system. Consequently, this chapter presents a proactive topology optimization and service restoration framework that enhances data-driven outage prediction and analysis.

1. Prior to a predicted outage, the proposed framework prescribes a topology that minimizes loads that would be left out of service if the outage occurs in the distribution network.

2. If an outage is unavoidable and occurs as predicted, the framework prescribes a topology to maximize the loads restored in the distribution network during service restoration.

The proposed framework (illustrated in Fig. 5.1) provides a holistic approach to outage management that integrates outage prediction with service restoration instead of treating both processes as silos. In most studies, the interaction between outage prediction and service restoration is not taken into consideration, but in reality, service restoration depends on processes, such as outage prediction, that precede it during outage management. Hence, the proposed framework in this work considers how to

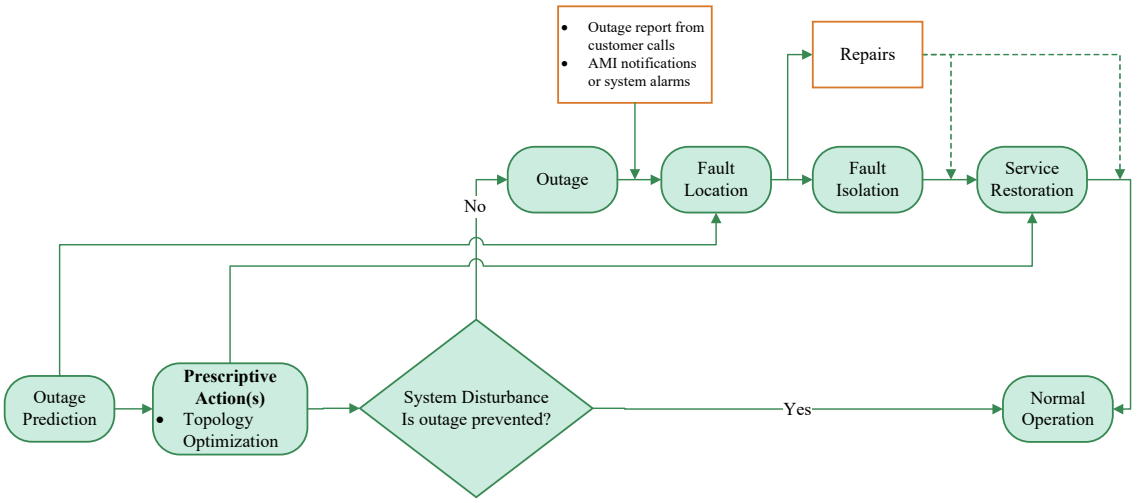

Figure 5.1: Proposed proactive outage management approach

transform outage forecasts into operational decisions regarding service restoration in the distribution network [86].

The framework assumes that the outage locations are provided from an outage prediction model (OPM). The OPM provides forecasts of possible outage locations in the distribution network using historical weather and outage data along with geographical information and weather forecasts. Although the design and details of OPM are beyond the scope of this dissertation, the following paragraphs provide a brief overview of how it interacts with the proposed proactive topology optimization and service restoration scheme.

The OPM produces forecasts of outage scenarios in the distribution network using inputs such as historical weather and outage data, geographic information, and customer information. Historical weather data could include measurements of wind speed, temperature, humidity, wind gust among others. Other possible inputs to the OPM include vegetation and social media information. As discussed in Chapters 2 and 4, trees often account for a large portion of outages, hence vegetation information could serve as valuable input to the OPM, especially if the distribution network is located in a woody geographical area. In the same vein, studies have demonstrated

the use of social media for outage detection purposes. The studies in [55, 114–116] demonstrated the use of tweets for power outage detection. Feature importance can be implemented as shown in Chapter 4 to determine which input variables contribute most to the predictive performance of the OPM.

Due to the uncertainty associated with weather forecasts and failure of distribution system components, a probabilistic OPM is assumed. In literature, probabilistic outage models have been developed to estimate the impact of outages caused by severe weather on distribution networks. The studies in [21,37–40] present OPMs to predict the impact of outages caused by severe weather such as thunderstorms, ice storms and hurricanes. [21, 39, 40] use tree-based machine learning models, whereas [37, 38] use generalized linear mixed models and negative binomial regression, respectively.

Outage scenarios could be generated using Monte Carlo simulations based on failure rates or fragility curves of grid components. This is done using the probability of severe weather along with the probability of asset failure due to severe weather. In [117], to estimate overhead distribution line failure rates, Monte Carlo simulations were used to estimate the prediction bounds of Poisson regressions and Bayesian network models. Similarly, [22] used weather radar measurements to simulate failure rates for grid assets with a Bayesian-based outage prediction model.

The outage scenarios generated from the OPM can assist distribution system operators in making decisions related to service restoration, including proactive topology optimization, crew coordination and dispatch planning, and resource allocation. The OPM could provide insights into distribution system equipment on the verge of failure, allowing operators to plan accordingly. This work assumes that the OPM generates a forecast of distribution lines (referred to as predicted outage locations in this work) likely to be impacted by severe weather or equipment failure in the distribution system. These lines are assumed to represent outage locations in the topology optimization and service restoration framework presented in the following sections.

5.3.1 Nomenclature

Sets

$\mathcal{B},\ \mathcal{B}_F,\ \mathcal{B}_S,\ \mathcal{V}_R$	Set of branches, subset of predicted outage locations, subset of switchable branches, subset of voltage regulators
$\mathcal{G}$	Set of generators
$\mathcal{L}$	Set of loads
$\mathcal{N},\ \mathcal{N}(i)$	Set of nodes, subset of nodes connected to node i

Binary Variables [0 - Disconnected/Offline, 1 - Energized/Online]

s_g^N	Status of the node to which generator g is connected
s_i^N	Status of node i
s_l^N	Status of the node to which load l is connected
x_g^G	Status of generator g
x_{ij}^{BR}	Status of branch/section ij
x_l^L	Status of load l

Continuous Variables

$P_{ij}^{BR},\ Q_{ij}^{BR}$	Real and reactive power flowing through branch/section ij
$P_i^G,\ Q_i^G$	Real and reactive power generated at node i
$P_i^L,\ Q_i^L$	Real and reactive power demand at node i
U_i	Square of the magnitude of voltage at node i

Parameters

a_{ij}	Effective regulator ratio of voltage regulator across section ij
M	Big-M
$P_g,\ Q_g$	Real and reactive power output of generator g

$P_g^{min},\ P_g^{max}$	Minimum and maximum real power rating of generator g
$Q_g^{min},\ Q_g^{max}$	Minimum and maximum reactive power rating of generator g
$P_l^{nom},\ Q_l^{nom}$	Nominal real and reactive power rating of load l
$r_{ij},\ \mathrm{x}_{ij}$	Resistance and reactance of branch ij
S_{ij}^{max}	Maximum kVA rating of branch/section ij
$V_i^{min},\ V_i^{max}$	Minimum and maximum voltage magnitude limits at node i

5.3.2 Mixed Integer Linear Programming (MILP) Problem Formulation

This work proposes a proactive topology optimization and service restoration framework that leverages outage forecasts to improve outage management in the distribution system. This involves prescribing switching actions that reduce the impact of predicted outages on the system by 1) minimizing the kW amount of loads that would be affected if the outage occurs and 2) maximizing the kW amount of load restored to the network after the outage. Both objectives are achieved through network reconfiguration using switchable lines in the network, resulting in optimal topologies for the network in both cases.

To find the optimal network topology, the proactive topology optimization and service restoration problem is formulated using mixed integer linear programming (MILP). The MILP formulation is adapted from [64]. The objectives of the problem are presented as follows:

1. Proactive Topology Optimization: In this stage of the framework, the distribution network is reconfigured using switchable lines so that the total load left out of service if the predicted outage occurs is minimized. This is achieved by minimizing the power flowing through the predicted outage locations as follows:

$$OF_1 : \min \sum |P_{ij}^{BR}| \qquad (i,j) \in \mathcal{B}_F \tag{5.6}$$

where P_{ij}^{BR} is the power flowing through branch ij and $\mathcal{B}_F$ is the set of predicted outage locations in the system. As previously mentioned, the predicted outage locations are assumed to be lines in the network. The objective function in (5.6) is linearized by introducing an auxiliary variable, z_{ij} to eliminate the absolute value function as follows:

$$\min \sum z_{ij}^{BR} \qquad (i,j) \in \mathcal{B}_F \tag{5.7a}$$

$$\text{s.t. } z_{ij} \geq P_{ij}^{BR} \qquad (i,j) \in \mathcal{B}_F \tag{5.7b}$$

$$z_{ij} \geq -P_{ij}^{BR} \qquad (i,j) \in \mathcal{B}_F \tag{5.7c}$$

The topology optimization stage could result in a new operational topology for the distribution network, if the new topology reduces the potential unserved loads in the original topology.

2. Service Restoration: In this stage, the distribution network is reconfigured using switchable lines to maximize the total amount of loads left in service (restorable loads) after the outage occurs at the predicted locations. This is represented below:

$$OF_2 : \max \sum_{i=1}^{n} x_i^L P_i^L \qquad i \in \mathcal{N} \tag{5.8}$$

where x_i^L is the status of the load connected to bus i, P_i^L is the load demand in kilowatts on the ith bus, and n represents the number of buses in the system.

The constraints considered in the MILP formulation are as follows:

1. Linear DistFlow Constraints: Distribution network power flow is solved using the linear DistFlow equations introduced in [80]. The nodal power balance equations are represented by equality constraints (5.9a) and (5.9b). Reactive power injection from capacitors in the distribution network is represented as reactive power generation, Q_i^G in constraint (5.9a). Inequality constraints (5.9c)

and (5.9d) ensure that only energized lines have power flowing through them. Constraints (5.9e) and (5.9f) are linear approximations of the power loss on each branch, $ij \in \mathcal{B}\backslash\mathcal{V}_R$, of the network, and they represent the voltage magnitude difference between the nodes, i and j of each energized branch (excluding voltage regulators). The big-M formulation [118] is used to activate or deactivate constraints (5.9c)–(5.9f) depending on the status, x_{ij}^{BR} of each line.

$$\sum_{h:(h,i)\in\mathcal{B}} P_{hi}^{BR} + P_i^G = \sum_{j:(i,j)\in\mathcal{B}} P_{ij}^{BR} + P_i^L \qquad i \in \mathcal{N} \tag{5.9a}$$

$$\sum_{h:(h,i)\in\mathcal{B}} Q_{hi}^{BR} + Q_i^G = \sum_{j:(i,j)\in\mathcal{B}} Q_{ij}^{BR} + Q_i^L \qquad i \in \mathcal{N} \tag{5.9b}$$

$$-M \cdot x_{ij}^{BR} \leq P_{ij}^{BR} \leq M \cdot x_{ij}^{BR} \qquad (i,j) \in \mathcal{B} \tag{5.9c}$$

$$-M \cdot x_{ij}^{BR} \leq Q_{ij}^{BR} \leq M \cdot x_{ij}^{BR} \qquad (i,j) \in \mathcal{B} \tag{5.9d}$$

$$U_i - U_j \;\leq\; 2(r_{ij} \cdot P_{ij}^{BR} \;+\; \mathrm{x}_{ij} \cdot Q_{ij}^{BR}) \;+\; M(1 - x_{ij}^{BR}) \quad (i,j) \in \mathcal{B}\backslash\mathcal{V}_R \tag{5.9e}$$

$$U_i - U_j \;\geq\; 2(r_{ij} \cdot P_{ij}^{BR} \;+\; \mathrm{x}_{ij} \cdot Q_{ij}^{BR}) \;-\; M(1 - x_{ij}^{BR}) \quad (i,j) \in \mathcal{B}\backslash\mathcal{V}_R \tag{5.9f}$$

$$-\; M(1 - x_{ij}^{BR}) \;\leq\; a_{ij}^2 \cdot U_j - U_i \;\leq\; M(1 - x_{ij}^{BR}) \qquad (i,j) \in \mathcal{V}_R \tag{5.9g}$$

Constraint (5.9g) represents the voltage magnitude difference on the both sides of a voltage regulator. The voltage regulators in the system are modeled using the Type B step-voltage regulator model in [119]. The effective regulator ratio, a is given by:

$$a = 1 + 0.00625 n^{tap} \tag{5.10}$$

where $n^{tap} \in \{-16, -15, ..., +15, +16\}$ is the tap position of the voltage regulator. Tap positions are assumed to be fixed for each voltage regulator in this work.

2. Load Model: The loads in the system are modeled as constant power (constant PQ). For energized loads (load status, $x_l^L = 1$), active and reactive load de-

mands, P_i^L and Q_i^L, are equal to nominal load ratings, P_l^{nom} and Q_l^{nom}, while power demand is zero for de-energized loads ($x_l^L = 0$). This is represented in (5.11) below:

$$P_i^L = x_l^L \cdot P_l^{nom} \qquad i \in \mathcal{N},\ l \in \mathcal{L} \tag{5.11a}$$

$$Q_i^L = x_l^L \cdot Q_l^{nom} \qquad i \in \mathcal{N},\ l \in \mathcal{L} \tag{5.11b}$$

3. Transformer and Line Loading Limits: The transformers and lines must be operated within their rated kVA capacity limits, S_{ij}^{max} as shown in (5.12).

$$\left(P_{ij}^{BR}\right)^2 + \left(Q_{ij}^{BR}\right)^2 \le \left(S_{ij}^{max}\right)^2 \qquad (i,j) \in \mathcal{B} \tag{5.12}$$

Constraint (5.12) is linearized as shown in [64, 120] to yield the following linear constraints:

$$-\sqrt{3}(P_{ij}^{BR} + S_{ij}) \le Q_{ij}^{BR} \le -\sqrt{3}(P_{ij}^{BR} - S_{ij}) \qquad (i,j) \in \mathcal{B} \tag{5.13a}$$

$$\big(-\sqrt{3}/2\big)S_{ij} \le Q_{ij}^{BR} \le \big(\sqrt{3}/2\big)S_{ij} \qquad (i,j) \in \mathcal{B} \tag{5.13b}$$

$$\sqrt{3}(P_{ij}^{BR} - S_{ij}) \le Q_{ij}^{BR} \le \sqrt{3}(P_{ij}^{BR} + S_{ij}) \qquad (i,j) \in \mathcal{B} \tag{5.13c}$$

4. Voltage Limits: Node voltages should be maintained within the acceptable limits of 0.95 and 1.05 p.u [103]. U_i represents the square of the magnitude of the voltage at node i.

$$s_i^N \cdot \big(V_i^{min}\big)^2 \le U_i \le s_i^N \cdot \big(V_i^{max}\big)^2 \qquad i \in \mathcal{N} \tag{5.14}$$

5. Switching Limits: To avoid mechanical wear and tear of the switches, the num-

ber of switching operations, n_s, is limited as follows:

$$\sum \left| x_{ij}^{BR} - x_{ij}^{BR_0} \right| \leq n_s \qquad (i,j) \in \mathcal{B}^S \tag{5.15}$$

where $x_{ij}^{BR_0}$ represents the initial status of switchable line ij, x_{ij}^{BR} is the status of switchable line ij after topology optimization, and n_s is the number of switching operations allowed. Constraint (5.15) is linearized by introducing an auxiliary variable, y_{ij} as follows:

$$\sum y_{ij} \leq n_s \qquad (i,j) \in \mathcal{B}^S \tag{5.16a}$$

$$y_{ij} \geq x_{ij}^{BR} - x_{ij}^{BR_0} \qquad (i,j) \in \mathcal{B}^S \tag{5.16b}$$

$$y_{ij} \geq x_{ij}^{BR_0} - x_{ij}^{BR} \qquad (i,j) \in \mathcal{B}^S \tag{5.16c}$$

6. Connectivity Constraints: These constraints ensure connectivity among energized components (nodes, lines and loads) in the network. Also, they determine which components should be connected during the topology optimization and service restoration process [64].

$$s_g^N = x_g^G \qquad g \in \mathcal{G} \tag{5.17a}$$

$$x_{ij}^{BR} \leq s_i^N \qquad (i,j) \in \mathcal{B}^S \backslash \mathcal{B}^F \tag{5.17b}$$

$$x_{ij}^{BR} \leq s_j^N \qquad (i,j) \in \mathcal{B}^S \backslash \mathcal{B}^F \tag{5.17c}$$

$$x_{ij}^{BR} = s_i^N = s_j^N \qquad (i,j) \in \mathcal{B} \backslash (\mathcal{B}^S \cup \mathcal{B}^F) \tag{5.17d}$$

$$x_l^L = s_l^N \qquad l \in \mathcal{L} \backslash \mathcal{L}^F \tag{5.17e}$$

In (5.17a), a node will be energized if it is connected to the substation node (or a node with a generator). In constraints (5.17b) and (5.17c), a switchable line, x_{ij}^{BR} will be energized when both its nodes, i and j are energized, that is s_i^N

and s_j^N are both equal to 1. On the other hand, a non-switchable line will be restored when either of its nodes are restored as shown in (5.17d). A load will be energized when connected to an energized node as shown in (5.17e).

7. Radiality Constraints: The topology resulting from the topology optimization and service restoration process must be radial. To gurarantee radiality, the following two conditions must be met: 1) the resulting topology should have no loops and 2) every node in the resulting topology asides the substation node, $\mathcal{N}_g$ should have only one parent [104].

$$\sum_{i\in\mathcal{N}} s_i^N \; - \; \sum_{(i,j)\in\mathcal{B}} x_{ij}^{BR} \; = \; \sum_{g\in\mathcal{G}} x_g^G \tag{5.18a}$$

$$b_{ij} \; + \; b_{ji} \; = \; x_{ij}^{BR} \qquad (i,j)\in\mathcal{B} \tag{5.18b}$$

$$\sum_{j\in\mathcal{N}(i)} b_{ij} \; = \; 1 \qquad i\in\mathcal{N}\backslash N_g \tag{5.18c}$$

$$b_{ij} \; = \; 0 \qquad i\in\mathcal{N}_g,\; j\in\mathcal{N}(i) \tag{5.18d}$$

Equations (5.18) ensure that every node except the substation node has exactly one parent node. Equation (5.18d) is enforced for the substation node, since it has no parents. In the second stage (that is, service restoration), (5.18c) is modified to allow for isolation of parts of the network affected by the outage as follows:

$$0 \; \leq \; \sum_{j\in\mathcal{N}(i)} b_{ij} \; \leq \; 1 \qquad i\in\mathcal{N}\backslash N_g \tag{5.19}$$

8. Other constraints are included in the problem as follows:

   (a) The substation node is energized throughout the topology optimization and service restoration process as shown in (5.20a), and its voltage, U_g is

regulated at U_s in (5.20b).

$$x_g^G = 1 \qquad g \in \mathcal{G} \tag{5.20a}$$

$$U_g = U_s \qquad g \in \mathcal{G} \tag{5.20b}$$

(b) Every node should be operational in the optimal topology resulting from the proactive topology optimization stage, since this is done prior to the outage occurring.

$$s_i^N = 1 \qquad i \in \mathcal{N} \tag{5.21}$$

(c) The constraint in (5.21) is relaxed in the service restoration stage, since some sections of the distribution network may be disconnected as a result of the predicted outages.

$$s_i^N \leq 1 \qquad i \in \mathcal{N} \tag{5.22}$$

(d) In addition, the predicted outage locations must remain operational during the proactive topology optimization stage unless they are switchable lines. Predicted outage locations that are switchable lines may remain energized or de-energized during proactive topology optimization to allow for more topology flexibility.

$$x_{ij}^{BR} = 1 \qquad (i,j) \in \mathcal{B}^F \backslash \mathcal{B}^S \tag{5.23}$$

(e) On the other hand, the status of the predicted outage locations during the service restoration process are assumed to be zero. It is assumed that the predicted outage locations are disconnected or isolated as a result of the

outage. This is represented as follows:

$$x_{ij}^{BR} = 0 \qquad (i,j) \in \mathcal{B}^F \tag{5.24}$$

The above MILP formulation for the proposed topology optimization and service restoration framework can be summarized as follows:

1. Proactive Topology Optimization

   Minimize $\sum z_{ij}^{BR} \quad \forall \ (i,j) \in \mathcal{B}_F$ *subject to*:

   (a) Constraints (5.7b) and (5.7c)

   (b) Linear DistFlow constraints given by (5.9)

   (c) Load limits given by (5.11)

   (d) Transformer and line loading limits given by (5.13a) to (5.13c)

   (e) Voltage limits given by (5.14)

   (f) Switching limits given by (5.16)

   (g) Connectivity constraints given by (5.17)

   (h) Radiality constraints given by (5.18a) to (5.18d), and

   (i) Other constraints given by (5.20), (5.21) and (5.23)

2. Service Restoration

   Maximize $\max \sum_{i=1}^{n} x_i^L P_i^L \quad \forall \ i \in \mathcal{N}$ *subject to*:

   (a) Linear DistFlow constraints given by (5.9)

   (b) Load limits given by (5.11)

   (c) Transformer and line loading limits given by (5.13a) to (5.13c)

   (d) Voltage limits given by (5.14)

   (e) Switching limits given by (5.16)

(f) Connectivity constraints given by (5.17)

(g) Radiality constraints given by (5.18a), (5.18b), (5.18d), and (5.19)

(h) Other constraints given by (5.20), (5.22) and (5.24)

5.4 Outage Optimization Cases

The previous section presented the MILP formulation of the proposed proactive topology optimization and service restoration framework. In this section, three outage optimization cases are considered for implementing the proposed framework: single outage, multiple outage and weighted multiple outage cases. These cases are summarized in Fig. 5.2 below and explained in detail in the following subsections.

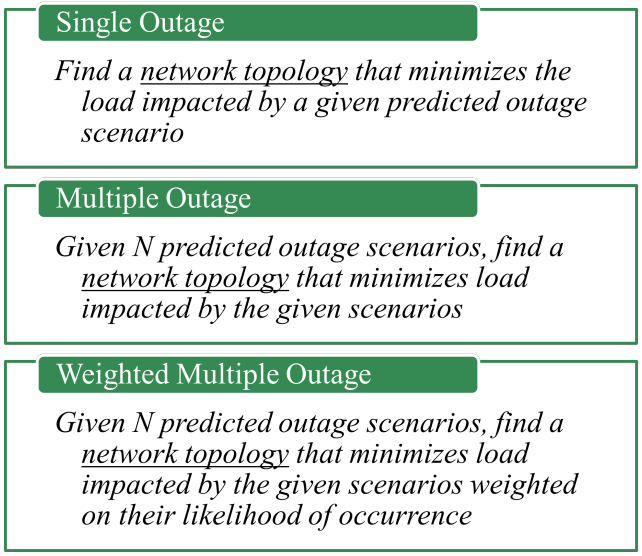

Figure 5.2: Summary of outage optimization cases

5.4.1 Single Outage Case

In the single outage case, each predicted outage scenario is considered individually, and the proposed topology optimization and service restoration framework is applied to each predicted outage scenario. It is assumed that outage scenarios are generated from an OPM, as mentioned in Section 5.3. In the single outage case, there may be one or more predicted outage locations (POLs) impacted in an outage scenario. In

other words, one or more lines or sections of the distribution network may be affected by an outage simultaneously.

The proposed topology optimization and service restoration process proceeds as follows. First, the topology optimization stage will find a topology that minimizes the loads left unserved (or out of service) in the event of the predicted outage, as indicated in (5.6). Using the MILP formulation presented in the previous section, this objective is achieved by minimizing the amount of power flowing through the predicted outage locations. If the original network topology is not optimal, a new topology would result from this stage. The new topology results from changing the status of switchable lines in the distribution system.

Having optimized the topology before the outage, the service restoration stage will focus on maximizing the restored load when the outage occurs as predicted. The predicted outage locations are now out of service, and the goal is to reconfigure the system to maximize the restored loads, as indicated in (5.8). Depending on the extent of the outage, some loads may be left unrestored in the service restoration stage. For example, loads that have only one supply path from the substation might be left unrestored if that path is affected by the outage.

5.4.2 Multiple Outage Case

The multiple outage case optimizes for several outage scenarios at the same time. The proposed topology optimization and service restoration framework is applied to minimize the impact of outages across these different scenarios. An outage scenario in the multiple outage case may affect one or more predicted outage locations simultaneously, just as in the single outage case.

In the multiple outage case, the proactive topology optimization process seeks to find an optimal topology, T_{opt}, that minimizes the total out-of-service loads across a set of two or more predicted outage scenarios. In the service restoration process, the aim is to determine the optimal topology that maximizes the load restored across the

set of predicted outage scenarios. The following paragraphs explain how the proposed framework is applied in the multiple outage case.

First, the MILP formulation presented in Section 5.3.2 is used to determine the optimal topology $T_i \ \forall \ i \in \{1, 2, ..., m\}$ that minimizes the out-of-service loads, L_{ij}, for each predicted outage scenario, S_j. L_{ij} represents the out-of-service loads or unserved demand (in kilowatts) in network topology T_i if outage scenario S_j occurs as predicted. For example, when outage scenario S_1 occurs in the distribution network, T_1 is the topology that results in the lowest out-of-service loads, L_{11}. While operating in topology T_1, L_{12} represents the out-of-service loads (in kilowatts) resulting from outage scenario S_1.

For n predicted outage scenarios, we may obtain up to n network topologies. However, in a case where the same topology is optimal for more than one outage scenario, the number of network topologies would be less than n. In summary, for n predicted outage scenarios and m optimal topologies, $m \times n$ values of out-of-service loads are obtained as shown in Table 5.2. Each scenario S_j results in the least amount out-of-service loads, L_{ij}, over all topologies when $i = j$. Hence, the diagonal terms, L_{11}, L_{22} and so on, are the minimum across the topologies considered in Table 5.2 for scenarios S_1, S_2 and so on.

To determine the optimal topology for the considered predicted scenarios, ΔL_{ij} is

Table 5.2: Multiple outage case: Out-of-service loads

Scenario	**Topology**			
	$\mathbf{T}_1$	$\mathbf{T}_2$	$\cdots$	$\mathbf{T}_m$
S_1	L_{11}	L_{21}	$\cdots$	L_{m1}
S_2	L_{12}	L_{22}	$\cdots$	L_{m2}
$\vdots$	$\vdots$	$\vdots$	$\ddots$	$\vdots$
S_n	L_{1n}	L_{2n}	$\cdots$	L_{mn}

Table 5.3: Computing additional out-of service loads to determine the optimal topology in the multiple outage case

Scenario	**Topology**			
	$\mathbf{T}_1$	$\mathbf{T}_2$	$\cdots$	$\mathbf{T}_m$
S_1	ΔL_{11}	ΔL_{21}	$\cdots$	ΔL_{m1}
S_2	ΔL_{12}	ΔL_{22}	$\cdots$	ΔL_{m2}
$\vdots$	$\vdots$	$\vdots$	$\ddots$	$\vdots$
S_n	ΔL_{1n}	ΔL_{2n}	$\cdots$	ΔL_{mn}
Average Cost	$\frac{1}{n}(\Delta L_{11} + \Delta L_{12} + \cdots + \Delta L_{1n})$	$\frac{1}{n}(\Delta L_{21} + \Delta L_{22} + \cdots + \Delta L_{2n})$	$\cdots$	$\frac{1}{n}(\Delta L_{n1} + \Delta L_{n2} + \cdots + \Delta L_{mn})$

obtained for all combinations of topology T_i and outage scenario, S_j as follows:

$$\Delta L_{ij} \;=\; L_{ij} \;-\; L_{ii} \tag{5.25}$$

When outage scenario S_j occurs, ΔL_{ij} represents the cost of not operating in the optimal topology T_i. In other words, $\Delta L_{ij}\ \forall\ i \neq j$ is the additional load left out of service while operating in a suboptimal topology T_i during outage scenario S_j. For instance in Table 5.3, if outage scenario S_2 occurs in the distribution network, ΔL_{12} represents the cost in kilowatts associated with operating in topology T_1. Topology T_2 is the optimal topology to operate in prior to outage scenario S_2; hence, operating in T_1, which is suboptimal for outage scenario S_2, would result in additional loads L_{12} being left out of service in the network.

It is worth noting that $\Delta L_{ij} = 0$ for cases where $i = j$. This is corresponds to operating in the optimal topology T_i, which results in the least amount of loads left out of service when outage scenario j occurs. Hence, the diagonal terms $\Delta L_{11}, \Delta L_{22}$ and so on in Table 5.3 are all equal to 0.

After obtaining ΔL_{ij} for all combinations of topologies and predicted outage sce-

narios, the average cost, C_i for each topology is calculated as follows:

$$C_i \;=\; \frac{1}{n} \cdot \sum_{j=1}^{n} \Delta L_{ij} \qquad \forall \;\; T_i \tag{5.26}$$

where n represents the number of outage scenarios, and ΔL_{ij} represents the cost (in kilowatts) associated with operating in a suboptimal topology, T_i for outage scenario S_j, as shown in (5.25). To eliminate the zero terms, that is $\Delta L_{ij} \;\forall\; i = j$, Equation (5.26) is rewritten as follows:

$$C_i \;=\; \frac{1}{n} \cdot \sum_{\substack{j=1 \\ j \neq i}}^{n} \Delta L_i^j \qquad \forall \;\; T_i \tag{5.27}$$

The topology T_i, with the lowest average cost C_i, across the n predicted outage scenarios as shown in Table 5.3, is chosen as the optimal topology, T_{opt}.

To illustrate the multiple outage case in practice, the case of a distribution network with three predicted outage scenarios from an OPM is presented in Table 5.4. As previously mentioned, each outage scenario could affect one or more locations (represented as line sections in this work) in the given distribution network. T_1, T_2 and T_3 represent the optimal distribution network topologies to operate in if outage scenarios S_1, S_2 and S_3 occur, respectively, as single outage cases. The diagonal terms, L_{11}, L_{22} and L_{33} are obtained from the first objective function, OF_1 of the MILP formulation in (5.6). They represent the out-of-service loads (in kilowatts) if the three predicted scenarios, S_1, S_2 and S_3 occur while operating in their respective optimal topologies, T_1, T_2 and T_3. The off-diagonal terms, $L_{ij} \;\forall\; i \neq j$, are obtained by estimating the loads left out of service due to outage scenario S_j while operating in topology T_i. For example, L_{12} represents the loads left out of service in topology T_1 in the event of outage scenario S_2.

Next, ΔL_{ij} is calculated for each topology and scenario using Equation (5.25). In

Table 5.4: Out-of-service loads in example multiple outage case with 3 predicted outages

Scenario	**Topology**		
	$\mathbf{T}_1$	$\mathbf{T}_2$	$\mathbf{T}_3$
S_1	L_{11}	L_{21}	L_{31}
S_2	L_{12}	L_{22}	L_{32}
S_3	L_{13}	L_{23}	L_{33}

Table 5.5: Additional out-of-service loads in example multiple outage case with 3 predicted outages

Scenario	**Topology**		
	$\mathbf{T}_1$	$\mathbf{T}_2$	$\mathbf{T}_3$
S_1	ΔL_{11}	ΔL_{21}	ΔL_{31}
S_2	ΔL_{12}	ΔL_{22}	ΔL_{32}
S_3	ΔL_{13}	ΔL_{23}	ΔL_{33}
Average Cost	$\frac{1}{3}(\Delta L_{11} + \Delta L_{12} + \Delta L_{13})$	$\frac{1}{3}(\Delta L_{21} + \Delta L_{22} + \Delta L_{23})$	$\frac{1}{3}(\Delta L_{31} + \Delta L_{32} + \Delta L_{33})$

Table 5.5, ΔL_{21} is the difference between L_{21} and L_{11}, ΔL_{31} is the difference between L_{31} and L_{11}, ΔL_{12} is the difference between L_{12} and L_{22}, ΔL_{32} is the difference between L_{32} and L_{22}, ΔL_{13} is the difference between L_{13} and L_{33}, and ΔL_{23} is the difference between L_{23} and L_{33}.

The diagonal terms, $\Delta L_{11}, \Delta L_{22}$, and ΔL_{33} are all equal to 0. This is because operating in the optimal topology does not result in additional loads being left out of service. For example, T_1, which is optimal for outage scenario, S_1, has the least amount of loads unserved (compared to T_2 and T_3) when outage scenario S_1 occurs. Thus, in the event of outage scenario S_1, $\Delta L_{11} = 0$, since no additional load is left out of service in topology T_1.

The off-diagonal terms, $\Delta L_{ij}\ \forall\ i \neq j$, in Table 5.5 represent the additional unserved loads due to operating in a suboptimal topology, T_i in the event of outage scenario S_j. For example, ΔL_{21} represents the additional load left out of service in T_2 when outage scenario S_1 occurs, while ΔL_{12} represents the additional load left out of service in T_1

when outage scenario S_2 occurs. The optimal topology, T_{opt} across all three scenarios is the topology with the least average cost, C_i, calculated as shown in (5.26) and Table 5.5. Since diagonal terms are equal to zero, they may be excluded in the calculation of average cost as shown in (5.27).

5.4.3 Weighted Multiple Outage Case

The multiple outage case presented in the previous subsection assumed that the predicted outage scenarios had equal likelihood of occurrence; however, this is unlikely to be the case. As a result, the weighted multiple outage case presented in this subsection extends the multiple outage case by finding a network topology that minimizes the impact of predicted outage scenarios weighted based on their likelihood of occurrence. Specifically, the weighted multiple outage case assigns weights to each outage scenario S_j based on its likelihood of occurring. In this work, the weights are chosen randomly to demonstrate how the weighted multiple outage case works. However, the weights can be derived from the output of a probabilistic outage prediction model (OPM). The weights, w_j assigned to the predicted outage scenarios sum up to 1 as shown in (5.28), with n representing the number of predicted outage scenarios.

$$\sum_{j=1}^{n} w_j = 1 \tag{5.28}$$

As in the multiple outage case, the optimal topology, T_i for each outage scenario S_j is derived from the MILP formulation presented in Section 5.3.2. The diagonal terms, $L_{ij}\ \forall\ i = j$, in Table 5.6, represent the loads left out of service (in kilowatts) in topology T_i when outage scenario S_j occurs. In each scenario, these terms correspond to the values of the objective function from the proactive topology optimization stage. On the other hand, the off-diagonal terms, $L_{ij}\ \forall\ i \neq j$, are obtained by estimating the loads left out of service due to outage scenario S_j while operating in topology T_i.

Next, ΔL_{ij} is calculated for each topology T_i and each outage scenario S_j as shown

Table 5.6: Computing additional out-of service loads to determine the optimal topology in the weighted multiple outage case

Scenario	**Topology**			
	$\mathbf{T}_1$	$\mathbf{T}_2$	$\cdots$	$\mathbf{T}_n$
S_1	$w_1 \cdot \Delta L_{11}$	$w_1 \cdot \Delta L_{21}$	$\cdots$	$w_1 \cdot \Delta L_{n1}$
S_2	$w_2 \cdot \Delta L_{12}$	$w_2 \cdot \Delta L_{22}$	$\cdots$	$w_2 \cdot \Delta L_{n2}$
$\vdots$	$\vdots$	$\vdots$	$\ddots$	$\vdots$
S_n	$w_n \cdot \Delta L_{1n}$	$w_n \cdot \Delta L_{2n}$	$\cdots$	$w_n \cdot \Delta L_{nn}$
Weighted Cost	$w_1 \cdot \Delta L_{11} +$ $w_2 \cdot \Delta L_{12} +$ $\cdots + w_n \cdot \Delta L_{1n}$	$w_1 \cdot \Delta L_{21} +$ $w_2 \cdot \Delta L_{22} +$ $\cdots + w_n \cdot \Delta L_{2n}$	$\cdots$	$w_1 \cdot \Delta L_{n1} +$ $w_2 \cdot \Delta L_{n2} +$ $\cdots + w_n \cdot \Delta L_{nn}$

in (5.25), after which the weighted cost, $w_j \cdot \Delta L_{ij}$ is computed as shown in Table 5.6. The optimal topology across the n outage scenarios is then determined by calculating the total weighed cost, ${}^wC_i$ for each topology as follows:

$$ {}^wC_i \;=\; \sum_{j=1}^{n} w_j \cdot \Delta L_{ij} \qquad\qquad \forall \;\; T_i \tag{5.29} $$

where n represents the number of outage scenarios, w_j is the weight assigned to outage scenario S_j, and ΔL_{ij} represents the cost of operating in a suboptimal topology, T_i when outage scenario j happens.

Since the diagonal terms, $\Delta L_{ij} = 0 \;\forall\; i = j$, (5.29) can be rewritten as follows to exclude the zero terms:

$$ {}^wC_i \;=\; \sum_{\substack{j=1 \\ j \neq i}} w_j \cdot \Delta L_{ij} \qquad\qquad \forall \;\; T_i \tag{5.30} $$

The topology, T_i with the lowest weighted cost, ${}^wC_i$ is chosen as the optimal topology, T_{opt} across the n predicted outage scenarios.

To demonstrate how the weighted multiple outage case works, the same distribution network from the multiple outage case is considered. There are three predicted

Table 5.7: Additional out-of-service loads in example weighted multiple outage case with 3 predicted outages

Scenario	**Topology**		
	$\mathbf{T}_1$	$\mathbf{T}_2$	$\mathbf{T}_3$
S_1	$w_1 \cdot \Delta L_{11}$	$w_1 \cdot \Delta L_{21}$	$w_1 \cdot \Delta L_{31}$
S_2	$w_2 \cdot \Delta L_{12}$	$w_2 \cdot \Delta L_{22}$	$w_2 \cdot \Delta L_{32}$
S_3	$w_3 \cdot \Delta L_{13}$	$w_3 \cdot \Delta L_{23}$	$w_3 \cdot \Delta L_{33}$
Weighted Cost	$w_1 \cdot \Delta L_{11}$ + $w_2 \cdot \Delta L_{12}$ + $w_3 \cdot \Delta L_{13}$	$w_1 \cdot \Delta L_{21}$ + $w_2 \cdot \Delta L_{22}$ + $w_3 \cdot \Delta L_{23}$	$w_1 \cdot \Delta L_{31}$ + $w_2 \cdot \Delta L_{32}$ + $w_3 \cdot \Delta L_{33}$

outage scenarios from an OPM as shown in Table 5.4. The optimal topologies, T_1, T_2 and T_3 are obtained from the topology optimization stage. The out-of-service load values, L_{11}, L_{22} and L_{33} in the diagonal, correspond to the values of objective function OF_1 when scenarios S_1, S_2, and S_3 occur. The off-diagonal terms, $L_{ij}\ \forall\ i \neq j$, ($L_{21}, L_{31}, L_{12}, L_{32}, L_{13}$ and L_{23}) are obtained by estimating the loads left out of service due to outage scenario S_j while operating in topology T_i.

In Table 5.7, the weights, w_1, w_2, and w_3, are the respective probabilities of outage scenarios S_1, S_2, and S_3, occurring in the distribution network. The three weights sum up to 1. For each scenario S_j, the weight w_j, is multiplied by ΔL_{ij}. For example, $w_1 \cdot \Delta L_{21}$ represents the weighted cost in kilowatts of operating in topology T_2 when outage scenario S_1 occurs.

Similar to the multiple outage case, the diagonal terms in Table 5.7 are also equal to zero since $\Delta L_{ij} = 0\ \forall\ i = j$. The optimal topology, T_{opt}, across all three scenarios is the one with the least total weighted cost, ${}^{w}C_i$, calculated using (5.30) as shown in Table 5.7.

The following is a summary of how to apply the proactive topology optimization framework in the multiple and weighted multiple outage cases:

1. Obtain the predicted outage scenarios, $S_j \in \{1, 2, ..., n\}$ from the OPM results.

   (a) For the multiple outage case, the predicted outages are assumed to have

the same weights or probabilities of occurrence.

(b) For the weighted multiple outage case, the weights w_j associated with each outage scenario is also obtained from the OPM.

2. Using the MILP formulation for the proactive topology optimization stage, obtain the following

   (a) T_i: Optimal topologies for each predicted scenario

   (b) L_{ij}: Unserved demand (kW) in topology T_i if outage scenario j occurs

3. Compute ΔL_{ij} for all combinations of topologies T_i and outage scenario, j.

   (a) ΔL_{ij} represents the cost associated with operating in topology T_i when outage scenario S_j occurs. In other words, ΔL_{ij} represents the additional load left out of service due to not operating in the optimal topology. Recall that ΔL_{ij} is equal to zero for all $i = j$. The topology T_i is optimal for all $i = j$.

   (b) For the weighted multiple outage case, ΔL_{ij} is multiplied by w_j for each scenario, S_j.

4. For the multiple outage case, calculate the average cost for each topology. For the weighted outage case, calculate the total weighted cost for each topology.

   (a) The topology with the lowest average cost or total weighted cost is the optimal topology, T_{opt} to operate in for the outage scenarios considered.

5.5 Summary

This chapter began with a brief overview of distribution system optimization followed by a detailed description of the proposed proactive topology optimization and service restoration framework.

The objective of the proactive topology optimization stage was to minimize the loads that would be left out of service in the event of a predicted outage in the distribution network. To accomplish this, the original network topology is reconfigured before the outage, so that the power flowing through the predicted outage locations is minimized. In the service restoration stage, the goal was to maximize the loads restored in the system following the predicted outage(s). The MILP formulation for the two stages including details of the problem constraints were also presented in this chapter.

Furthermore, three outage optimization cases were presented: single outage, multiple outage, and weighted multiple outage. In each case, it is assumed that the predicted outage locations were derived from an outage prediction model (OPM). In the single outage case, the aim is to find the optimal topology that would result in the least amount of out-of-service loads when the predicted outage occurs. In the multiple outage case, the goal is to find the topology that results in the least amount of out-of-service loads across two or more outage scenarios with equal probabilities. On the other hand, the goal of the weighted multiple outage case is to find a network topology that minimizes the impact of predicted outage scenarios weighted on their likelihood of occurrence.

CHAPTER 6: CASE STUDIES AND RESULTS

6.1 Overview

In this chapter, the proposed proactive topology optimization and service restoration framework presented in Chapter 5 is tested and validated using modified versions of the IEEE 13-bus and 123-bus test feeders [121]. The three optimization cases presented in the previous chapter, single outage, multiple outage, and weighted multiple outage, are applied to both test systems. The MILP model is implemented using Pyomo, a Python-based, open-source optimization software package [122,123] it is solved with the CPLEX 20.1.0.1 solver on an Intel® Core™ i7-8565U CPU, 1.80GHz, 16GB RAM and 64-bit operating system PC.

6.2 Test Feeders

This work uses modified versions of the IEEE 13-bus feeder and IEEE 123-bus feeder adapted from [121] and [124] to demonstrate the proposed proactive network reconfiguration and service restoration framework. Both systems are assumed to be three-phase balanced systems. Data for the 13-bus feeder are presented in detail in the following section while data for the 123-bus feeder are presented in Appendix A.

6.2.1 Modified IEEE 13-bus Feeder

The IEEE 13-bus test feeder [121, 125] is modified into a balanced system with a total load of 1150 kW and 700 kVar. To allow for topological flexibility, it is assumed that all the lines in the feeder are switchable as shown in Fig. 6.1 and are thus available for network reconfiguration purposes. Three lines, 633–692, 646–611 and 675–680 are assumed to be normally-open, while the remaining twelve lines are assumed to be normally-closed. Additionally, the system includes capacitors at nodes 611 and 675

and a voltage regulator on line segment 650–632. Tables 6.1 to 6.5 provide details of the system parameters, including line and load parameters, which were adapted from [64, 121].

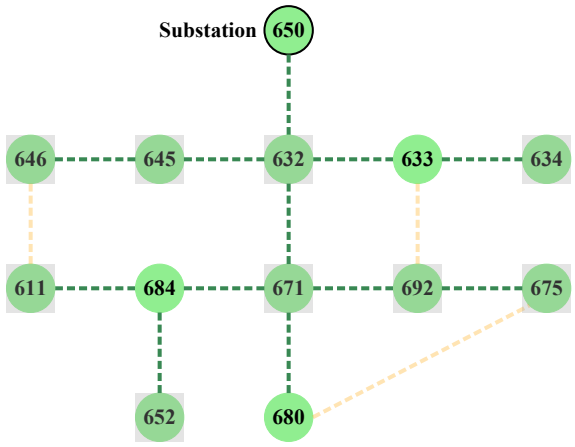

Figure 6.1: Modified IEEE 13-bus feeder showing normally-closed switches (green dotted lines) and normally-open switches (orange dotted lines)

Table 6.1: Line parameters for modified IEEE 13-bus feeder

Line No.	From Node	To Node	Length (ft)	Capacity (kVA)	Config.
1	650	632	2000	1500	601
2	632	633	500	1000	602
3	633	634	200	500	XFM-1
4	632	645	500	1000	603
5	645	646	300	800	603
6	632	671	2000	1500	601
7	671	692	10	800	Switch
8	692	675	500	800	606
9	671	684	300	800	604
10	684	611	300	800	605
11	684	652	800	800	607
12	671	680	1000	1500	601
13	633	692	2000	1000	602
14	646	611	2000	800	603
15	675	680	1500	1000	601

Table 6.2: Line impedances for modified IEEE 13-bus feeder

Config.	Resistance (Ohms/mi)	Reactance (Ohms/mi)
601	0.3418	1.0335
602	0.7479	1.1970
603	1.3266	1.3520
604	1.3266	1.3520
605	1.3292	1.3475
606	0.7952	0.4322
607	1.3425	0.5124
XFM-1	1.0051	1.8274
Switch	0.0001	0.0001

Table 6.3: Load parameters for modified IEEE 13-bus feeder

Load Name	P (kW)	Q (kVar)
L632	65	40
L634	135	95
L645	55	40
L646	75	45
L671	385	220
L692	55	50
L675	280	155
L611	55	25
L652	45	30

Table 6.4: Transformer and regulator data for modified IEEE 13-bus feeder

	kVA	kV-high	kV-low	Tap Position
Substation	5000	115	4.16	–
XFM-1	500	4.16	0.48	–
RG 650-632	–	4.16	4.16	1

Table 6.5: Capacitor data for modified IEEE 13-bus feeder

Node	kVar
675	200
611	30

6.2.2 Modified IEEE 123-bus Feeder

Fig. 6.2 shows a one-line diagram of the modified IEEE 123-bus feeder, which is used to test and demonstrate the scalability of the proposed topology optimization and service restoration framework. The three-phase feeder is assumed to be balanced with a load of 1185 kW and 610 kVar. Additionally, there are twelve switchable lines in the feeder used for network reconfiguration as follows: 1–7, 13–18, 13–152, 18–135, 23–25, 54–94, 60–160, 76–77, 87–89, 97–197, 150–149, and 151–300. Two of the switchable lines, 54–94 and 151–300, are assumed to be normally open while the remaining ten are assumed to be normally closed. In the one-line diagram in Fig. 6.2, the green dotted lines represent normally closed switchable lines while the orange dotted lines represent normally open switchable lines. Green solid lines represent non-switchable lines in the system. Four voltage regulators are connected to the following line sections: 150–149, 9–14, 25–26 and 160–67 and four capacitors are connected at nodes 83, 88, 90 and 92 respectively. Details of the line parameters, load parameters, voltage regulator tap settings and capacitor ratings in the system are presented in Appendix A.1.

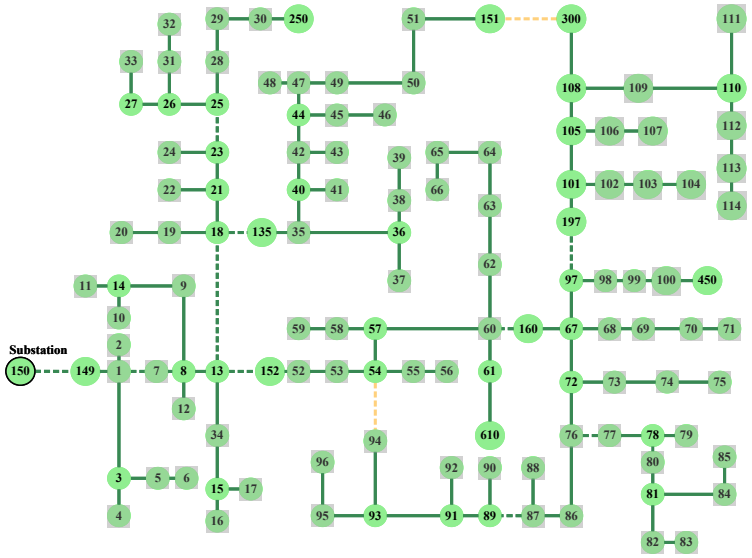

Figure 6.2: Modified IEEE 123-bus feeder showing normally-closed switches (green dotted lines) and normally-open switches (orange dotted lines)

6.3 Case Studies

This section presents case studies based on the three optimization cases discussed in Chapter 5.

6.3.1 Case I: Single Outage Case

6.3.1.1 Case I.A: IEEE 13-bus Feeder

For the single outage case in the modified IEEE 13-bus feeder, three cases are considered with predicted outage locations in the test feeder listed in Table 6.6; the number of allowed switching operations, n_s in (5.16a) of the MILP formulation is limited to four. Table 6.6 presents the results of proactive network reconfiguration and service restoration for each case.

In Case A, branch 671–684 is the predicted outage location as shown in Fig. 6.3(a). If an outage were to occur at this location, 100 kW of loads (L611 and L652) would be left out of service as shown in Fig. 6.3(b). In the first stage of the proposed framework, the network is proactively reconfigured, resulting in the network displayed in Fig. 6.3(c). The new topology is achieved in four switch operations by switching off lines 671–692 and 684–611 and switching on lines 675–680 and 646–611.

An outage at branch 671–684 would leave 45 kW (load at 652) unserved in the new topology as shown in Fig. 6.3(d). Reconfiguring the network to minimize the power

Table 6.6: Single Outage Case: Results from modified IEEE 13-bus feeder

Case	**Predicted Outage Location(s)**	**Stage 1 Unserved Loads (kW)**		**Stage 2 Unserved Loads (kW)**	**Comp. Time (s)**
		Original Config.	**Proactive Config.**		
A	671–684	100	45	0	0.45
B	632–633	135	135	0	0.49
C	671–684 | 671–692	435	100	0	0.51

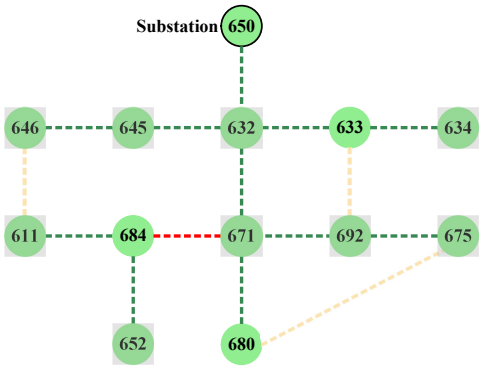

(a) Original topology with predicted outage location 671–684 shown in red

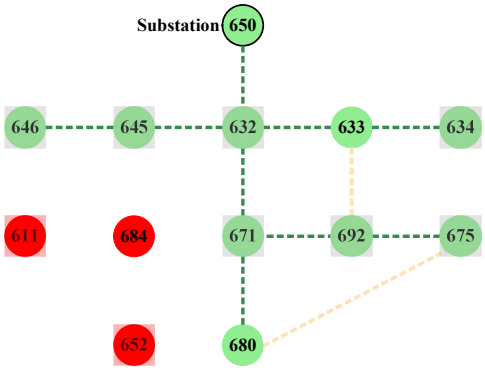

(b) Original topology showing loads that would be impacted by predicted outage at branch 671–684

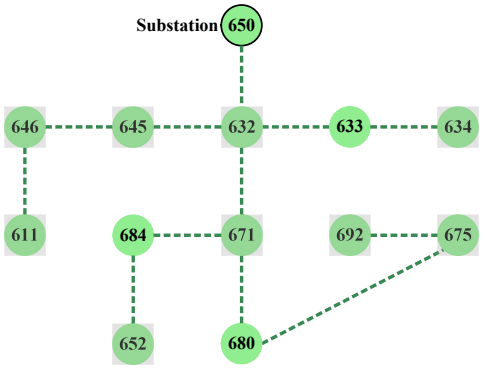

(c) Proactive topology

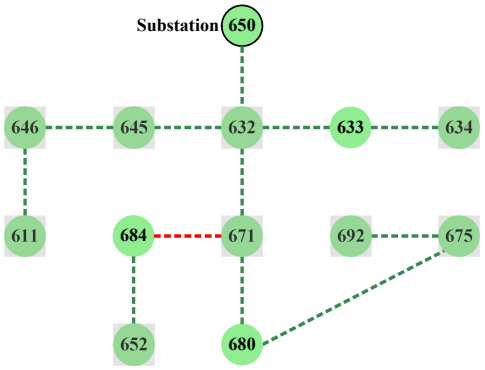

(d) Proactive topology with predicted outage locations 671–684 shown in red

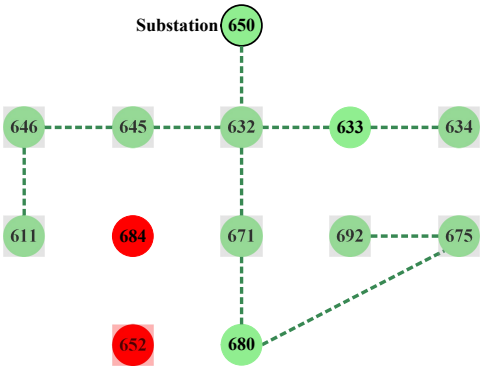

(e) Proactive topology showing loads that would be impacted by predicted outage at branch 671–684

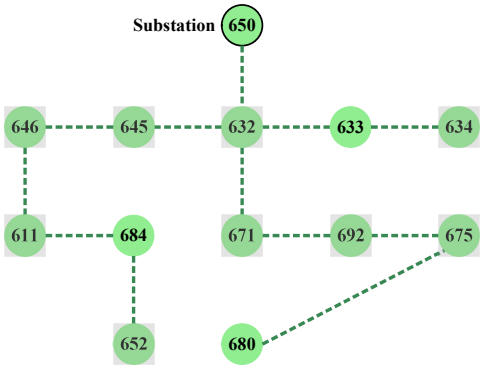

(f) New topology after the predicted outage location is isolated

Figure 6.3: Case A: One-line diagrams of modified IEEE 13-bus test feeder showing network topology before and after implementing the proactive topology optimization and service restoration framework

flowing through branch 671–684 reduces the loads that would be left out of service by 55%, from 100 kW to 45 kW. Therefore, minimizing the power flowing through line 671–684 results in a reduction in the load impacted on the network in the event of a predicted outage on line 671–684.

It is worth mentioning that due to the flexibility of the distribution feeder (all the lines are assumed to be switchable), other topologies may result in the same objective function value of 45 kW for the topology optimization stage. Topology options can be limited by expanding the objective function in (5.7) to minimize the number of switching operations allowed or to minimize the maximum deviation in node voltage along the feeder. It is important to note that if line 671–684 were turned off in the new topology, the out-of-service loads be 0 kW, the lowest possible value of the objective function; however, this would be a trivial solution since in reality, the predicted outage locations may not always be switchable.

The next step is the service restoration process. This stage assumes that the outage has occurred and the faulted branch has been disconnected, as shown in Fig. 6.3(e); hence the feeder is reconfigured to maximize the load restored after the outage. In this case, all the loads (1150 kW) in the feeder are restored as shown in Fig. 6.3(f).

In Case B, the outage is predicted to occur on line 632–633; in the original topology shown in Fig. 6.1, the power flow, P_{ij}^{BR} through this line is 135 kW. An outage on line 632–633 would leave load L634 (135 kW) out of service in the original network topology. In the topology optimization stage, branch 671–680 is opened and branch 675–680 is closed to reconfigure the network. The value of objective function, OF_1 is 135 kW; the unserved load due to the outage is also 135 kW (load L634). Since there is no other path in the network to node 634 from the substation besides 650–632–633–634, the predicted outage would leave 135 kW out of service in the new and original topologies. Hence, the network can be operated in either topology prior to the outage. In the service restoration stage, branch 632–633 is isolated following the

Table 6.7: Single Outage Case: Switch operations in modified IEEE 13-bus feeder

Case	POL(s)	Stage 1			Stage 2		
		No. of Sw. ops	**Opened Switches**	**Closed Switches**	**No. of Sw. ops**	**Opened Switches**	**Closed Switches**
A	671–684	4	671–692 684–611	646–611 675–680	3	671–680	671–692 684–611
B	632–633	2	671–680	675–680	3	675–680	671–680 633–692
C	671–684 671–692	4	692–675 684–611	646–611 675–680	2	–	692–675 684–611

outage, and the network is reconfigured. The resulting topology restores all loads in the system. The new topology is achieved in three switch operations as shown in Table 6.7 by opening line 675–680 and closing lines 671–680 and 633–692.

In Case C, the number of predicted outage locations is increased to two: branches 671–684 and 671–692. If the outage occurs as predicted, topology optimization reduces the unserved loads from 435 kW in the original topology to 100 kW in the new topology in the first stage. The new topology is achieved by opening lines 692–675 and 684–611 and closing lines 646–611 and 675–680 in four switching operations. Loads L611, L652, L675 and L692 would be out of service in the original topology, while only loads L652 and L692 are affected in the new topology in the event of the predicted outage. In the second stage, we assume that the outage occurs as predicted, and service restoration proceeds by isolating the predicted outage locations (671–684 and 671–692) and reconfiguring the system to restore the maximum loads possible. All loads are restored in two switching operations (closing lines 692–675 and 684–611).

In the three cases presented, it can be seen that the value of objective function OF_1 from (5.7) is equal to the sum of loads left out of service if the outage occurred as predicted. However, this may not be the case when predicted outage locations are located on the same lateral in the distribution network, or in a larger distribution network with fewer switchable lines.

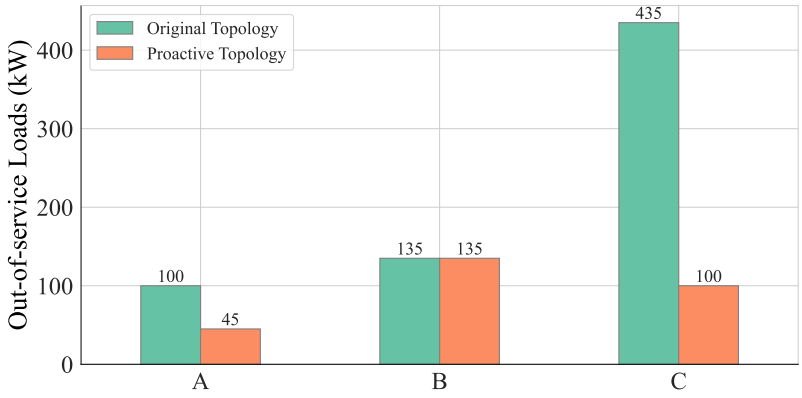

Figure 6.4: IEEE 13-bus feeder: Out-of-service loads in Stage 1 due to predicted outages in original and proactive network topologies

Fig. 6.4 compares the out-of-service loads that resulted from predicted outages in the original and proactive topologies of the three cases discussed. The plot shows that proactive topology optimization reduces the loads that would be impacted by outages at predicted outage locations in cases A and C. For case B, the unserved loads are the same for both the original and proactive topologies. In all three cases, proactive topology optimization yields a reduction between 0% and 75% in the out-of-service loads. One-line diagrams of the feeder showing the original and proactive topologies for Cases B and C are provided in Appendix B.1.

6.3.1.2 Case I.B: IEEE 123-bus Feeder

In this section, four cases are tested to demonstrate the scalability of the proposed framework using the modified IEEE 123-bus feeder presented in Section 6.2.2. The same MILP formulation presented in Chapter 5 is used, but the number of switching operations allowed, n_s in (5.16a) is increased to six to provide more topological flexibility in this larger system with fewer switchable lines. The results for the four cases are presented in Table 6.8 and discussed in the following paragraphs.

In Case A, the predicted outage locations are branches 67–72 and 67–97, both non-switchable lines, as shown in Fig. 6.5(a). An outage at these locations would leave 455 kW of loads out of service as shown in Fig. 6.5(b). The sum of power flowing through

Table 6.8: Single Outage Case: Results from modified IEEE 123-bus feeder

Case	**Predicted Outage Location(s)**	**Stage 1 Unserved Loads (kW)**		**Stage 2 Unserved Loads (kW)**	**Comp. Time (s)**
		Original Config.	**Proactive Config.**		
A	67–72 67–97	455	85	0	1.28
B	13–18 57–60	1000	505	485	1.25
C	26–27 | 72–76 97–197 | 160–67	510	145	145	1.26
D	13–18 | 30–250 49–50 | 72–76	630	555	355	1.23

both lines in the original topology shown in Fig. 6.2 is also 455 kW. To minimize the impact of an outage on both lines, the network is proactively reconfigured in the first stage resulting in the topology shown in Fig. 6.5(c). The new topology is achieved by opening switchable lines 60–160 and 97–197 and closing switchable lines 54–94 and 151–300. In the event of the outage in the new topology, the unserved demand is reduced from 455 kW in the original topology to 85 kW (an 81% reduction) as illustrated in Fig. 6.5(e). Power flowing through branches 67-72 and 67-97 is also reduced to 130 kW. It is important to point out that the value of OF_1 (130 kW) is not the same as the out-of-service loads (85 kW) because branches 67-72 and 67-97 are located on the same lateral of the distribution network. In the second stage, service restoration is carried out and the network is reconfigured to maximize the loads restored in the network by closing lines 60–160 and 97–197. All the loads are restored as shown in Fig. 6.5(f).

In Case B, the predicted outage locations are lines 13–18 and 57–60. An outage affecting these lines will have a significant impact on the network since they are among the longest and highest capacity lines in the network. In the original topology, an outage affecting lines 13–18 and 57–60 would impact 1000 kW of loads (almost 85% of

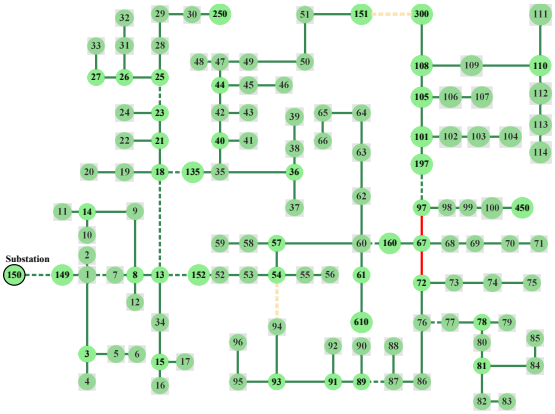

(a) Original topology with predicted outage locations 67–97 and 67–72 shown in red

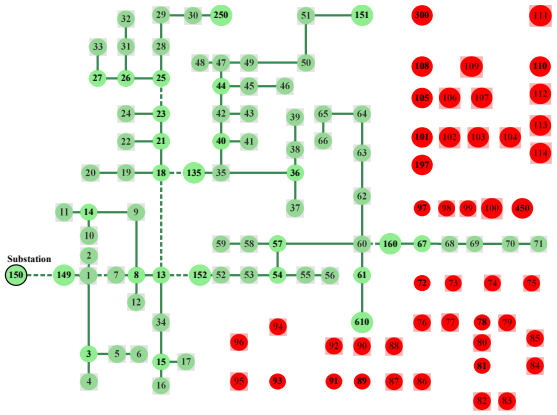

(b) Original topology showing loads that would be impacted by predicted outage at branches 67–97 and 67–72

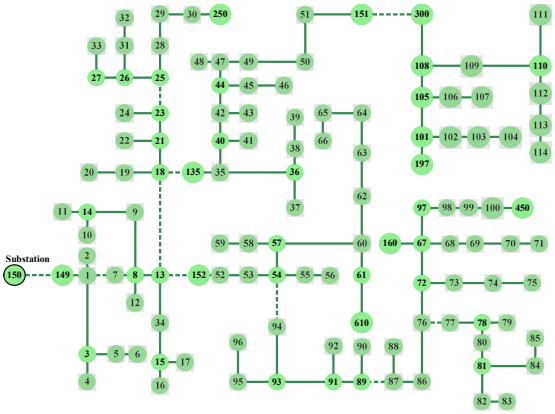

(c) Proactive topology

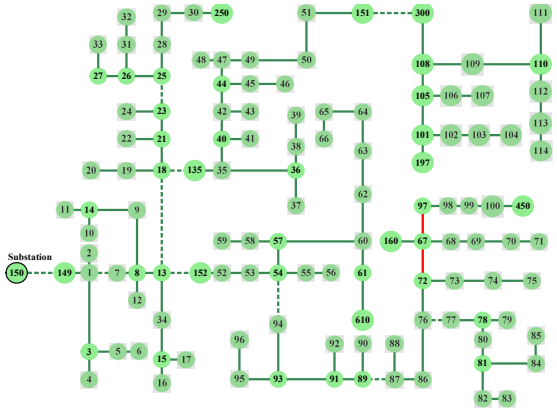

(d) Proactive topology with predicted outage locations 67–97 and 67–72 shown in red

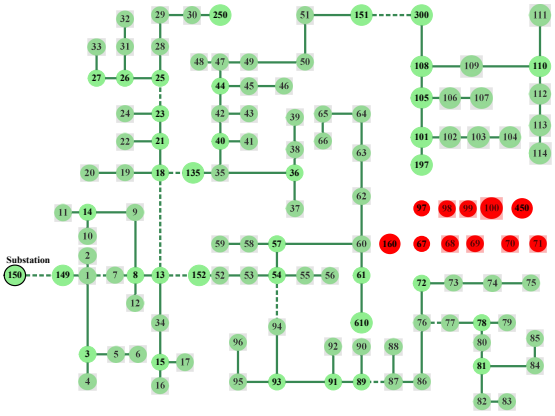

(e) Proactive topology showing loads that would be impacted by predicted outage at branches 67–97 and 67–72

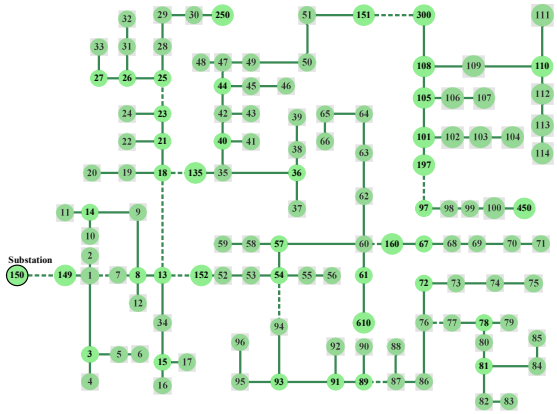

(f) New topology after the predicted outage locations are isolated

Figure 6.5: Case A: One-line diagrams of modified IEEE 123-bus feeder showing network topology before and after implementing the proactive topology optimization and service restoration framework

the system load). Optimizing the network topology reduces the loads impacted to 505 kW. In this case, both values (1000 kW and 505 kW) also correspond to the loads left out of service in the original and proactive topologies, respectively. Hence, topology optimization reduced the out-of-service loads by almost 50% as shown in Fig. 6.6. The proactive topology is achieved in two switch operations by opening line 60–160 and closing line 54–94. In the second stage, the network is again reconfigured during service restoration to maximize the amount of loads restored after the outage affecting lines 13–18 and 57–60 occurs. By closing line 60–160 and opening line 97–197, 700 kW of loads are restored, leaving 485 kW of loads unserved in the system.

To further test the robustness of the proposed proactive topology optimization and service restoration framework, the number of predicted outage locations is increased to four in cases C and D.

In Case C, a potential outage at lines 26–27, 72–76, 97–197 and 160–67 would leave 510 kW out of service. By optimizing the network topology in the first stage, the unserved loads are reduced by 72% to 145 kW in four switch operations by opening lines 60–160 and 97–197 and closing lines 54–94 and 151–300. The sum of power flowing through these lines (that is, the value of OF_1) is reduced from 875 kW to 145 kW.

In the second stage, the predicted outage locations are isolated during service restoration; however, the topology remains the same since none of the switchable lines are operated. Loads L68, L69, L70, L98, L99 and L100 remain unrestored since lines 97–197 and 160–67 are affected by the outage, leaving no alternative path to reconnect these loads to the network. Also, load L33 which is downstream of line 26–27, one of the predicted outage locations, is left out of service for a similar reason. Thus, it may be beneficial to have DGs connected at end nodes in the network or to have more switchable lines connecting different laterals in the network.

In Case D, the outage is predicted to occur at lines 13–18, 30–250, 49–50 and 72–

76. Outages at these locations would result in 630 kW of load left out of service in the original topology; this number is reduced to 555 kW by implementing proactive topology optimization (opening lines 18–135 and 87-89 and closing lines 54–94 and 151–300). A further reduction in the unserved loads (especially those downstream of node 18 in the original topology) cannot be achieved since line 49–50 is one of the potential outage locations. A potential outage at line 49–50 would restrict power flowing from the substation through switchable line 151–300. By installing more switchable lines in the network that bypass the predicted outage location (such as one connecting nodes 51 and 250), there could be a further reduction in power flowing through 13-18, and therefore lower out-of-service loads. In the second stage, 830 kW of loads are restored by closing line 87–89; an additional 200 kW of loads are picked up, leaving 355 kW of loads unrestored. As in the first stage, loads downstream of node 50 in the post-outage topology are left unrestored due to the isolation of line 49–50.

The plot in Fig. 6.6 shows the out-of-service loads due to the predicted outages in the four cases presented for the modified IEEE 123-node test feeder. In the four cases, out-of-service loads are compared between the original and proactive topologies. Operating in the proactive topologies reduces the amount of out-of-service loads due to the predicted outages by at least 10% in all four cases. Table 6.9 shows the number of switch operations in both stages of the proposed framework for all four cases. In each case, the maximum number of switch operations is four even though the number of switching operations, n_s is limited to six. Also, all proactive topologies in the first stage were achieved by closing either 54-94 or 151-300 or both switchable lines. One-line diagrams of the feeder showing the original and proactive topologies for cases B, C and D are provided in Appendices B.3 to B.5.

Table 6.9: Single Outage Case: Switch operations in modified IEEE 123-bus feeder

Case	POL(s)	Stage 1			Stage 2		
		No. of Sw. ops	Opened Switches	Closed Switches	No. of Sw. ops	Opened Switches	Closed Switches
A	67–72 67–97	4	60–160 97–197	54–94 151–300	2	–	60–160 97–197
B	13–18 57–60	2	60–160	54–94	2	97–197	60–160
C	26–27 | 72–76 97–197 | 160–67	4	60–160 97–197	54–94 151–300	0	–	–
D	13–18 | 30–250 49–50 | 72–76	4	18–135 87–89	54–94 151–300	1	–	87–89

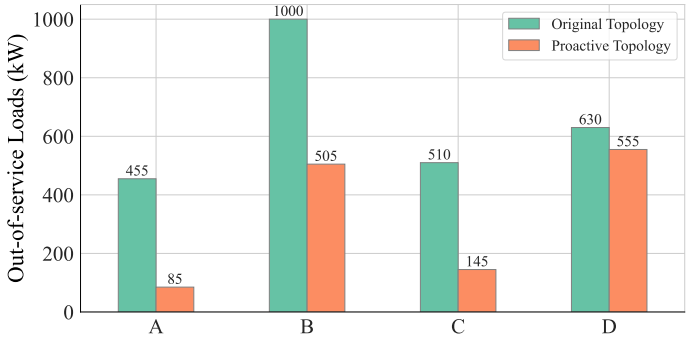

Figure 6.6: IEEE 123-bus feeder: Out-of-service loads due to predicted outages in original and proactive topologies

6.3.2 Case II: Multiple Outage Case

In the multiple outage case, the proposed topology optimization and service restoration framework is applied to minimize the impact of predicted outages across different outage scenarios. Each outage scenario could involve one or more predicted outage locations. Topology optimization involves finding an optimal topology, T_{opt} that minimizes the total out-of-service loads across several predicted outage scenarios, $\{S_1, S_2, ..., S_n\}$. The service restoration stage involves determining the topology that maximizes the loads restored across predicted outage scenarios after the outages have occurred.

In this section, the multiple outage case is demonstrated in the following subsections

using modified versions of the IEEE 13-bus and 123-bus feeders.

6.3.2.1 Case II.A: IEEE 13-bus Feeder

The multiple outage case is applied to the modified IEEE 13-bus feeder by considering two cases involving three predicted outage scenarios. The lines affected in each outage scenario are listed in Table 6.10. Each outage scenario is assumed to have an equal probability of occurrence. With three outage scenarios, this represents a 33.33% chance of occurrence for each scenario.

In Case A, three outage scenarios are considered, each with equal probability of occurrence on the following lines in the network: 671–684, 671–692 and 632–645. As presented in Section 5.4.2, the optimal topologies, T_1, T_2 and T_3 for the outage scenarios are first determined. The status of each line in the three topologies is listed in Table 6.11. Then the out-of-service loads, L_{ij} in each topology, T_i is determined for each predicted outage scenario S_j. Table 6.12 presents the out-of-service loads (in kilowatts) when each scenario occurs while operating in topologies T_1, T_2 and T_3, respectively. T_1 is the optimal topology to operate in if outage scenario S_1 occurs at line 671–684. Outage scenario S_1 (predicted outage at 671–692) leaves 45 kW of loads out of service in topology T_1; this is represented as L_{11} in Table 6.12. If scenario S_2 (predicted outage at 671–692) occurs while operating in T_1, 335 kW (L_{12}) of loads are left unserved, and so on. For scenario S_1, the unserved loads, L_{11} and L_{21} in topologies T_1 and T_2 are the same (45 kW). Load L652 would be left unserved in both

Table 6.10: Modified IEEE 13-bus feeder: Outage scenarios and predicted outage locations

Case	**Scenarios**		
	Scenario 1	**Scenario 2**	**Scenario 3**
A	671–684	671–692	632–645
B	692–675	671–684 671–692	632–633 632–645

Table 6.11: Status of switchable lines in multiple outage cases: Modified IEEE 13-bus feeder

Line No.	From Node	To Node	Line Status				
			Case A			Case B	
			T_1	T_2	T_3	$T_1 = T_3$	T_2
1	650	632	ON	ON	ON	ON	ON
2	632	633	ON	ON	ON	ON	ON
3	633	634	ON	ON	ON	ON	ON
4	632	645	ON	ON	ON	ON	ON
5	645	646	ON	ON	OFF	OFF	ON
6	632	671	ON	ON	ON	ON	ON
7	671	692	ON	ON	ON	ON	ON
8	692	675	ON	OFF	ON	ON	ON
9	671	684	ON	ON	ON	ON	ON
10	684	611	OFF	OFF	ON	ON	OFF
11	684	652	ON	ON	ON	ON	ON
12	671	680	ON	ON	OFF	ON	OFF
13	633	692	OFF	OFF	OFF	OFF	OFF
14	646	611	ON	ON	ON	ON	ON
15	675	680	OFF	ON	ON	OFF	ON

Table 6.12: Multiple Outage Case A: Out-of-service loads (kW) in modified IEEE 13-bus feeder

Scenario	**Topology**		
	$\mathbf{T}_1$	$\mathbf{T}_2$	$\mathbf{T}_3$
S_1	$L_{11} = 45$	$L_{21} = 45$	$L_{31} = 175$
S_2	$L_{12} = 335$	$L_{22} = 55$	$L_{32} = 335$
S_3	$L_{13} = 185$	$L_{23} = 185$	$L_{33} = 55$

topologies due to scenario S_1. The diagonal terms, L_{11}, L_{22} and L_{33} in Table 6.12 represent the unserved loads in the optimal topologies, and they are the least for scenarios S_1, S_2, and S_3, respectively. Also, $L_{12} = L_{32}$ since scenario S_2 would leave loads L675 and L692 out of service in topologies T_1 and T_3. Similarly, $L_{13} = L_{23}$ since scenario S_3 would leave loads L611, L645 and L646 unserved in topologies T_1 and T_2.

The costs ΔL_{ij} of not operating in the optimal topologies are estimated from Equation (5.25) as shown in Table 6.13. $\Delta L_{ij} = 0$ for the optimal topologies for each scenario, that is when $i = j$. Also, $\Delta L_{ij} = 0$ if the considered topology leaves the same amount of loads unserved as the optimal topology. For example, ΔL_{21} is the

Table 6.13: Multiple Outage Case A: Additional out-of-service loads (kW) in modified IEEE 13-bus Feeder

Scenario	**Topology**		
	$\mathbf{T}_1$	$\mathbf{T}_2$	$\mathbf{T}_3$
S_1	$\Delta L_{11} = L_{11} - L_{11}$ $= 45 - 45 = 0$	$\Delta L_{21} = L_{21} - L_{11}$ $= 45 - 45 = 0$	$\Delta L_{31} = L_{31} - L_{11}$ $= 175 - 45 = 130$
S_2	$\Delta L_{12} = L_{12} - L_{22}$ $= 335 - 55 = 280$	$\Delta L_{22} = L_{22} - L_{22}$ $= 55 - 55 = 0$	$\Delta L_{32} = L_{32} - L_{22}$ $= 335 - 55 = 280$
S_3	$\Delta L_{13} = L_{13} - L_{33}$ $= 185 - 55 = 130$	$\Delta L_{23} = L_{23} - L_{33}$ $= 185 - 55 = 130$	$\Delta L_{33} = L_{33} - L_{33}$ $= 55 - 55 = 0$
Average Cost	$\frac{1}{3}(0 + 280 + 130) =$ 136.67 kW	$\frac{1}{3}(0 + 0 + 130) =$ 43.33 kW	$\frac{1}{3}(130 + 280 + 0) =$ 136.67 kW

same as ΔL_{11} since scenario S_1 results in the same amount of loads left unserved in topologies T_1 (the optimal topology) and T_2. Hence, the additional loads left unserved in both topologies are zero. On the other hand, topologies with higher costs are suboptimal. For example, topology T_3 is the least optimal topology to operate in if predicted outage scenario S_1 occurs, since it has a higher cost of 130 kW compared to T_1 and T_2 which both have a cost of 0 kW.

The average cost, C_i for each topology is then calculated by taking the average of the costs ΔL_{ij} across the three outage scenarios. T_2 is the optimum topology for the three predicted outage scenarios as shown in Table 6.13 since it results in the lowest average cost (43.33 kW). On average, the additional out-of-service loads in T_2 (43.33 kW) due to the predicted outages would be three times less than the additional out-of-service loads (136.67 kW) in either T_1 or T_3. Therefore, it is recommended to operate in T_2 if the three scenarios have equal likelihood of occurring.

In case B, the three scenarios are predicted outages at lines 692–675 (S_1), 671–684 and 671–692 (S_2), and 632–633 and 632–645 (S_3), respectively. The topologies that minimize the unserved loads in these three scenarios are listed as T_1 to T_3 in Table 6.14 along with the corresponding values of the unserved loads. It is important

Table 6.14: Multiple Outage Case B: Out-of-service loads (kW) in modified IEEE 13-bus Feeder

Scenario	**Topology**	
	$\mathbf{T}_1 = \mathbf{T}_3$	$\mathbf{T}_2$
S_1	$L_{11} = 280$	$L_{21} = 280$
S_2	$L_{12} = 510$	$L_{22} = 380$
S_3	$L_{13} = 190$	$L_{23} = 320$

Table 6.15: Multiple Outage Case B: Additional out-of-service loads (kW) in modified IEEE 13-bus Feeder

Scenario	**Topology**	
	$\mathbf{T}_1 = \mathbf{T}_3$	$\mathbf{T}_2$
S_1	$\Delta L_{11} = L_{11} - L_{11}$ $= 280 - 280 = 0$	$\Delta L_{21} = L_{21} - L_{11}$ $= 280 - 280 = 0$
S_2	$\Delta L_{12} = L_{12} - L_{22}$ $= 510 - 380 = 130$	$\Delta L_{22} = L_{22} - L_{22}$ $= 380 - 380 = 0$
S_3	$\Delta L_{13} = L_{13} - L_{33}$ $= 190 - 190 = 0$	$\Delta L_{23} = L_{23} - L_{33}$ $= 320 - 190 = 130$
Average Cost	$\frac{1}{3}(0 + 130 + 0) =$ 43.33 kW	$\frac{1}{3}(0 + 0 + 130) =$ 43.33 kW

to note that topologies T_1 and T_3 are the same in this case; this is denoted as $T_1 = T_3$. The status of each line in these topologies is listed in Table 6.11. This means that $\Delta L_{13} = \Delta L_{11}$, $\Delta L_{32} = \Delta L_{12}$ and $\Delta L_{33} = \Delta L_{13}$. The results show that scenario S_1 would result in the same amount of unserved loads in topologies T_1 and T_2 even though both topologies are different.

Next, the costs ΔL_{ij} are computed as displayed in Table 6.15. Since there is no additional load left unserved when scenario S_1 occurs while operating in T_1 or when scenario S_2 occurs while operating in T_2, ΔL_{11} and ΔL_{22} are both equal to 0 kW. Similarly, ΔL_{13} is also equal to 0 kW since $T_1 = T_3$. In scenario S_1, ΔL_{21} is also equal to zero, since the same amount of load, 280 kW, is left unserved in topologies T_1 and T_2. The average cost of each topology is computed; T_1 and T_2 have the same average

cost (43.33 kW). Hence, the network can be operated in either topology when the predicted outage scenarios have the same probability of occurring.

6.3.2.2 Case II.B: IEEE 123-bus Feeder

In this section, the multiple outage case is implemented on the modified IEEE 123-bus test feeder by considering two cases involving three predicted outage scenarios with the outage locations presented in Table 6.16. It is assumed that each outage scenario has an equal likelihood of occurrence (33.33%).

In case A, three outage scenarios are considered, each with an equal probability of occurrence on the following lines in the network: lines 67–72 and 67–97 (S_1), 13–18 and 57–60 (S_2) and lines 49–50 and 93–94 (S_3). First, the optimal topologies, T_1, T_2 and T_3 for each outage scenario are determined during the topology optimization stage. Table 6.17 lists the status of the switchable lines for each topology, and Table 6.18 shows the out-of-service loads (in kilowatts), L_{ij} for each topology T_i and scenario S_j. As expected, the diagonal terms, L_{11}, L_{22} and L_{33} are the lowest for each outage scenario.

Table 6.19 presents the costs or additional out-of-service loads, ΔL_{ij}. ΔL_{ij} represents the difference between unserved loads in suboptimal topology T_i and unserved loads in the optimal topology T_j in case of outage scenario S_j. Therefore, the diagonal terms $\Delta L_{11}, \Delta L_{22}$ and ΔL_{33} are all 0 kW. In scenario S_1, T_3 has a cost of 370 kW; this means that an additional 370 kW of loads (L_{31}) are left unserved in T_3 compared

Table 6.16: Modified IEEE 123-bus Feeder: Outage scenarios and predicted outage locations

Case	**Scenarios**		
	Scenario 1	**Scenario 2**	**Scenario 3**
A	67–72 | 67–97	13–18 | 57–60	49–50 | 93–94
B	13–18 | 30–250 49–50 | 72–76	26–27 | 72–76 97–197 | 160–67	67–72 | 67–97 13–18 | 57–60

Table 6.17: Status of switchable lines in multiple outage cases: Modified IEEE 123-bus feeder

Line No.	From Node	To Node	Line Status				
			Case A			Case B	
			T_1	T_2	T_3	T_1	$T_2 = T_3$
1	1	7	ON	ON	ON	ON	ON
2	13	18	ON	ON	ON	ON	ON
3	13	152	ON	ON	ON	ON	ON
4	18	135	ON	ON	ON	OFF	ON
5	23	25	ON	ON	ON	ON	ON
6	54	94	ON	ON	OFF	ON	ON
7	60	160	OFF	OFF	ON	ON	OFF
8	76	77	ON	ON	ON	ON	ON
9	87	89	ON	ON	ON	OFF	ON
10	97	197	ON	OFF	ON	ON	OFF
11	150	149	ON	ON	ON	ON	ON
12	151	300	OFF	ON	OFF	ON	ON

Table 6.18: Multiple Outage Case A: Out-of-service loads (kW) in modified IEEE 123-bus feeder

Scenario	**Topology**		
	$\mathbf{T}_1$	$\mathbf{T}_2$	$\mathbf{T}_3$
S_1	$L_{11} = 85$	$L_{21} = 195$	$L_{31} = 455$
S_2	$L_{12} = 615$	$L_{22} = 505$	$L_{32} = 1000$
S_3	$L_{13} = 500$	$L_{23} = 500$	$L_{33} = 35$

Table 6.19: Multiple Outage Case A: Additional out-of-service loads (kW) in modified IEEE 123-bus feeder

Scenario	**Topology**		
	$\mathbf{T}_1$	$\mathbf{T}_2$	$\mathbf{T}_3$
S_1	0	110	370
S_2	110	0	495
S_3	465	465	0
Average Cost	191.67 kW	191.67 kW	288.33 kW

to the unserved loads in optimal topology T_1.

Similarly, operating in T_3 results in the highest amount of additional unserved loads, L_{32} when outage scenario S_2 occurs. In scenario S_3, the additional unserved loads are the same for T_1 and T_2, that is, $\Delta L_{13} = \Delta L_{23} = 465$ kW; this is because

the same loads are affected in both topologies during outage scenario S_3. Next, the average costs for each topology across the three scenarios are computed, and the results in Table 6.19 show that T_1 and T_2 have the least average costs (191.67 kW). On average, the three scenarios would leave 1.5 times more addional loads unserved in T_3 compared to T_1 or T_2. Therefore, if the three scenarios have the same probability of occurrence, it would be optimum to operate in either topology T_1 or topology T_2, since on average, they would have the minimum loads left unserved or out of service during the predicted outages.

Case B considers three outage scenarios, each with four lines as predicted outage locations as shown in Table 6.16. Using the MILP formulation, the optimal topology T_i for each scenario is determined in the proactive topology optimization stage. The optimal topologies for scenarios S_1, S_2 and S_3 are topologies T_1, T_2 and T_3, respectively. In this case, topologies T_2 and T_3 are the same, and this is denoted as $T_2 = T_3$. The status of the switchable lines for each topology is presented in Table 6.17.

Table 6.20 presents the out-of-service loads, L_{ij} in each topology T_i in the event of each scenario S_j. In scenario S_1, the unserved loads are lowest when operating in topology T_1. In scenarios S_2 and S_3, the unserved loads are lowest when operating in topology $T_2 = T_3$. Next, the additional unserved loads, ΔL_{ij} in each topology during each scenario are estimated and shown in Table 6.21. As expected, ΔL_{11} and ΔL_{22} are both 0 kW since there are no additional unserved loads when operating in the optimal topology. Similarly, ΔL_{23} is also 0 kW since T_2 is the optimal topology for scenario S_3. The results show that T_2 has a lower average cost (20 kW) compared to T_1 (266.67 kW). Operating in T_1 prior to the predicted outages would result in about ten times additional unserved loads compared to T_2. Hence, it is more optimal to operate in T_2 ahead of the predicted outages when they have equal probability of occurring.

Overall, the multiple outage cases presented could assist distribution system op-

Table 6.20: Multiple Outage Case B: Out-of-service loads (kW) in modified IEEE 123-bus feeder

Scenario	**Topology**	
	$\mathbf{T}_1$	$\mathbf{T}_2 = \mathbf{T}_3$
S_1	$L_{11} = 555$	$L_{21} = 615$
S_2	$L_{12} = 700$	$L_{22} = 145$
S_3	$L_{13} = 945$	$L_{23} = 700$

Table 6.21: Multiple Outage Case B: Additional out-of-service loads (kW) in modified IEEE 123-bus feeder

Scenario	**Topology**	
	$\mathbf{T}_1$	$\mathbf{T}_2 = \mathbf{T}_3$
S_1	0	60
S_2	555	0
S_3	245	0
Average Cost	266.67 kW	20.00 kW

erators in deciding which topology to operate in when faced with a set of outage scenarios with equal probability or likelihood of occurring. The chosen topologies in the cases considered resulted in the lowest additional out-of-service loads compared to the other topologies. Although the multiple outage case presented in this work has been limited to just three outage scenarios, it can be expanded to include more scenarios. This could result in more topologies depending on the number of switchable lines and the topological flexibility of the system. Alternatively, a topology may be optimal for more than one outage scenario, as shown in cases B in both feeders. This reduces the computation required to determine the optimal topology.

6.3.3 Case III: Weighted Multiple Outage Case

A limitation of the multiple outage case is that it assumes each outage scenario has the same chance of occurring; however, this is unlikely to be the case. Hence, the weighted multiple outage case extends the multiple outage case by finding a network topology that minimizes the impact of predicted outage scenarios weighted

based on their likelihood of occurring. Each predicted scenario is assigned weights corresponding to its probability of occurring in the distribution network. In the following sections, the weighted multiple outage case is tested on the modified IEEE 13-node and 123-node test feeders. In addition, a sensitivity analysis is carried out by changing the weights assigned to each scenario to see how that affects the optimal topology chosen.

6.3.3.1 Case III.A: IEEE 13-bus Feeder

The weighted multiple outage case is applied to the modified IEEE 13-bus feeder using the same scenarios from the multiple outage case presented in Table 6.10. Each outage scenario is given a weight based on its likelihood of occurring, and the weights for all scenarios sum up to 1. In the two cases considered in this section (Cases A and B), the three scenarios are randomly assigned weights of 68%, 17% and 15% respectively as shown in Table 6.22. Therefore, scenario S_1 is assumed to have the highest chance of occurring (68% probability), followed by scenario S_2 (17% probability) and then scenario S_3 (15% probability). The most likely scenario is scenario S_1 (68% probability), followed by scenario S_2 (17% probability) and finally scenario S_3 (15% probability). The out-of-service loads, L_{ij} and additional out-of-service loads, ΔL_{ij} are estimated as in the multiple outage case (see Tables 6.12 and 6.13). Then, the weights are multiplied by the additional unserved loads in each scenario as shown in Table 6.22. The product of each scenario weight and the out-of-service loads in each topology is summed to obtain the weighted cost of each topology, ${}^{w}C_i$, as represented in (5.30).

In Case A, the results show that T_2 is the optimum topology since it has the lowest weighted cost compared to the other two topologies.

Furthermore, a sensitivity analysis is performed by varying the weight for each outage scenario between 0 and 1 in increments of 10% (0.1) for a total of 66 possible scenarios. The analysis also includes the case where each outage scenario has the

Table 6.22: Weighted Multiple Outage Case A: Computing weighted cost for modified IEEE 13-bus feeder

Scenario	**Weight** (w)	**Topology**		
		$\mathbf{T}_1$	$\mathbf{T}_2$	$\mathbf{T}_3$
S_1	0.68	$w_1 \cdot \Delta L_{11}$ $= 0.68(0) = 0$	$w_1 \cdot \Delta L_{21}$ $= 0.68(0) = 0$	$w_1 \cdot \Delta L_{31}$ $= 0.68(130) = 88.40$
S_2	0.17	$w_2 \cdot \Delta L_{12}$ $= 0.17(280) = 47.60$	$w_2 \cdot \Delta L_{22}$ $= 0.17(0) = 0$	$w_2 \cdot \Delta L_{32}$ $= 0.17(280) = 47.60$
S_3	0.15	$w_3 \cdot \Delta L_{13}$ $= 0.15(130) = 19.50$	$w_3 \cdot \Delta L_{23}$ $= 0.15(130) = 19.50$	$w_3 \cdot \Delta L_{33}$ $= 0.15(0) = 0$
Weighted Cost		67.10 kW	19.50 kW	136.00 kW

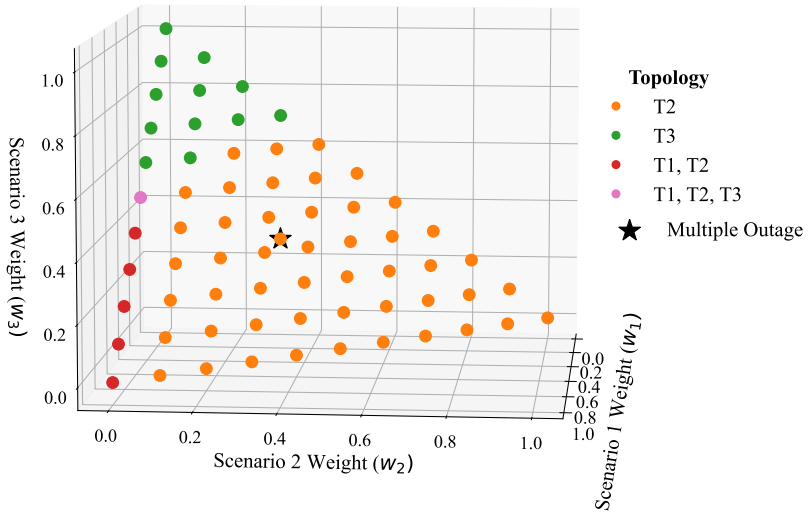

Figure 6.7: IEEE 13-bus Weighted Multiple Outage Case A: Sensitivity analysis

same likelihood of occurring (33.33%). Fig. 6.7 shows a 3D scatterplot of the optimal topologies chosen as the weights for the three outage scenarios in case A are varied between 0 and 1. Based on the plot, T_2 (represented by the orange dots) is the optimal topology for most scenarios (over 70%), while T_3 (represented by the green dots) is chosen as optimal in 18% of the scenarios. For 7% of the scenarios, operating in either T_1 or T_2 would be optimal. In the scenario where $w_1 = 0.5, w_2 = 0$ and $w_3 = 0.5$ (represented by the pink dot), it would be optimal to operate in any of the three topologies. The point denoted by the black star corresponds to when the three

outage scenarios have the same probability of occurrence (33.33%) as demonstrated in the multiple outage case.

The results for Case B are presented in Table 6.23. T_2 has the lower weighted cost, and is therefore the optimal topology to operate in prior to the predicted outages. Fig. 6.8 shows the results of sensitivity analysis in the weighted multiple outage for case B of the modified IEEE 13-node test feeder. T_1 and T_2 are chosen as the optimal topologies for the same number of cases, about 45% , respectively. Recall from Table 6.14 that topologies T_1 and T_3 are the same (hence the notation $T_1 = T_3$). In

Table 6.23: Weighted Multiple Outage Case B: Computing weighted cost for modified IEEE 13-bus feeder

Scenario	**Weight** (w)	**Topology**	
		$\mathbf{T}_1 = \mathbf{T}_3$	$\mathbf{T}_2$
S_1	0.68	$w_1 \cdot \Delta L_{11}$ $= 0.68(0) = 0$	$w_1 \cdot \Delta L_{21}$ $= 0.68(0) = 0$
S_2	0.17	$w_2 \cdot \Delta L_{12}$ $= 0.17(130) = 22.10$	$w_2 \cdot \Delta L_{22}$ $= 0.17(0) = 0$
S_3	0.15	$w_3 \cdot \Delta L_{13}$ $= 0.15(0) = 0$	$w_3 \cdot \Delta L_{23}$ $= 0.15(130) = 19.50$
Weighted Cost		22.10 kW	19.50 kW

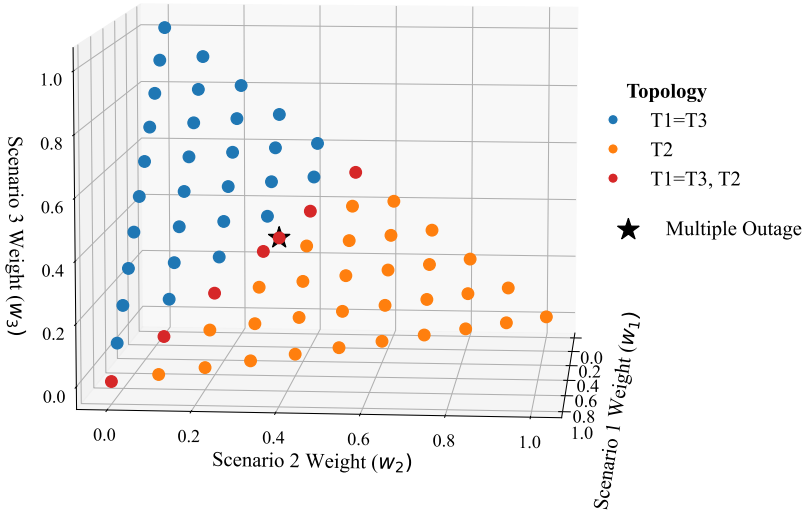

Figure 6.8: IEEE 13-bus Weighted Multiple Outage Case B: Sensitivity analysis

the remaining 10% of the cases, it is optimum to operate in either T_1 or T_2 (indicated by the red dots in the scatterplot in Fig. 6.8); these points form the boundary between cases where operating in T_1 is optimal and cases where operating in T_2 is optimal. A list of the weighted costs for each topology for all combinations of w_1, w_2, and w_3 can be found in Table C.1 of Appendix C.1.

6.3.3.2 Case III.B: IEEE 123-bus Feeder

In this section, the weighted multiple outage case is demonstrated with the modified IEEE 123-bus feeder using the same scenarios presented in Table 6.16 for the multiple outage cases. For the three outage scenarios considered, the same weights of 68%, 17%, and 15% from the modified 13-bus feeder are used. As previously described, this corresponds with the assumption that the first outage scenario, S_1 has a probability of 68% while scenarios S_2 and S_3 have probabilities of 17% and 15%, respectively.

As described in the previous section, the optimal topology for each outage scenario is first determined from the topology optimization stage as shown in Section 6.3.1.2. Then, the out-of-service loads, L_{ij} and additional out-of-service loads, ΔL_{ij} are estimated as shown in Table 6.18 from the multiple outage case. In each topology, the additional out-of-service loads are multiplied by the weights, w_j, of each scenario. The weighted cost, ${}^{w}C_i$ for each topology, T_i, is calculated by summing the products from the previous step.

In Case A, the weighted costs are presented in Table 6.24. Since T_1 has the lowest weighted cost, it is chosen as the optimal topology. In the multiple outage case, which assumed equal weights for each outage scenario, T_1 and T_2 were chosen as the optimal topologies. In contrast, the higher weight (68%) assigned to scenario S_1 in the weighted case gives its optimum topology, T_1 a higher preference (and reduces its weighted cost). Hence, T_1 is chosen as the optimum in the weighted case.

A sensitivity analysis is performed by varying the weight of each outage scenario from 0 to 1 in 10% increments. Fig. 6.9 displays a 3D scatterplot of the optimal

Table 6.24: Weighted Multiple Outage Case A: Computing weighted cost for modified IEEE 123-bus feeder

Scenario	**Weight** (w)	**Topology**		
		$\mathbf{T}_1$	$\mathbf{T}_2$	$\mathbf{T}_3$
S_1	0.68	0	74.80	251.60
S_2	0.17	18.70	0	84.15
S_3	0.15	69.75	69.75	0
Weighted Cost		88.45 kW	144.55 kW	335.75 kW

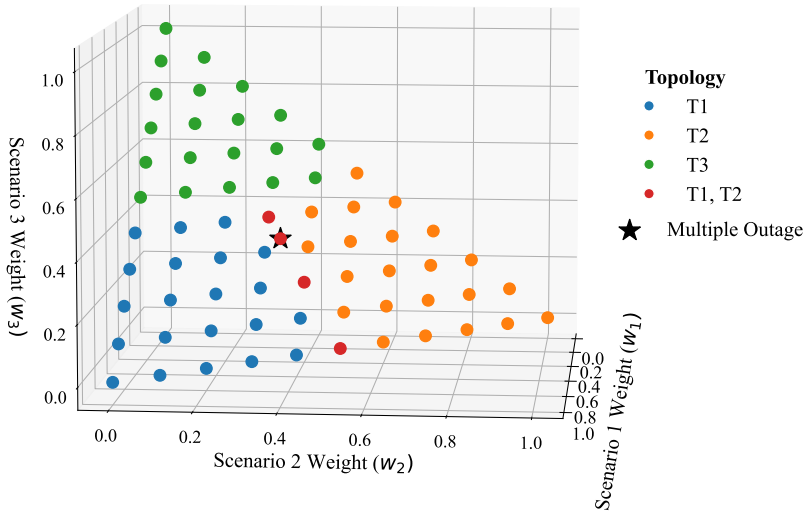

Figure 6.9: IEEE 123-bus Weighted Multiple Outage Case A: Sensitivity analysis

topologies chosen as the weights for the three outage scenarios are varied from 0 to 1. T_1 (blue dots) is optimal in approximately 30% of weight combinations. This is also true for T_2 (orange dots) and T_3 (green dots). Furthermore, T_1 is the optimal topology for at least 95% of the weight combinations in which $w_1 \geq 0.5$. T_2 is the optimal topology (or at least one of the optimal topologies) chosen when $w_2 \geq 0.5$, while T_3 is the optimal topology chosen when $w_3 \geq 0.5$. In about 6% of the weight combinations, where $w_1 = w_2$ and $0.3 \leq (w_1, w_2) \leq 0.5$, T_1 and T_2 have the same weighted costs; hence it is possible to operate in either T_1 or T_2 in these cases.

In case B, the optimal topologies for outage scenarios S_2 and S_3 are the same and this is denoted as $T_2 = T_3$ in Table 6.25. Topology $T_2 = T_3$ is the chosen optimal

Table 6.25: Weighted Multiple Outage Case B: Computing weighted cost for modified IEEE 123-bus feeder

Scenario	**Weight** (w)	**Topology**	
		$\mathbf{T}_1$	$\mathbf{T}_2 = \mathbf{T}_3$
S_1	0.68	0	40.80
S_2	0.17	94.35	0
S_3	0.15	36.75	0
Weighted Cost		131.10 kW	40.80 kW

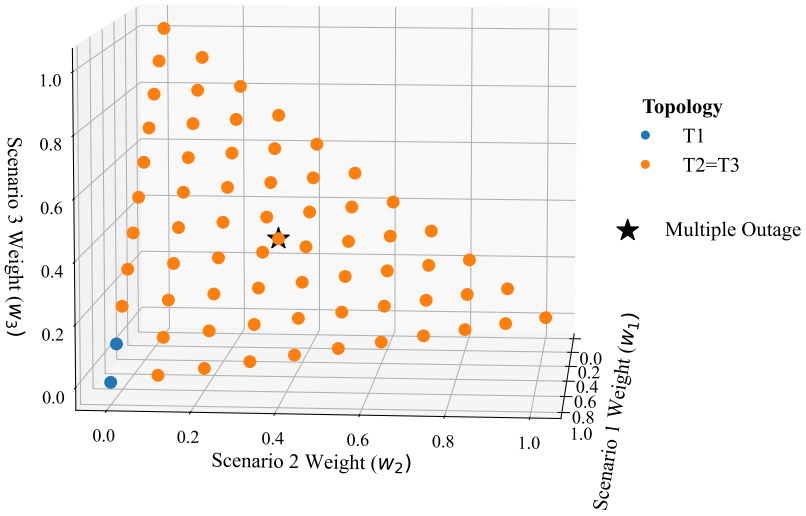

Figure 6.10: IEEE 123-bus Weighted Multiple Outage Case B: Sensitivity analysis

topology for the three outage scenarios since it has the lower weighted cost (40.80 kW) compared to T_1 (131.10 kW). This case shows that the optimal topology for the scenario with the highest probability is not automatically selected as the optimal topology across the outage scenarios considered. The additional loads left out-of-service in each topology are taken into consideration when determining the overall optimal topology.

Again, a sensitivity analysis is conducted by varying the scenario weights as previously described. Fig. 6.10 displays a 3D scatterplot of the selected topologies based on combinations of the outage scenario weights w_1, w_2 and w_3. For 97% of the weight combinations considered, topology $T_2 = T_3$ (orange dots) is selected, while T_1 (blue

dots) is selected for just two cases ($w_1 = 0.9, w_3 = 0.1$) and ($w_1 = 1.0$). This is because on average, $T_2 = T_3$ has less additional out-of-service loads compared to T_1. Hence, in the given outage scenarios, if prior knowledge about the probability of each outage is unknown, then the network can be operated in topologies $T_2 = T_3$. This would result in a lower amount of out-of-service loads on average.

The points denoted by the black star in Figures 6.9 and 6.10 represent the case where the three outage scenarios have the same probability of occurrence as shown in Tables 6.19 and 6.21 for the multiple outage case. Table C.2 in Appendix C.2 provides the values of weighted costs and selected topologies for the combinations of w_1, w_2 and w_3 considered in the cases presented for the modified IEEE 123-bus feeder.

6.4 Validation of MILP Power Flow Model

The linear power flow model used in the MILP formulation presented in this work (in (5.9a) to (5.9g)) is based on the DistFlow equations presented in [80, 113]. In this section, the linear power flow model is validated by comparing power flow results from the MILP model to power flow results from OpenDSS, an electric power distribution system simulator [126]. This is done using the modified IEEE 13-bus and 123-bus feeders that were presented earlier in this chapter in Section 6.2. A comparison of power flow results is also performed with different loading conditions for each feeder.

6.4.1 Modified IEEE 13-bus Feeder

For the modified 13-bus test feeder, Tables 6.26, 6.27 and 6.28 compare voltage magnitude (p.u.), active power (kW) and reactive power (kW) values, respectively, from the linear power flow model with values from OpenDSS.

Overall, the node voltages from OpenDSS are lower than those from the MILP. A maximum error of 0.0168 p.u. was recorded at bus 675, and an average error of 0.0092 p.u. was recorded across all buses. The average errors for real and reactive power are approximately 0.55% and 3.52%, respectively. The OpenDSS line flows are

all higher than the MILP line flows, primarily because line losses are not considered in the MILP model. As a result, the MILP model error in power flowing from the substation (19.01 kW + j50.91 kVar) is approximately equal to the OpenDSS total feeder losses (19.0 kW + j52.2 kVar).

In addition, the loading conditions are varied by adjusting every load in the modified 13-bus feeder from 30% to 110% of its rated value. All node voltages are maintained between 0.95 p.u. and 1.05 p.u., while the substation bus voltage (bus 650) is maintained at 1.05 p.u. Fig. 6.11 shows a plot of OpenDSS line apparent power (kVA) versus MILP line apparent power (calculated from values of P_{ij}^{BR} and Q_{ij}^{BR}). The data points in the plot are colored based on the load multipliers used (from 30% to 110%). The plot shows a high positive correlation ($R^2 = 0.9979$) between the MILP and OpenDSS line apparent power results (kVA).

Overall, the results show that the MILP model provides a reasonable approximation of the nonlinear power flow model.

Table 6.26: Power flow results for modified IEEE 13-bus feeder: Voltage magnitude (p.u.)

Node	**Voltage Magnitude (p.u.)**		**Error (p.u.)**
	MILP	OpenDSS	
650	1.0500	1.0499	0.0001
632	1.0435	1.0429	0.0006
633	1.0419	1.0395	0.0024
634	1.0412	1.0375	0.0037
675	1.0200	1.0032	0.0168
645	1.0420	1.0383	0.0037
646	1.0415	1.0368	0.0047
671	1.0203	1.0065	0.0138
680	1.0203	1.0065	0.0138
684	1.0199	1.0049	0.0150
611	1.0199	1.0043	0.0156
652	1.0191	1.0029	0.0162
692	1.0203	1.0065	0.0138

Table 6.27: Power flow results for modified IEEE 13-bus feeder: Real power (kW)

Line No.	From Node	To Node	Real Power (kW)		Error (kW)
			MILP	OpenDSS	
1	650	632	1150	1169.01	19.01
2	632	633	135	135.48	0.48
3	633	634	135	135.17	0.17
4	632	645	130	130.58	0.58
5	645	646	75	75.09	0.09
6	632	671	820	837.65	17.65
7	671	692	335	336.05	1.05
8	692	675	280	281.05	1.05
9	671	684	100	100.28	0.28
10	684	611	55	55.04	0.04
11	684	652	45	45.10	0.10
12	671	680	0	0	0
13	633	692	0	0	0
14	646	611	0	0	0
15	675	680	0	0	0

Table 6.28: Power flow results for modified IEEE 13-bus feeder: Reactive power (kVar)

Line No.	From Node	To Node	Reactive Power (kVar)		Error (kVar)
			MILP	OpenDSS	
1	650	632	470	520.91	50.91
2	632	633	95	95.80	0.80
3	633	634	95	95.30	0.30
4	632	645	85	85.59	0.59
5	645	646	45	45.09	0.09
6	632	671	250	298.62	48.62
7	671	692	5	4.31	0.69
8	692	675	-45	-45.69	0.69
9	671	684	25	24.97	0.03
10	684	611	-5	-5.21	0.21
11	684	652	30	30.04	0.04
12	671	680	0	0	0
13	633	692	0	0	0
14	646	611	0	0	0
15	675	680	0	0	0

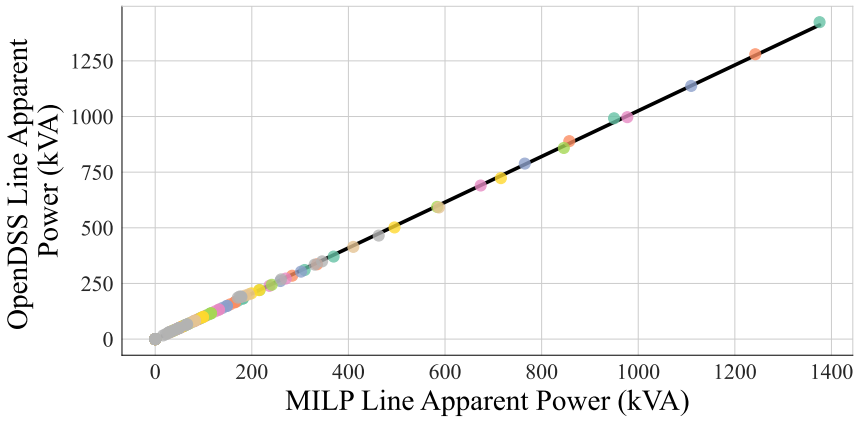

Figure 6.11: Correlation between MILP power flow results and OpenDSS results: Line apparent power (kVA) in modified IEEE 13-bus feeder

6.4.2 Modified IEEE 123-bus Feeder

The MILP model is also validated using the modified IEEE 123-bus feeder to demonstrate its performance on a larger system. Detailed results of voltage magnitude (p.u.) and line flows (kW and kVar) from the MILP power flow and OpenDSS are presented in Tables A.6 to A.8 in Appendix A.1.1.

The MILP and OpenDSS voltage results show that all the node voltages lie within the required limits of 0.95 p.u. and 1.05 p.u. For voltages, the maximum error is 0.0321 p.u. at bus 66, and the average error is 0.0215 p.u. The node voltages from OpenDSS are all lower than those from the MILP. For real power, the average error is 0.40% (2.47 kW) while the average error for reactive power line flow is 1.59%. Line flows from OpenDSS are all higher than MILP line flows for this system, due to line losses that are not included in the MILP model. The error in power flowing from the substation in the MILP model (46.78 kW + j95.578 kVar) corresponds to the total feeder losses in the OpenDSS model (46.8 kW + j105.8 kVar). The larger error in reactive power flow may be a result of the higher number of voltage regulators and capacitors in the system compared to the modified IEEE 13-bus system.

Additionally, the loading conditions in the feeder are varied by adjusting the feeder

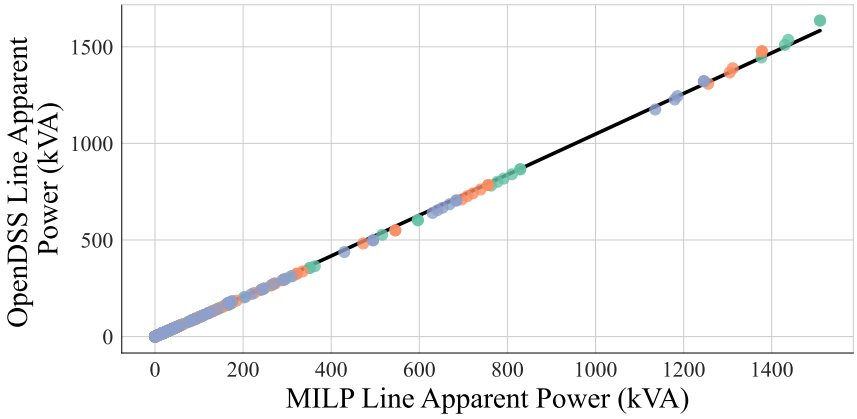

Figure 6.12: Correlation between MILP power flow results and OpenDSS results: Line apparent power (kVA) in modified IEEE 123-bus feeder

loads from 100% to 120% of their rated values. Fig. 6.12 shows the relationship between the line apparent power values from the MILP and OpenDSS models. The plot shows a high correlation between the MILP and OpenDSS line apparent power results (kVA) ($R^2 = 0.9995$).

6.5 Summary

In this chapter, the proposed proactive topology optimization and service restoration framework was applied to modified versions of the IEEE 13-bus and IEEE 123-bus test feeders. Both systems were assumed to be balanced. For topological flexibility in the distribution network, all the lines in the 13-bus system were assumed to be switchable. Both systems were tested with three optimization cases: single outage, multiple outage and weighted multiple outage.

For the single outage cases, the proposed framework was applied to determine the optimal topology that minimizes the impact of a given predicted outage scenario. The results in the single outage cases showed that reducing the power flowing through the predicted outage locations also reduced the loads that would be left unserved if the outages occurred as predicted. In both stages, the new topologies led to a decrease in the unserved loads in most of the cases considered. Additionally, these topologies were achieved within the specified number of switching operations. The computation

time was less than 2 seconds in each case. The proposed method was able to find feasible topologies even for the 123-bus system, which had fewer switchable lines than the 13-bus system.

For the multiple outage cases, the proposed topology optimization and service restoration framework was applied to minimize the impact of outages across different outage scenarios. The out-of-service loads and additional loads left out of service were estimated for each combination of topologies and scenarios considered. The topology (or topologies) with the lowest average cost was selected as the optimal topology to operate in prior to the predicted outage.

The weighted multiple outage cases extended the multiple outage cases by minimizing the impact of the predicted outage scenarios weighted on their likelihood of occurrence. The optimal operating topology was determined by selecting the topology (or topologies) with the lowest weighted costs. Furthermore, sensitivity analyses were performed by assigning different weights to each outage scenario. The results showed that the optimal topology for the scenario with the highest weight may not be the overall optimal; it is important to consider the loads left out of service for each topology during each outage scenario. Based on the results of the sensitivity analyses, the operating topology may be selected even without prior knowledge of the probability of each outage scenario.

Lastly, the linear power flow model used in the MILP formulation of the proposed framework was validated using results from OpenDSS, an open-source simulation tool for electric power distribution systems. In both test systems, the values of voltage magnitude (p.u.), active power (kW), and reactive power (kVar) through the lines from the MILP power flow were compared with OpenDSS results. The errors in the results were within acceptable limits.

CHAPTER 7: CONCLUSION AND FUTURE WORK

7.1 Overview

This chapter summarizes the contributions and key findings of this dissertation, followed by recommendations and ideas for future research.

7.2 Concluding Remarks

The work presented in this dissertation addresses the need for a more proactive approach to outage management in distribution systems. To improve current outage management practices, which are largely reactive, it would be beneficial to implement a holistic approach that integrates outage forecasts into the service restoration process.

As a first step, this work presented a detailed analysis of outage data to determine what features have the most impact on outage frequency and average duration in a distribution network. Two machine learning methods, random forest and gradient boosting, were used to rank the importance of each outage variable with regard to average outage duration. Climatic description, failed equipment and wind speed were found to be the top three features explaining the variability of outage duration for the distribution network considered.

Furthermore, this dissertation presented a proactive topology optimization and service restoration framework that leveraged outage forecasts to mitigate the impacts of distribution system outages. The proposed framework was formulated as a mixed integer linear programming (MILP) problem with two stages: a topology optimization stage that minimized the loads left out of service prior to the predicted outage, and a service restoration stage that maximized the loads restored in the network af-

ter the predicted outage occurred. The resulting network topology from each stage was derived by changing the status of switchable lines in the network to achieve each objective subject to the specified problem constraints. The results of topology optimization showed that by minimizing power flow through the predicted outage locations, the loads left out of service as a result of the outage were minimized.

To implement the proposed framework, three optimization cases were considered as follows: single outage, multiple outage and weighted multiple outage. Also, a sensitivity analysis was performed by assigning different weights to each outage scenario to assess how the weights affected the selected optimal topology.

In most of the single outage cases considered, the proposed framework was able to determine an optimal topology that led to a reduction of at least 10% in the loads left out of service due to the predicted outage compared to the original network topology. In the multiple outage cases, it was observed that more than one topology may be optimal across the predicted outage scenarios considered. Based on results from the weighted multiple outage cases, the optimal topology for the outage scenario with the highest weight may not necessarily be the overall optimum for all the scenarios considered. So, it is crucial to take into account the loads left out of service in each topology during each outage scenario. Furthermore, using plots from sensitivity analysis results, the optimal operational topology may be selected even without prior knowledge of the weights assigned to each outage scenario.

In general, this dissertation provides a method for improving situational awareness within the distribution system. Using the proposed approach, distribution system operators can determine what topology to operate in ahead of predicted outages, thereby reducing the loads left out of service.

7.3 Summary of Contributions

The contributions of this work are summarized as follows:

- A topology optimization and service restoration framework was proposed for

proactive outage management in the distribution system. The framework was formulated using mixed integer linear programming (MILP) with the following objectives: 1) minimize the loads left out of service prior to the outage and 2) maximize the restorable load when the outage occurs as predicted. The proposed framework was implemented by considering three sets of optimization cases as follows: single outage, multiple outage and weighted multiple outage cases.

- A sensitivity analysis based on the weighted multiple outage case was presented in order to determine the optimal topology to operate in given a range of probabilities for the outage locations in the distribution system.

- The frequency and duration of power system outages in a distribution system were analyzed based on several features in an outage management dataset. The following features were considered in this analysis: outage cause, interrupted phase, voltage level of the affected circuit, climatic description, and calendar variables. Two machine learning techniques, random forest and gradient boosting were used to rank these features based on their significance in predicting average outage duration.

7.4 Future Work

This section discusses some ideas to extend the work presented in this dissertation as well as its limitations.

- The test feeders used to demonstrate the proposed framework in this dissertation were assumed to be balanced three-phase systems. Real-world distribution networks, however, are inherently unbalanced. The proposed MILP formulation can thus be extended to accommodate unbalanced three-phase power flows. To further test the scalability of the framework, it can be applied to larger test

systems such as the EPRI Test Circuits and [121]. The proposed method may be further investigated by including distributed energy resource (DER) in the test feeders.

- Similarly, the problem could be formulated as a robust optimization model that incorporates the uncertainty associated with outages occurring in the distribution network. In this case, outage locations would be predicted using actual forecasts. Moreover, a robust optimization model would better capture the variations in the system due to changing load demand.

- Another consideration is the issue of priority or critical customers such as hospitals, fire departments, airports, etc. The MILP formulation in this work assumed that all loads in the distribution network have the same priority during the service restoration process. It is possible to prioritize critical loads in the service restoration stage by assigning weights to all loads, with higher weights assigned to critical loads. This would involve incorporating the weights into the load constraints of the MILP problem. Furthermore, the objective function would be modified so that it maximizes the amount of critical loads that can be restored while also maximizing the amount of overall load that can be restored in the distribution system. In the resulting multiobjective problem, critical loads would be prioritized during service restoration.

- Reliability is of critical importance in distribution systems. In this work, power system reliability indices such as SAIDI, SAIFI and CAIDI could be considered by modifying the objective function in either stage of the proposed framework so that outage duration or number of customers affected by an outage is minimized.

- Finally, distribution system operators can gain even deeper and more actionable insights into proactively managing outages by combining modeling and simulation results from this work with interactive visualizations.

REFERENCES

[1] H. Farhangi, "The path of the smart grid," *IEEE Power and Energy Magazine*, vol. 8, pp. 18–28, Jan/Feb 2010.

[2] V. C. Gungor, D. Sahin, T. Kocak, S. Ergut, C. Buccella, C. Cecati, and G. P. Hancke, "A Survey on smart grid potential applications and communication requirements," *IEEE Transactions on Industrial Informatics*, vol. 9, pp. 28–42, Feb 2013.

[3] J. W. Busby, K. Baker, M. D. Bazilian, A. Q. Gilbert, E. Grubert, V. Rai, J. D. Rhodes, S. Shidore, C. A. Smith, and M. E. Webber, "Cascading risks: Understanding the 2021 winter blackout in texas," *Energy Research & Social Science*, vol. 77, p. 102106, 2021.

[4] M. Puleo, "Damages from Feb. winter storms could be as high as $155 billion." [Online], March 2021. Accessed: Sep 3, 2021.

[5] W. A. Wulf, "Great Achievements and Grand Challenges," *The Bridge*, vol. 30, no. 3 & 4, pp. 5–10, 2000.

[6] G. Constable and B. Somerville, eds., *A Century of Innovation: Twenty Engineering Achievements that Transformed our Lives*. Washington, DC: The National Academies Press, 2003.

[7] "Resilience Framework, Methods, and Metrics for the Electricity Sector," tech. rep., IEEE Power & Energy Society Industry Technical Support Leadership Committee Task Force, Oct 2020.

[8] W. Scott, "Automating the restoration of distribution services in major emergencies," *IEEE Transactions on Power Delivery*, vol. 5, pp. 1034–1039, Apr 1990.

[9] C. L. Benner, R. A. Peterson, and B. D. Russell, "Application of DFA Technology for Improved Reliability and Operations," *2017 IEEE Rural Electric Power Conference (REPC)*, 2017.

[10] T. Nielsen, "Improving outage restoration efforts using rule-based prediction and advanced analysis," in *2002 IEEE Power Engineering Society Winter Meeting. Conference Proceedings (Cat. No.02CH37309)*, vol. 2, (New York, NY), pp. 866–869, IEEE, Jan 2002.

[11] C. Chen, J. Wang, and D. Ton, "Modernizing Distribution System Restoration to Achieve Grid Resiliency Against Extreme Weather Events: An Integrated Solution," *Proceedings of the IEEE*, vol. 105, pp. 1267–1288, Jul 2017.

[12] R. Mitra, R. Kota, S. Bandyopadhyay, V. Arya, B. Sullivan, R. Mueller, H. Storey, and G. Labut, "Voltage Correlations in Smart Meter Data," in *Proceedings of the 21th ACM SIGKDD International Conference on Knowledge Discovery and Data Mining*, KDD '15, (New York, NY, USA), pp. 1999–2008, Association for Computing Machinery, Aug 2015.

[13] T. A. Short, "Advanced Metering for Phase Identification, Transformer Identification, and Secondary Modeling," *IEEE Transactions on Smart Grid*, vol. 4, pp. 651–658, Jun 2013.

[14] "Electric Power Annual 2019," tech. rep., U.S. Energy Information Administration (EIA), Washington DC, Feb 2021.

[15] N. Yu, S. Shah, R. Johnson, R. Sherick, M. Hong, and K. Loparo, "Big data analytics in power distribution systems," in *2015 IEEE Power & Energy Society Innovative Smart Grid Technologies Conference (ISGT)*, (Washington DC), pp. 1–5, IEEE, Feb 2015.

[16] H. Tram, "Technical and operation considerations in using Smart Metering for outage management," in *2008 IEEE/PES Transmission and Distribution Conference and Exposition*, pp. 1–3, IEEE, Apr 2008.

[17] G. Pritchard, "Reading Deeper," *IEEE Power and Energy Magazine*, vol. 8, pp. 85–87, Nov 2010.

[18] "Advanced Metering Infrastructure and Customer Systems - Results from the Smart Grid Investment Grant Program," tech. rep., Office of Electricity Delivery and Energy Reliability, U.S. Department of Energy, Sep 2016.

[19] Z. Li, F. Yang, S. Mohagheghi, Z. Wang, J. Tournier, and Y. Wang, "Toward smart distribution management by integrating advanced metering infrastructure," *Electric Power Systems Research*, vol. 105, pp. 51–56, Dec 2013.

[20] M. Doostan and B. H. Chowdhury, "Power distribution system equipment failure identification using machine learning algorithms," in *2017 IEEE Power & Energy Society General Meeting*, pp. 1–5, IEEE, Jul 2017.

[21] D. Cerrai, D. W. Wanik, M. A. E. Bhuiyan, X. Zhang, J. Yang, M. E. B. Frediani, and E. N. Anagnostou, "Predicting Storm Outages Through New Representations of Weather and Vegetation," *IEEE Access*, vol. 7, pp. 29639–29654, Mar 2019.

[22] M. Yue, T. Toto, M. P. Jensen, S. E. Giangrande, and R. Lofaro, "A Bayesian Approach-Based Outage Prediction in Electric Utility Systems Using Radar Measurement Data," *IEEE Transactions on Smart Grid*, vol. 9, pp. 6149–6159, Nov 2018.

[23] M. S. Bashkari, A. Sami, and M. Rastegar, "Outage Cause Detection in Power Distribution Systems Based on Data Mining," *IEEE Transactions on Industrial Informatics*, vol. 17, pp. 640–649, Jan 2021.

[24] M. Sullivan, J. Schellenberg, and M. Blundell, "Updated Value of Service Reliability Estimates for Electric Utility Customers in the United States," Tech. Rep. LBNL-6941E, Lawrence Berkeley National Laboratory (LBNL), Berkeley, CA (United States), Jan 2015.

[25] M. Matousek, "Delta says it lost up to $50 million because of the Atlanta airport power outage." [Online], December 2017. Accessed: Sep 6, 2021.

[26] P. M. Curtis, *Energy and Cyber Security and its Effect on Business Resiliency*, ch. 2, p. 39. John Wiley & Sons, Ltd, 2020.

[27] "IEEE Guide for Collecting, Categorizing, and Utilizing Information Related to Electric Power Distribution Interruption Events," *IEEE Std 1782-2014*, pp. 1–98, Aug 2014.

[28] American Public Power Association, "Infographic: Top causes for power outages." [Online], March 2017. Accessed: Sep 29, 2021.

[29] Mo-Yuen Chow and L. Taylor, "A novel approach for distribution fault analysis," *IEEE Transactions on Power Delivery*, vol. 8, no. 4, pp. 1882–1889, 1993.

[30] L. Xu and M. Y. Chow, "Power distribution systems fault cause identification using logistic regression and artificial neural network," in *Proceedings of the 13th International Conference on Intelligent Systems Application to Power Systems, ISAP'05*, pp. 163–168, IEEE, 2005.

[31] L. Xu, M. Y. Chow, and J. Timmis, "Power distribution outage cause identification using Fuzzy Artificial Immune Recognition Systems (FAIRS) algorithm," in *2007 IEEE Power Engineering Society General Meeting, PES*, pp. 1–8, IEEE, Jun 2007.

[32] L. Xu and M. Y. Chow, "Distribution fault diagnosis using a hybrid algorithm of Fuzzy classification and Artificial Immune systems," in *IEEE Power and Energy Society 2008 General Meeting: Conversion and Delivery of Electrical Energy in the 21st Century, PES*, pp. 1–6, IEEE, Jul 2008.

[33] M. Doostan, R. Sohrabi, and B. Chowdhury, "A data-driven approach for predicting vegetation-related outages in power distribution systems," *International Transactions on Electrical Energy Systems*, vol. 30, Jan 2020.

[34] D. Radmer, P. Kuntz, R. Christie, S. Venkata, and R. Fletcher, "Predicting vegetation-related failure rates for overhead distribution feeders," *IEEE Transactions on Power Delivery*, vol. 17, pp. 1170–1175, Oct 2002.

[35] T. Dokic and M. Kezunovic, "Predictive Risk Management for Dynamic Tree Trimming Scheduling for Distribution Networks," *IEEE Transactions on Smart Grid*, vol. 10, pp. 4776–4785, Sep 2018.

[36] M. Kezunovic, Z. Obradovic, T. Dokic, B. Zhang, J. Stojanovic, P. Dehghanian, and P.-C. Chen, "Predicting Spatiotemporal Impacts of Weather on Power Systems Using Big Data Science," in *Data Science and Big Data: An Environment of Computational Intelligence* (W. Pedrycz and S.-M. Chen, eds.), vol. 24 of *Studies in Big Data*, pp. 265–299, Springer, Cham, 2017.

[37] H. Liu, R. A. Davidson, D. V. Rosowsky, and J. R. Stedinger, "Negative Binomial Regression of Electric Power Outages in Hurricanes," *Journal of Infrastructure Systems*, vol. 11, pp. 258–267, Dec 2005.

[38] H. Liu, R. A. Davidson, and T. V. Apanasovich, "Spatial generalized linear mixed models of electric power outages due to hurricanes and ice storms," *Reliability Engineering & System Safety*, vol. 93, pp. 897–912, Jun 2008.

[39] D. W. Wanik, E. N. Anagnostou, B. M. Hartman, M. E. B. Frediani, and M. Astitha, "Storm outage modeling for an electric distribution network in Northeastern USA," *Natural Hazards*, vol. 79, pp. 1359–1384, Nov 2015.

[40] J. He, D. W. Wanik, B. M. Hartman, E. N. Anagnostou, M. Astitha, and M. E. B. Frediani, "Nonparametric Tree-Based Predictive Modeling of Storm Outages on an Electric Distribution Network," *Risk Analysis*, vol. 37, pp. 441–458, Mar 2017.

[41] M. Doostan and B. Chowdhury, "Statistical Analysis of Animal-Related Outages in Power Distribution Systems - A Case Study," in *2019 IEEE Power & Energy Society General Meeting (PESGM)*, (Atlanta, GA), pp. 1–5, IEEE, Aug 2019.

[42] S. Sahai and A. Pahwa, "A Probabilistic Approach for Animal-Caused Outages in Overhead Distribution Systems," in *2006 International Conference on Probabilistic Methods Applied to Power Systems*, pp. 1–7, IEEE, Jun 2006.

[43] P. Kankanala, A. Pahwa, and S. Das, "Estimating Animal-Related Outages on Overhead Distribution Feeders Using Boosting," *IFAC-PapersOnLine*, vol. 48, pp. 270–275, Jan 2015.

[44] M. Gui, A. Pahwa, and S. Das, "Bayesian network model with Monte Carlo simulations for analysis of animal-related outages in overhead distribution systems," *IEEE Transactions on Power Systems*, vol. 26, pp. 1618–1624, Aug 2011.

[45] M.-Y. Chow, S. O. Yee, and L. S. Taylor, "Recognizing Animal-Caused Faults in Power Distribution Systems Using Artificial Neural Networks," *IEEE Transactions on Power Delivery*, vol. 8, pp. 1268–1274, Jul 1993.

[46] M. Gui, A. Pahwa, and S. Das, "Analysis of animal-related outages in overhead distribution systems with wavelet decomposition and immune systems-based neural networks," *IEEE Transactions on Power Systems*, vol. 24, pp. 1765–1771, Nov 2009.

[47] "IEEE Guide for Electric Power Distribution Reliability Indices," *IEEE Std 1366-2012 (Revision of IEEE Std 1366-2003)*, pp. 1–43, May 2012.

[48] M.-Y. Chow, L. S. Taylor, and M. S. Chow, "Time of outage restoration analysis in distribution systems," *IEEE Transactions on Power Delivery*, vol. 11, no. 3, pp. 1652–1658, 1996.

[49] M. Doostan and B. H. Chowdhury, "A data-driven analysis of outage duration in power distribution systems," in *2017 North American Power Symposium, NAPS 2017*, pp. 1–6, IEEE, Sep 2017.

[50] A. Jaech, B. Zhang, M. Ostendorf, and D. S. Kirschen, "Real-Time Prediction of the Duration of Distribution System Outages," *IEEE Transactions on Power Systems*, vol. 34, pp. 773–781, Jan 2019.

[51] R. Eskandarpour and A. Khodaei, "Machine Learning Based Power Grid Outage Prediction in Response to Extreme Events," *IEEE Transactions on Power Systems*, vol. 32, pp. 3315–3316, Jul 2017.

[52] P. Kankanala, A. Pahwa, and S. Das, "Regression models for outages due to wind and lightning on overhead distribution feeders," in *2011 IEEE Power and Energy Society General Meeting*, (Detroit, MI), pp. 1–4, IEEE, Jul 2011.

[53] P. Kankanala, A. Pahwa, and S. Das, "Exponential regression models for wind and lightning caused outages on overhead distribution feeders," in *NAPS 2011 - 43rd North American Power Symposium*, pp. 1–4, IEEE, Aug 2011.

[54] R. Eskandarpour, A. Khodaei, and A. Arab, "Improving power grid resilience through predictive outage estimation," in *2017 North American Power Symposium (NAPS)*, pp. 1–5, IEEE, Sep 2017.

[55] H. Sun, Z. Wang, J. Wang, Z. Huang, N. Carrington, and J. Liao, "Data-Driven Power Outage Detection by Social Sensors," *IEEE Transactions on Smart Grid*, vol. 7, pp. 2516–2524, Sep 2016.

[56] K. Aoki, K. Nara, M. Itoh, T. Satoh, and H. Kuwabara, "A new algorithm for service restoration in distribution systems," *IEEE Transactions on Power Delivery*, vol. 4, pp. 1832–1839, Jul 1989.

[57] S. Ćurčić, C. Özveren, L. Crowe, and P. Lo, "Electric power distribution network restoration: a survey of papers and a review of the restoration problem," *Electric Power Systems Research*, vol. 35, pp. 73–86, Nov 1995.

[58] S. Singh, G. Raju, G. Rao, and M. Afsari, "A heuristic method for feeder reconfiguration and service restoration in distribution networks," *International Journal of Electrical Power & Energy Systems*, vol. 31, pp. 309–314, Sep 2009.

[59] B. J. D. Costa, L. R. de Araujo, and D. R. R. Penido, "A Heuristic Method of Restoring Distribution Systems Using Field Measurements," *IEEE Systems Journal*, vol. 13, pp. 1841–1850, Jun 2019.

[60] A. Morelato and A. Monticelli, "Heuristic search approach to distribution system restoration," *IEEE Transactions on Power Delivery*, vol. 4, pp. 2235–2241, Oct 1989.

[61] T. Nagata, H. Sasaki, and R. Yokoyama, "Power system restoration by joint usage of expert system and mathematical programming approach," *IEEE Transactions on Power Systems*, vol. 10, pp. 1473–1479, Jun 1995.

[62] H. Fudo, S. Toune, T. Genji, Y. Fukuyama, and Y. Nakanishi, "An application of reactive tabu search for service restoration in distribution systems and its comparison with the genetic algorithm and parallel simulated annealing," *Electrical Engineering in Japan*, vol. 133, pp. 71–82, Aug 2000.

[63] Y. Fukuyama and Y. Ueki, "Application of genetic algorithms to service restoration in distribution systems," *Electrical Engineering in Japan*, vol. 115, pp. 30–38, Jun 1995.

[64] B. Chen, C. Chen, J. Wang, and K. L. Butler-Purry, "Multi-Time Step Service Restoration for Advanced Distribution Systems and Microgrids," *IEEE Transactions on Smart Grid*, vol. 9, pp. 6793–6805, Nov 2018.

[65] S. Poudel and A. Dubey, "A two-stage service restoration method for electric power distribution systems," *IET Smart Grid*, vol. 4, pp. 500–521, Oct 2021.

[66] J. Wang, N. Zhou, and Q. Wang, "Data-driven stochastic service restoration in unbalanced active distribution networks with multi-terminal soft open points," *International Journal of Electrical Power & Energy Systems*, vol. 121, p. 106069, Oct 2020.

[67] Y. Li, J. Xiao, C. Chen, Y. Tan, and Y. Cao, "Service Restoration Model With Mixed-Integer Second-Order Cone Programming for Distribution Network With Distributed Generations," *IEEE Transactions on Smart Grid*, vol. 10, pp. 4138–4150, Jul 2019.

[68] N. C. Koutsoukis, P. A. Karafotis, P. S. Georgilakis, and N. D. Hatziargyriou, "Optimal service restoration of power distribution networks considering voltage regulation," in *2017 IEEE Manchester PowerTech, Powertech 2017*, Institute of Electrical and Electronics Engineers Inc., Jul 2017.

[69] Z. Wang and J. Wang, "Service restoration based on AMI and networked MGs under extreme weather events," *IET Generation, Transmission & Distribution*, vol. 11, pp. 401–408, Jan 2017.

[70] H. Ahmadi and J. R. Marti, "Distribution System Optimization Based on a Linear Power-Flow Formulation," *IEEE Transactions on Power Delivery*, vol. 30, pp. 25–33, Feb 2015.

[71] R. Romero, J. F. Franco, F. B. Leao, M. J. Rider, and E. S. de Souza, "A New Mathematical Model for the Restoration Problem in Balanced Radial Distribution Systems," *IEEE Transactions on Power Systems*, vol. 31, pp. 1259–1268, Mar 2016.

[72] Z. Wang and J. Wang, "Self-Healing Resilient Distribution Systems Based on Sectionalization into Microgrids," *IEEE Transactions on Power Systems*, vol. 30, pp. 3139–3149, Nov 2015.

[73] C. Ucak and A. Pahwa, "An analytical approach for step-by-step restoration of distribution systems following extended outages," *IEEE Transactions on Power Delivery*, vol. 9, pp. 1717–1723, Jul 1994.

[74] V. Widiputra, F. H. Jufri, and J. Jung, "Development of service restoration algorithm under cold load pickup condition using conservation voltage reduction and particle swarm optimization," *International Transactions on Electrical Energy Systems*, Jul 2020.

[75] Wen-Hui Chen, "Quantitative Decision-Making Model for Distribution System Restoration," *IEEE Transactions on Power Systems*, vol. 25, pp. 313–321, Feb 2010.

[76] Qin Zhou, D. Shirmohammadi, and W.-H. Liu, "Distribution feeder reconfiguration for service restoration and load balancing," *IEEE Transactions on Power Systems*, vol. 12, pp. 724–729, May 1997.

[77] Y. Kumar, B. Das, and J. Sharma, "Multiobjective, Multiconstraint Service Restoration of Electric Power Distribution System With Priority Customers," *IEEE Transactions on Power Delivery*, vol. 23, pp. 261–270, Jan 2008.

[78] F. Wang, C. Chen, C. Li, Y. Cao, Y. Li, B. Zhou, and X. Dong, "A Multi-Stage Restoration Method for Medium-Voltage Distribution System With DGs," *IEEE Transactions on Smart Grid*, vol. 8, pp. 2627–2636, Nov 2017.

[79] M. Mahdavi, H. H. Alhelou, N. D. Hatziargyriou, and A. Al-Hinai, "An Efficient Mathematical Model for Distribution System Reconfiguration Using AMPL," *IEEE Access*, vol. 9, pp. 79961–79993, 2021.

[80] M. Baran and F. Wu, "Network reconfiguration in distribution systems for loss reduction and load balancing," *IEEE Transactions on Power Delivery*, vol. 4, pp. 1401–1407, Apr 1989.

[81] W. Chen, X. Lou, X. Ding, and C. Guo, "Unified data-driven stochastic and robust service restoration method using non-parametric estimation in distribution networks with soft open points," *IET Generation, Transmission & Distribution*, vol. 14, pp. 3433–3443, Sep 2020.

[82] V. Kumar, H. Kumar, I. Gupta, and H. Gupta, "DG Integrated Approach for Service Restoration Under Cold Load Pickup," *IEEE Transactions on Power Delivery*, vol. 25, pp. 398–406, Jan 2010.

[83] A. Sharma, D. Srinivasan, and A. Trivedi, "A Decentralized Multi-Agent Approach for Service Restoration in Uncertain Environment," *IEEE Transactions on Smart Grid*, vol. 9, pp. 3394–3405, Jul 2018.

[84] S. Ma, S. Li, Z. Wang, A. Arif, and K. Ma, "A Novel MILP Formulation for Fault Isolation and Network Reconfiguration in Active Distribution Systems," in *2018 IEEE Power & Energy Society General Meeting (PESGM)*, pp. 1–5, IEEE, Aug 2018.

[85] B. Chen, C. Chen, J. Wang, and K. L. Butler-Purry, "Sequential Service Restoration for Unbalanced Distribution Systems and Microgrids," *IEEE Transactions on Power Systems*, vol. 33, pp. 1507–1520, Mar 2018.

[86] S. Zhu, H. Wang, Y. Xie, and H. M. Stewart, "Data-Driven Optimization for Atlanta Police Zone Design," Mar 2021.

[87] S. Ma, B. Chen, and Z. Wang, "Resilience Enhancement Strategy for Distribution Systems Under Extreme Weather Events," *IEEE Transactions on Smart Grid*, vol. 9, pp. 1442–1451, Mar 2018.

[88] S. Ma, S. Li, Z. Wang, and F. Qiu, "Resilience-Oriented Design of Distribution Systems," *IEEE Transactions on Power Systems*, vol. 34, pp. 2880–2891, Jul 2019.

[89] T. Lawanson, V. Sharma, V. Cecchi, and T. Hong, "Analysis of outage frequency and duration in distribution systems using machine learning," in *2020 52nd North American Power Symposium (NAPS)*, pp. 1–6, 2021.

[90] Mo-Yuen Chow, L. Taylor, and Mo-Suk Chow, "Time of outage restoration analysis in distribution systems," *IEEE Transactions on Power Delivery*, vol. 11, pp. 1652–1658, Jul 1996.

[91] M. Doostan and B. H. Chowdhury, "A data-driven analysis of outage duration in power distribution systems," in *2017 North American Power Symposium, NAPS 2017*, pp. 1–6, IEEE, Sep 2017.

[92] L. Xu, M.-y. Chow, and L. Taylor, "Data Mining and Analysis of Tree-Caused Faults in Power Distribution Systems," in *2006 IEEE PES Power Systems Conference and Exposition*, (Atlanta, GA), pp. 1221–1227, IEEE, 2006.

[93] Mo-Yuen Chow and L. Taylor, "Analysis and prevention of animal-caused faults in power distribution systems," *IEEE Transactions on Power Delivery*, vol. 10, pp. 995–1001, Apr 1995.

[94] "OpenWeatherMap." Accessed: May 13, 2020.

[95] J. D. Glover, M. S. Sarma, and T. J. Overbye, "Unsymmetrical faults," in *Power System Analysis and Design*, ch. 9, p. 471, Stamford, CT: Cengage Learning, 5th ed., 2012.

[96] F. Pedregosa, G. Varoquaux, A. Gramfort, V. Michel, B. Thirion, O. Grisel, M. Blondel, P. Prettenhofer, R. Weiss, V. Dubourg, J. Vanderplas, A. Passos, D. Cournapeau, M. Brucher, M. Perrot, and E. Duchesnay, "Scikit-learn: Machine learning in Python," *Journal of Machine Learning Research*, vol. 12, pp. 2825–2830, 2011.

[97] S. Ronaghan, "The Mathematics of Decision Trees, Random Forest and Feature Importance in Scikit-learn and Spark," Nov 2019.

[98] L. Breiman, "Random forests," *Machine learning*, vol. 45, no. 1, pp. 5–32, 2001.

[99] B. Wolff, O. Kramer, and D. Heinemann, "Selection of Numerical Weather Forecast Features for PV Power Predictions with Random Forests," in *Data Analytics for Renewable Energy Integration* (W. L. Woon, Z. Aung, O. Kramer, and S. Madnick, eds.), (Cham), pp. 78–91, Springer International Publishing, 2017.

[100] J. H. Friedman, "Stochastic gradient boosting," *Computational Statistics & Data Analysis*, vol. 38, no. 4, pp. 367 – 378, 2002. Nonlinear Methods and Data Mining.

[101] S. B. Taieb and R. J. Hyndman, "A gradient boosting approach to the kaggle load forecasting competition," *International Journal of Forecasting*, vol. 30, no. 2, pp. 382 – 394, 2014.

[102] A. Soroudi, *Power System Optimization Modeling in GAMS*. Cham: Springer International Publishing AG, 1st ed., 2017.

[103] "American National Standard for Electric Power Systems and Equipment - Voltage Ratings (60Hz)," 2020.

[104] R. A. Jabr, R. Singh, and B. C. Pal, "Minimum Loss Network Reconfiguration Using Mixed-Integer Convex Programming," *IEEE Transactions on Power Systems*, vol. 27, pp. 1106–1115, May 2012.

[105] H. Ahmadi and J. R. Martí, "Mathematical representation of radiality constraint in distribution system reconfiguration problem," *International Journal of Electrical Power & Energy Systems*, vol. 64, pp. 293–299, Jan 2015.

[106] S. Lei, C. Chen, Y. Song, and Y. Hou, "Radiality Constraints for Resilient Reconfiguration of Distribution Systems: Formulation and Application to Microgrid Formation," *IEEE Transactions on Smart Grid*, vol. 11, pp. 3944–3956, Sep 2020.

[107] M. Lavorato, J. F. Franco, M. J. Rider, and R. Romero, "Imposing Radiality Constraints in Distribution System Optimization Problems," *IEEE Transactions on Power Systems*, vol. 27, pp. 172–180, Feb 2012.

[108] Gurobi Optimization, LLC, "Gurobi Optimizer Reference Manual," 2022.

[109] K. Bestuzheva, M. Besançon, W.-K. Chen, A. Chmiela, T. Donkiewicz, J. van Doornmalen, L. Eifler, O. Gaul, G. Gamrath, A. Gleixner, L. Gottwald, C. Graczyk, K. Halbig, A. Hoen, C. Hojny, R. van der Hulst, T. Koch, M. Lübbecke, S. J. Maher, F. Matter, E. Mühmer, B. Müller, M. E. Pfetsch, D. Rehfeldt, S. Schlein, F. Schlösser, F. Serrano, Y. Shinano, B. Sofranac, M. Turner, S. Vigerske, F. Wegscheider, P. Wellner, D. Weninger, and J. Witzig, "The SCIP Optimization Suite 8.0," technical report, Optimization Online, December 2021.

[110] J. Forrest, T. Ralphs, H. G. Santos, S. Vigerske, J. Forrest, L. Hafer, B. Kristjansson, jpfasano, EdwinStraver, M. Lubin, and et al., "coin-or/cbc: Release releases/2.10.8," May 2022. COIN-OR Branch-and-Cut solver.

[111] Z. Yang, K. Xie, J. Yu, H. Zhong, N. Zhang, and Q. X. Xia, "A General Formulation of Linear Power Flow Models: Basic Theory and Error Analysis," *IEEE Transactions on Power Systems*, vol. 34, pp. 1315–1324, Mar 2019.

[112] M. Li, Y. Du, J. Mohammadi, C. Crozier, K. Baker, and S. Kar, "Numerical Comparisons of Linear Power Flow Approximations: Optimality, Feasibility, and Computation Time," in *2022 IEEE Power & Energy Society General Meeting (PESGM)*, pp. 1–5, IEEE, Jul 2022.

[113] M. Baran and F. Wu, "Optimal sizing of capacitors placed on a radial distribution system," *IEEE Transactions on Power Delivery*, vol. 4, pp. 735–743, Jan 1989.

[114] K. Bauman, A. Tuzhilin, and R. Zaczynski, "Virtual Power Outage Detection Using Social Sensors," *NYU Working Paper No.*, Sep 2015.

[115] K. Bauman, A. Tuzhilin, and R. Zaczynski, "Using Social Sensors for Detecting Emergency Events: A Case of Power Outages in the Electrical Utility Industry," *ACM Trans. Manage. Inf. Syst*, vol. 8, Jun 2017.

[116] H. Mao, G. Thakur, K. Sparks, J. Sanyal, and B. Bhaduri, "Mapping near-real-time power outages from social media," *International Journal of Digital Earth*, vol. 12, pp. 1285–1299, Nov 2019.

[117] Y. Zhou, A. Pahwa, and S. S. Yang, "Modeling weather-related failures of overhead distribution lines," *IEEE Transactions on Power Systems*, vol. 21, pp. 1683–1690, Nov 2006.

[118] H. P. Williams, *Model Building in Mathematical Programming*. West Sussex: John Wiley & Sons Ltd, 5th ed., March 2013.

[119] W. H. Kersting, *Distribution System Modeling and Analysis*. Electric Power Engineering, Boca Raton, FL, USA: CRC Press LLC, 1st ed., Aug 2001.

[120] H. Ahmadi and J. R. Martí, "Linear current flow equations with application to distribution systems reconfiguration," *IEEE Transactions on Power Systems*, vol. 30, no. 4, pp. 2073–2080, 2015.

[121] "IEEE PES Test Feeder." [Online]. Accessed: Mar 23, 2022.

[122] W. E. Hart, C. D. Laird, J.-P. Watson, D. L. Woodruff, G. A. Hackebeil, B. L. Nicholson, and J. D. Siirola, *Pyomo — Optimization Modeling in Python*, vol. 67 of *Springer Optimization and Its Applications*. Cham: Springer International Publishing, 2017.

[123] W. E. Hart, J.-P. Watson, and D. L. Woodruff, "Pyomo: modeling and solving mathematical programs in Python," *Mathematical Programming Computation*, vol. 3, no. 3, pp. 219–260, 2011.

[124] B. Chen, *Black Start Restoration for Electric Distribution Systems and Microgrids*. PhD dissertation, Texas A&M University, 2017.

[125] W. Kersting, "Radial distribution test feeders," in *2001 IEEE Power Engineering Society Winter Meeting. Conference Proceedings (Cat. No.01CH37194)*, vol. 2, pp. 908–912, 2001.

[126] "OpenDSS: EPRI Distribution System Simulator," 2008.

APPENDIX A: FEEDER DATA

A.1 Modified IEEE 123-bus Test Feeder

Table A.1: Line parameters for modified IEEE 123-bus feeder

Line No.	From Node	To Node	Length (ft)	Capacity (kVA)	Line Type	Config.
1	1	2	175	960	Non-switchable	10
2	1	3	250	960	Non-switchable	11
3	1	7	300	2200	Switchable	1
4	3	4	200	960	Non-switchable	11
5	3	5	325	960	Non-switchable	11
6	5	6	250	960	Non-switchable	11
7	7	8	200	2200	Non-switchable	1
8	8	12	225	960	Non-switchable	10
9	8	9	225	960	Non-switchable	9
10	8	13	300	2200	Non-switchable	1
11	9	14	425	960	Non-switchable	9
12	13	34	150	960	Non-switchable	11
13	13	18	825	2200	Switchable	2
14	13	152	10	3700	Switchable	13
15	14	11	250	960	Non-switchable	9
16	14	10	250	960	Non-switchable	9
17	15	16	375	960	Non-switchable	11
18	15	17	350	960	Non-switchable	11
19	18	19	250	960	Non-switchable	9
20	18	21	300	2200	Non-switchable	2
21	18	135	10	3700	Switchable	13
22	19	20	325	960	Non-switchable	9
23	21	22	525	960	Non-switchable	10
24	21	23	250	2200	Non-switchable	2
25	23	24	550	960	Non-switchable	11
26	23	25	275	2200	Switchable	2
27	25	26	350	2200	Non-switchable	7
28	25	28	200	2200	Non-switchable	2
29	26	27	275	2200	Non-switchable	7
30	26	31	225	960	Non-switchable	11
31	27	33	500	960	Non-switchable	9
32	28	29	300	2200	Non-switchable	2
33	29	30	350	2200	Non-switchable	2
34	30	250	200	2200	Non-switchable	2
35	31	32	300	960	Non-switchable	11

Line No.	From Node	To Node	Length (ft)	Capacity (kVA)	Line Type	Config.
36	34	15	100	960	Non-switchable	11
37	35	36	650	2200	Non-switchable	8
38	35	40	250	2200	Non-switchable	1
39	36	37	300	960	Non-switchable	9
40	36	38	250	960	Non-switchable	10
41	38	39	325	960	Non-switchable	10
42	40	41	325	960	Non-switchable	11
43	40	42	250	2200	Non-switchable	1
44	42	43	500	960	Non-switchable	10
45	42	44	200	2200	Non-switchable	1
46	44	45	200	960	Non-switchable	9
47	44	47	250	2200	Non-switchable	1
48	45	46	300	960	Non-switchable	9
49	47	48	150	2200	Non-switchable	4
50	47	49	250	2200	Non-switchable	4
51	49	50	250	2200	Non-switchable	4
52	50	51	250	2200	Non-switchable	4
53	51	151	500	2200	Non-switchable	13
54	52	53	200	2200	Non-switchable	1
55	53	54	125	2200	Non-switchable	1
56	54	55	275	2200	Non-switchable	1
57	54	57	350	2200	Non-switchable	3
58	54	94	10	3700	Switchable	13
59	55	56	275	2200	Non-switchable	1
60	57	58	250	960	Non-switchable	10
61	57	60	750	2200	Non-switchable	3
62	58	59	250	960	Non-switchable	10
63	60	61	550	2200	Non-switchable	5
64	60	62	250	730	Non-switchable	12
65	60	160	10	3700	Switchable	13
66	61	610	10	150	Non-switchable	13
67	62	63	175	730	Non-switchable	12
68	63	64	350	730	Non-switchable	12
69	64	65	425	730	Non-switchable	12
70	65	66	325	730	Non-switchable	12
71	67	68	200	960	Non-switchable	9
72	67	72	275	2200	Non-switchable	3
73	67	97	250	2200	Non-switchable	3
74	68	69	275	960	Non-switchable	9
75	69	70	325	960	Non-switchable	9
76	70	71	275	960	Non-switchable	9
77	72	73	275	960	Non-switchable	11

Line No.	From Node	To Node	Length (ft)	Capacity (kVA)	Line Type	Config.
78	72	76	200	2200	Non-switchable	3
79	73	74	350	960	Non-switchable	11
80	74	75	400	960	Non-switchable	11
81	76	77	400	2200	Switchable	6
82	76	86	700	2200	Non-switchable	3
83	77	78	100	2200	Non-switchable	6
84	78	79	225	2200	Non-switchable	6
85	78	80	475	2200	Non-switchable	6
86	80	81	475	2200	Non-switchable	6
87	81	82	250	2200	Non-switchable	6
88	81	84	675	960	Non-switchable	11
89	82	83	250	2200	Non-switchable	6
90	84	85	475	960	Non-switchable	11
91	86	87	450	2200	Non-switchable	6
92	87	88	175	960	Non-switchable	9
93	87	89	275	2200	Switchable	6
94	89	90	225	960	Non-switchable	10
95	89	91	225	2200	Non-switchable	6
96	91	92	300	960	Non-switchable	11
97	91	93	225	2200	Non-switchable	6
98	93	94	275	960	Non-switchable	9
99	93	95	300	2200	Non-switchable	6
100	95	96	200	960	Non-switchable	10
101	97	98	275	2200	Non-switchable	3
102	97	197	10	3700	Switchable	13
103	98	99	550	2200	Non-switchable	3
104	99	100	300	2200	Non-switchable	3
105	100	450	800	2200	Non-switchable	3
106	101	102	225	960	Non-switchable	11
107	101	105	275	2200	Non-switchable	3
108	102	103	325	960	Non-switchable	11
109	103	104	700	960	Non-switchable	11
110	105	106	225	960	Non-switchable	10
111	105	108	325	2200	Non-switchable	3
112	106	107	575	960	Non-switchable	10
113	108	109	450	960	Non-switchable	9
114	108	300	1000	2200	Non-switchable	3
115	109	110	300	960	Non-switchable	9
116	110	111	575	960	Non-switchable	9
117	110	112	125	960	Non-switchable	9
118	112	113	525	960	Non-switchable	9
119	113	114	325	960	Non-switchable	9

Line No.	From Node	To Node	Length (ft)	Capacity (kVA)	Line Type	Config.
120	135	35	375	2200	Non-switchable	4
121	149	1	400	2200	Non-switchable	1
122	150	149	10	3700	Switchable	13
123	151	300	10	3700	Switchable	13
124	152	52	400	2200	Non-switchable	1
125	160	67	350	2200	Non-switchable	6
126	197	101	250	2200	Non-switchable	3

Table A.2: Line impedances for modified IEEE 123-bus feeder

Config.	Resistance (Ohms/mi)	Reactance (Ohms/mi)
1	0.4619	1.0638
2	0.4619	1.0638
3	0.4619	1.0638
4	0.4619	1.0638
5	0.4619	1.0638
6	0.4619	1.0638
7	0.4576	1.0780
8	0.4596	1.0716
9	1.3292	1.3475
10	1.3292	1.3475
11	1.3292	1.3475
12	1.5249	0.7401
13	0.0100	0.0100

Table A.3: Load parameters for modified IEEE 123-bus feeder

Load Name	P (kW)	Q (kVar)	Load Name	P (kW)	Q (kVar)	Load Name	P (kW)	Q (kVar)
L1	15	5	L43	15	5	L79	15	5
L2	5	5	L45	5	5	L80	15	5
L4	15	5	L46	5	5	L82	15	5
L5	5	5	L47	35	25	L83	5	5
L6	15	5	L48	70	50	L84	5	5
L7	5	5	L49	45	30	L85	15	5
L9	15	5	L50	15	5	L86	5	5
L10	5	5	L51	5	5	L87	15	5
L11	15	5	L52	15	5	L88	15	5
L12	5	5	L53	15	5	L90	15	5

Load Name	P (kW)	Q (kVar)	Load Name	P (kW)	Q (kVar)	Load Name	P (kW)	Q (kVar)
L16	15	5	L55	5	5	L92	15	5
L17	5	5	L56	5	5	L94	15	5
L19	15	5	L58	5	5	L95	5	5
L20	15	5	L59	5	5	L96	5	5
L22	15	5	L60	5	5	L98	15	5
L24	15	5	L62	15	5	L99	15	5
L28	15	5	L63	15	5	L100	15	5
L29	15	5	L64	25	10	L102	5	5
L30	15	5	L65	45	35	L103	15	5
L31	5	5	L66	25	10	L104	15	5
L32	5	5	L68	5	5	L106	15	5
L33	15	5	L69	15	5	L107	15	5
L34	15	5	L70	5	5	L109	15	5
L35	15	5	L71	15	5	L111	5	5
L37	15	5	L73	15	5	L112	5	5
L38	5	5	L74	15	5	L113	15	5
L39	5	5	L75	15	5	L114	5	5
L41	5	5	L76	80	60			
L42	5	5	L77	15	5			

Table A.4: Capacitor data for modified IEEE 123-bus feeder

Node	kVar
83	180
88	15
90	15
92	15

Table A.5: Transformer and regulator data for modified IEEE 123-bus feeder

	kVA	kV-high	kV-low	Tap Position
Substation	5000	115	4.16	–
XFM-1	150	4.16	0.48	–
RG 150-149	–	4.16	4.16	-7
RG 9-14	–	4.16	4.16	1
RG 25-26	–	4.16	4.16	1
RG 160-67	–	4.16	4.16	-4

A.1.1 Power Flow Results

Table A.6: Power flow results for modified 123-bus feeder: Voltage magnitude (p.u.)

Node	**Voltage Magnitude (p.u.)**		**Error (p.u.)**	**Node**	**Voltage Magnitude (p.u.)**		**Error (p.u.)**
	MILP	OpenDSS			MILP	OpenDSS	
150	1.0000	1.0000	0.0000	65	1.0117	0.9800	0.0318
149	1.0458	1.0500	0.0042	66	1.0116	0.9795	0.0321
1	1.0389	1.0366	0.0023	18	1.0197	1.0012	0.0185
2	1.0389	1.0365	0.0024	135	1.0196	1.0012	0.0184
3	1.0387	1.0360	0.0027	35	1.0175	0.9977	0.0198
4	1.0387	1.0359	0.0028	36	1.0171	0.9971	0.0201
5	1.0386	1.0356	0.0030	37	1.0171	0.9968	0.0203
6	1.0386	1.0354	0.0032	38	1.0170	0.9968	0.0202
7	1.0340	1.0271	0.0069	39	1.0170	0.9967	0.0203
8	1.0308	1.0209	0.0099	40	1.0163	0.9956	0.0206
12	1.0307	1.0208	0.0099	41	1.0162	0.9955	0.0207
13	1.0261	1.0121	0.0140	42	1.0151	0.9937	0.0214
152	1.0260	1.0121	0.0139	43	1.0149	0.9932	0.0217
52	1.0232	1.0061	0.0171	44	1.0142	0.9922	0.0219
53	1.0218	1.0032	0.0186	45	1.0141	0.9921	0.0221
54	1.0210	1.0015	0.0195	46	1.0141	0.9919	0.0221
55	1.0209	1.0013	0.0196	47	1.0132	0.9906	0.0226
56	1.0208	1.0013	0.0195	48	1.0129	0.9902	0.0227
57	1.0187	0.9968	0.0219	49	1.0128	0.9900	0.0228
58	1.0186	0.9966	0.0221	50	1.0127	0.9898	0.0229
59	1.0186	0.9965	0.0221	51	1.0127	0.9897	0.0229
60	1.0141	0.9874	0.0268	151	1.0127	0.9897	0.0229
160	1.0141	0.9874	0.0267	300	1.0383	1.0124	0.0259
67	1.0401	1.0156	0.0245	108	1.0383	1.0124	0.0259
68	1.0400	1.0150	0.0250	105	1.0386	1.0129	0.0257
69	1.0398	1.0144	0.0254	101	1.0389	1.0136	0.0253
70	1.0397	1.0140	0.0257	102	1.0388	1.0131	0.0257
71	1.0396	1.0138	0.0258	103	1.0387	1.0125	0.0262
72	1.0401	1.0151	0.0250	104	1.0385	1.0119	0.0266
73	1.0399	1.0144	0.0255	197	1.0394	1.0144	0.0250
74	1.0398	1.0138	0.0260	106	1.0385	1.0125	0.0260
75	1.0397	1.0134	0.0263	107	1.0383	1.0120	0.0263
76	1.0402	1.0150	0.0252	109	1.0379	1.0111	0.0268
77	1.0415	1.0166	0.0249	110	1.0377	1.0104	0.0273
78	1.0418	1.0170	0.0248	111	1.0376	1.0101	0.0275

Node	Voltage Magnitude (p.u.)		Error (p.u.)	Node	Voltage Magnitude (p.u.)		Error (p.u.)
	MILP	OpenDSS			MILP	OpenDSS	
79	1.0418	1.0169	0.0249	112	1.0376	1.0102	0.0274
80	1.0435	1.0193	0.0242	113	1.0374	1.0095	0.0279
81	1.0453	1.0217	0.0236	114	1.0373	1.0094	0.0279
82	1.0463	1.0232	0.0231	19	1.0196	1.0007	0.0189
83	1.0474	1.0247	0.0227	20	1.0195	1.0005	0.0190
84	1.0451	1.0208	0.0243	21	1.0192	1.0003	0.0189
85	1.0449	1.0204	0.0245	22	1.0191	0.9999	0.0192
86	1.0399	1.0142	0.0257	23	1.0188	0.9997	0.0191
87	1.0398	1.0138	0.0260	24	1.0187	0.9992	0.0195
88	1.0398	1.0138	0.0260	25	1.0185	0.9991	0.0194
89	1.0397	1.0136	0.0261	26	1.0122	0.9863	0.0259
90	1.0398	1.0136	0.0262	27	1.0121	0.9862	0.0259
91	1.0397	1.0134	0.0263	33	1.0120	0.9857	0.0262
92	1.0397	1.0134	0.0263	31	1.0121	0.9861	0.0260
93	1.0395	1.0132	0.0263	32	1.0120	0.9860	0.0261
94	1.0395	1.0130	0.0265	28	1.0183	0.9989	0.0195
95	1.0394	1.0131	0.0263	29	1.0182	0.9986	0.0196
96	1.0394	1.0130	0.0264	30	1.0181	0.9985	0.0197
97	1.0395	1.0144	0.0251	250	1.0181	0.9985	0.0197
98	1.0393	1.0141	0.0252	34	1.0260	1.0117	0.0143
99	1.0390	1.0136	0.0254	15	1.0260	1.0116	0.0144
100	1.0390	1.0135	0.0255	16	1.0259	1.0113	0.0146
450	1.0390	1.0135	0.0255	17	1.0259	1.0115	0.0144
61	1.0141	0.9874	0.0268	9	1.0306	1.0204	0.0102
610	1.0141	0.9874	0.0268	14	1.0242	1.0071	0.0171
62	1.0135	0.9854	0.0281	10	1.0242	1.0070	0.0172
63	1.0131	0.9841	0.0290	11	1.0242	1.0069	0.0173
64	1.0124	0.9820	0.0305				

Table A.7: Power flow results for modified 123-bus feeder: Real power (kW)

From Node	To Node	Real Power (kW)		Error (kW)	From Node	To Node	Real Power (kW)		Error (kW)
		MILP	OpenDSS				MILP	OpenDSS	
150	149	1185	1231.78	46.78	64	65	70	70.17	0.17
149	1	1185	1231.77	46.77	65	66	25	25.01	0.01
1	2	5	5.00	0.00	13	18	375	378.84	3.83
1	3	35	35.03	0.03	18	135	245	246.34	1.34
3	4	15	15.00	0.00	135	35	245	246.34	1.34
3	5	20	20.01	0.01	35	36	25	25.01	0.01
5	6	15	15.00	0.00	36	37	15	15.00	0.00
1	7	1130	1167.13	37.13	36	38	10	10.00	0.00
7	8	1125	1155.56	30.56	38	39	5	5.00	0.00
8	12	5	5.00	0.00	35	40	205	205.83	0.82
8	13	1085	1111.21	26.21	40	41	5	5.00	0.00
13	152	675	691.33	16.33	40	42	200	200.59	0.59
152	52	675	691.32	16.32	42	43	15	15.01	0.01
52	53	660	673.38	13.38	42	44	180	180.36	0.36
53	54	645	656.98	11.98	44	45	10	10.00	0.00
54	55	10	10.00	0.00	45	46	5	5.00	0.00
55	56	5	5.00	0.00	44	47	170	170.21	0.21
54	57	635	646.14	11.14	47	48	70	70.02	0.02
57	58	10	10.00	0.00	47	49	65	65.02	0.02
58	59	5	5.00	0.00	49	50	20	20.00	0.00
57	60	625	633.87	8.87	50	51	5	5.00	0.00
60	160	495	498.40	3.39	51	151	0	0.00	0.00
160	67	495	498.39	3.39	151	300	0	0.00	0.00
67	68	40	40.04	0.04	108	300	0	0.00	0.00
68	69	35	35.03	0.03	105	108	45	45.10	0.10
69	70	20	20.01	0.01	101	105	75	75.14	0.14
70	71	15	15.00	0.00	101	102	35	35.04	0.04
67	72	300	301.72	1.72	102	103	30	30.02	0.02
72	73	45	45.05	0.05	103	104	15	15.01	0.01
73	74	30	30.02	0.02	197	101	110	110.23	0.23
74	75	15	15.00	0.00	97	197	110	110.23	0.23
72	76	255	256.28	1.28	105	106	30	30.02	0.02
76	77	85	85.89	0.89	106	107	15	15.01	0.01
77	78	70	70.72	0.72	108	109	45	45.09	0.09
78	79	15	15.00	0.00	109	110	30	30.03	0.03
78	80	55	55.67	0.67	110	111	5	5.00	0.00
80	81	40	40.47	0.47	110	112	25	25.02	0.02
81	82	20	20.24	0.24	112	113	20	20.01	0.01
82	83	5	5.12	0.12	113	114	5	5.00	0.00
81	84	20	20.02	0.02	18	19	30	30.01	0.01
84	85	15	15.01	0.01	19	20	15	15.00	0.00
76	86	90	90.17	0.17	18	21	100	100.15	0.15
86	87	85	85.08	0.08	21	22	15	15.01	0.01
87	88	15	15.00	0.00	21	23	85	85.09	0.09
87	89	55	55.03	0.03	23	24	15	15.01	0.01
89	90	15	15.00	0.00	23	25	70	70.05	0.05
89	91	40	40.02	0.02	25	26	25	25.01	0.01
91	92	15	15.00	0.00	26	27	15	15.01	0.01
91	93	25	25.01	0.01	27	33	15	15.01	0.01
93	94	15	15.00	0.00	26	31	10	10.00	0.00
54	94	0	0.00	0.00	31	32	5	5.00	0.00
93	95	10	10.00	0.00	25	28	45	45.01	0.01
95	96	5	5.00	0.00	28	29	30	30.01	0.01
67	97	155	155.35	0.35	29	30	15	15.00	0.00
97	98	45	45.02	0.02	30	250	0	0.00	0.00
98	99	30	30.01	0.01	13	34	35	35.02	0.02
99	100	15	15.00	0.00	34	15	20	20.01	0.01
100	450	0	0.00	0.00	15	16	15	15.00	0.00
60	61	0	0.00	0.00	15	17	5	5.00	0.00

From Node	To Node	Real Power (kW)		Error (kW)	From Node	To Node	Real Power (kW)		Error (kW)
		MILP	OpenDSS				MILP	OpenDSS	
61	610	0	0.00	0.00	8	9	35	35.03	0.03
60	62	125	125.79	0.79	9	14	20	20.01	0.01
62	63	110	110.53	0.53	14	10	5	5.00	0.00
63	64	95	95.39	0.39	14	11	15	15.00	0.00

Table A.8: Power flow results for modified 123-bus feeder: Reactive power (kVar)

From Node	To Node	Reactive Power (kVar)		Error (kVar)	From Node	To Node	Reactive Power (kVar)		Error (kVar)
		MILP	OpenDSS				MILP	OpenDSS	
150	149	385.00	480.58	95.58	64	65	45.00	45.08	0.08
149	1	385.00	480.57	95.57	65	66	10.00	10.01	0.01
1	2	5.00	5.00	0.00	13	18	210.00	218.76	8.76
1	3	15.00	15.03	0.03	18	135	160.00	163.05	3.05
3	4	5.00	5.00	0.00	135	35	160.00	163.05	3.05
3	5	10.00	10.01	0.01	35	36	15.00	15.02	0.02
5	6	5.00	5.00	0.00	36	37	5.00	5.00	0.00
1	7	360.00	433.39	73.39	36	38	10.00	10.00	0.00
7	8	355.00	413.28	58.28	38	39	5.00	5.00	0.00
8	12	5.00	5.00	0.00	35	40	140.00	141.89	1.88
8	13	335.00	383.28	48.28	40	41	5.00	5.00	0.00
13	152	110.00	135.62	25.62	40	42	135.00	136.34	1.34
152	52	110.00	135.62	25.62	42	43	5.00	5.01	0.01
52	53	105.00	123.85	18.85	42	44	125.00	125.81	0.81
53	54	100.00	115.61	15.61	44	45	10.00	10.00	0.00
54	55	10.00	10.00	0.00	45	46	5.00	5.00	0.00
55	56	5.00	5.00	0.00	44	47	115.00	115.47	0.47
54	57	90.00	103.68	13.68	47	48	50.00	50.04	0.04
57	58	10.00	10.00	0.00	47	49	40.00	40.06	0.06
58	59	5.00	5.00	0.00	49	50	10.00	10.00	0.00
57	60	80.00	88.46	8.46	50	51	5.00	5.00	0.00
60	160	10.00	7.28	2.72	51	151	0.00	0.00	0.00
160	67	10.00	7.27	2.73	151	300	0.00	0.00	0.00
67	68	20.00	20.04	0.04	108	300	0.00	0.00	0.00
68	69	15.00	15.03	0.03	105	108	25.00	25.11	0.11
69	70	10.00	10.01	0.01	101	105	35.00	35.19	0.19
70	71	5.00	5.00	0.00	101	102	15.00	15.03	0.03
67	72	-75.00	-81.33	6.33	102	103	10.00	10.02	0.02
72	73	15.00	15.04	0.04	103	104	5.00	5.01	0.01
73	74	10.00	10.02	0.02	197	101	50.00	50.35	0.35
74	75	5.00	5.00	0.00	97	197	50.00	50.35	0.35
72	76	-90.00	-97.29	7.29	105	106	10.00	10.02	0.02
76	77	-145.00	-151.94	6.94	106	107	5.00	5.01	0.01
77	78	-150.00	-157.35	7.35	108	109	25.00	25.08	0.08
78	79	5.00	5.00	0.00	109	110	20.00	20.03	0.03
78	80	-155.00	-162.45	7.45	110	111	5.00	5.00	0.00
80	81	-160.00	-167.93	7.93	110	112	15.00	15.02	0.02
81	82	-170.00	-178.42	8.42	112	113	10.00	10.01	0.01
82	83	-175.00	-183.69	8.69	113	114	5.00	5.00	0.00
81	84	10.00	10.02	0.02	18	19	10.00	10.01	0.01
84	85	5.00	5.00	0.00	19	20	5.00	5.00	0.00
76	86	-5.00	-5.86	0.86	18	21	40.00	40.31	0.31
86	87	-10.00	-11.05	1.05	21	22	5.00	5.01	0.01
87	88	-10.00	-10.41	0.41	21	23	35.00	35.18	0.18
87	89	-5.00	-5.75	0.75	23	24	5.00	5.01	0.01
89	90	-10.00	-10.40	0.40	23	25	30.00	30.10	0.10
89	91	5.00	4.63	0.37	25	26	15.00	15.02	0.02
91	92	-10.00	-10.40	0.40	26	27	5.00	5.01	0.01
91	93	15.00	15.01	0.01	27	33	5.00	5.01	0.01

From Node	To Node	Reactive Power (kVar)		Error (kVar)	From Node	To Node	Reactive Power (kVar)		Error (kVar)
		MILP	OpenDSS				MILP	OpenDSS	
93	94	5.00	5.00	0.00	26	31	10.00	10.00	0.00
54	94	0.00	0.00	0.00	31	32	5.00	5.00	0.00
93	95	10.00	10.00	0.00	25	28	15.00	15.03	0.03
95	96	5.00	5.00	0.00	28	29	10.00	10.01	0.01
67	97	65.00	65.63	0.63	29	30	5.00	5.00	0.00
97	98	15.00	15.04	0.04	30	250	0.00	0.00	0.00
98	99	10.00	10.02	0.02	13	34	15.00	15.02	0.02
99	100	5.00	5.00	0.00	34	15	10.00	10.01	0.01
100	450	0.00	0.00	0.00	15	16	5.00	5.00	0.00
60	61	0.00	0.00	0.00	15	17	5.00	5.00	0.00
61	610	0.00	0.00	0.00	8	9	15.00	15.03	0.03
60	62	65.00	65.38	0.38	9	14	10.00	10.01	0.01
62	63	60.00	60.26	0.26	14	10	5.00	5.00	0.00
63	64	55.00	55.19	0.19	14	11	5.00	5.00	0.00

APPENDIX B: SINGLE OUTAGE CASE: FEEDER IMAGES

B.1 Modified IEEE 13-bus Test Feeder Case B

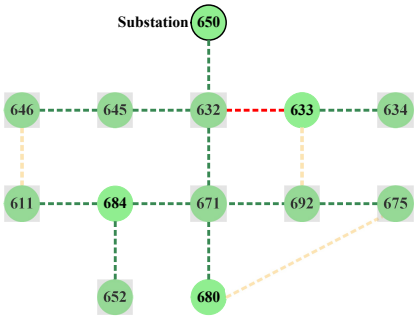

(a) Original topology with predicted outage location 632–633 shown in red

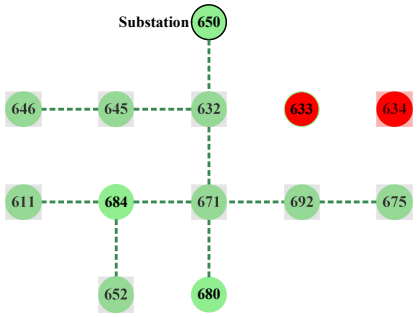

(b) Original topology showing loads that would be impacted by predicted outage

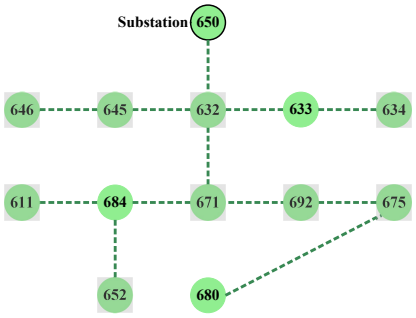

(c) Proactive topology

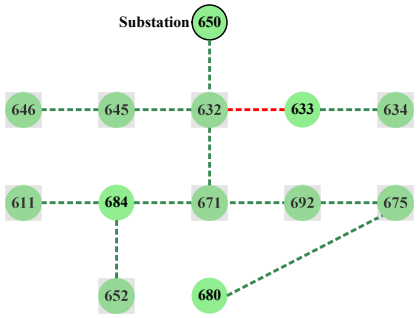

(d) Proactive topology with predicted outage location branch 632–633 shown in red

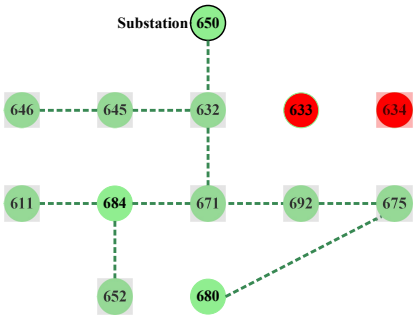

(e) Proactive topology showing loads that would be impacted by predicted outage

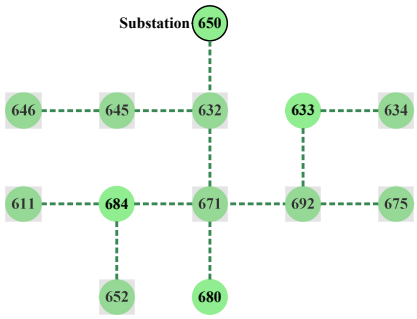

(f) New topology after the predicted outage locations are isolated

Figure B.1: Case B: One-line diagrams of modified IEEE 13-node test feeder showing network topology before and after implementing the proactive topology optimization and service restoration framework

B.2 Modified IEEE 13-bus Test Feeder Case C

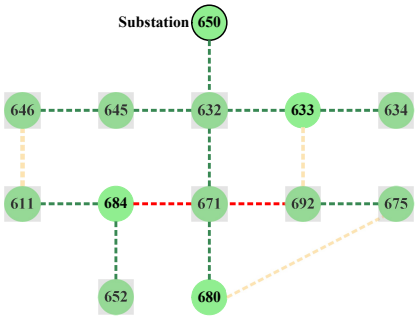

(a) Original topology with predicted outage locations 671–684 and 671–692 shown in red

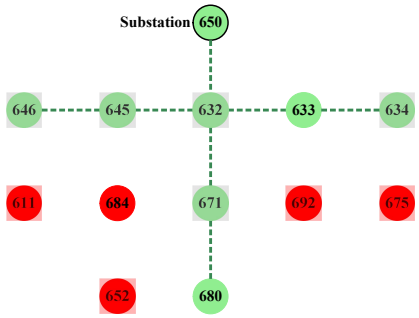

(b) Original topology showing loads that would be impacted by predicted outage

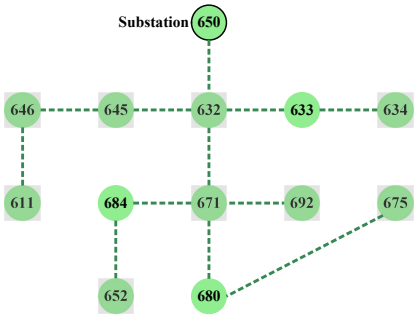

(c) Proactive topology

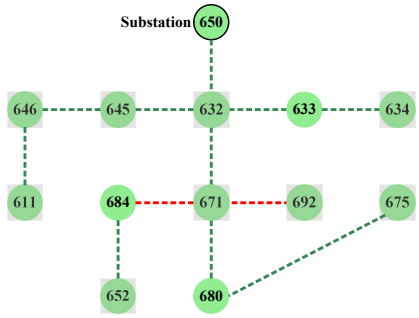

(d) Proactive topology with predicted outage locations 671–684 and 671–692 shown in red

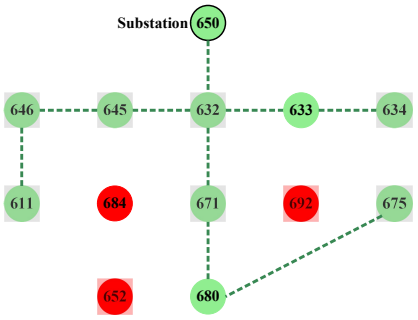

(e) Proactive topology showing loads that would be impacted by predicted outage

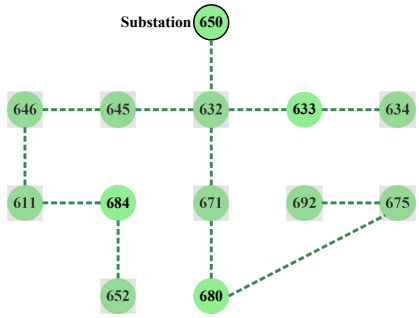

(f) New topology after the predicted outage locations are isolated

Figure B.2: Case C: One-line diagrams of modified IEEE 13-node test feeder showing network topology before and after implementing the proactive topology optimization and service restoration framework

B.3 Modified IEEE 123-bus Test Feeder Case B

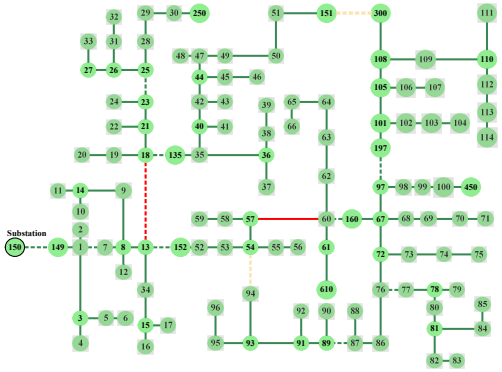

(a) Original topology with predicted outage locations 13–18 and 57–60 shown in red

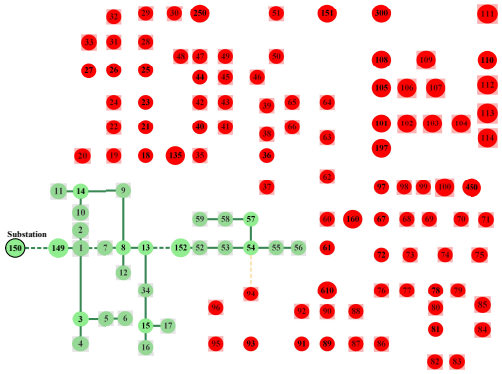

(b) Original topology showing loads that would be impacted by predicted outage

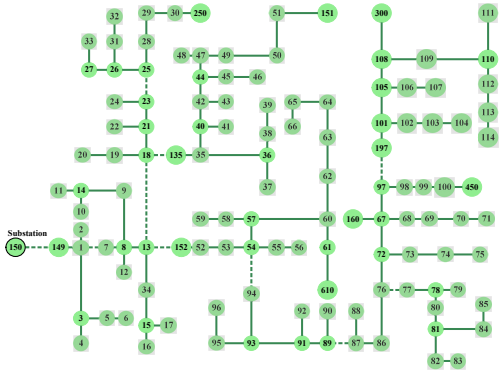

(c) Proactive topology

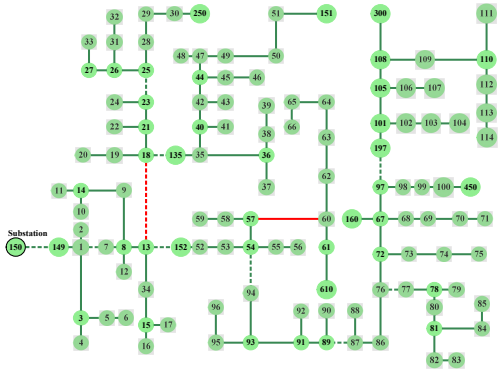

(d) Proactive topology with predicted outage locations 13–18 and 57–60 shown in red

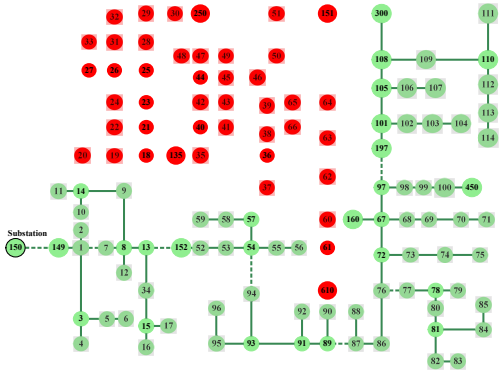

(e) Proactive topology showing loads that would be impacted by predicted outage

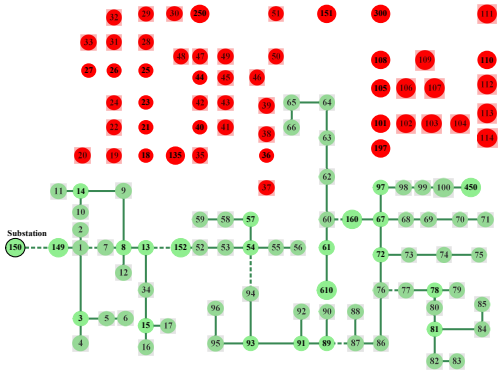

(f) New topology after the predicted outage locations are isolated

Figure B.3: Case B: One-line diagrams of modified IEEE 123-node test feeder showing network topology before and after implementing the proactive topology optimization and service restoration framework

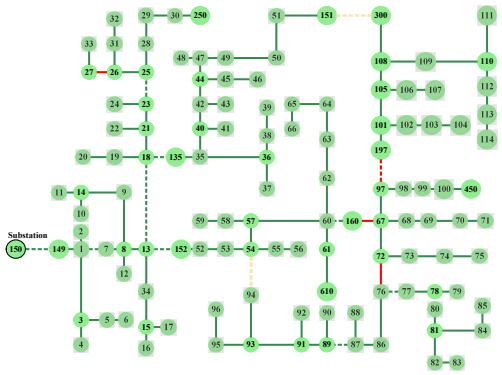

(a) Original topology with predicted outage locations 26–27, 72–76, 97–197 and 160–67 shown in red

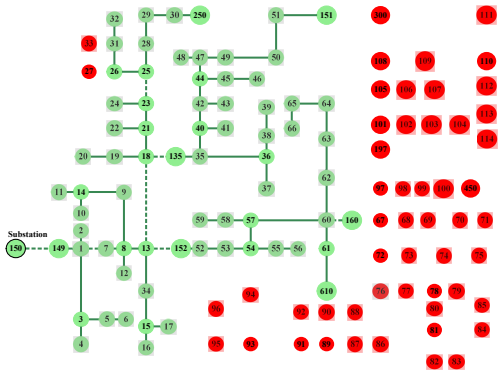

(b) Original topology showing loads that would be impacted by predicted outage

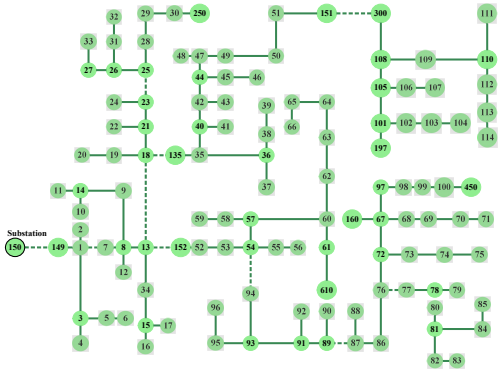

(c) Proactive topology

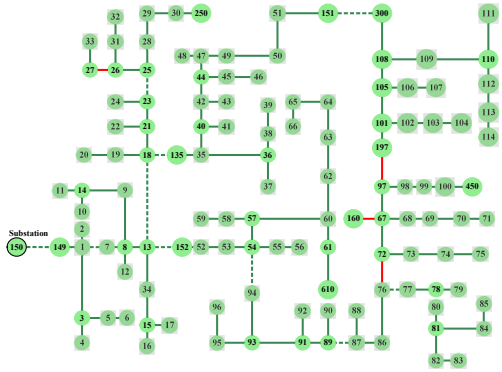

(d) Proactive topology with predicted outage locations shown in red

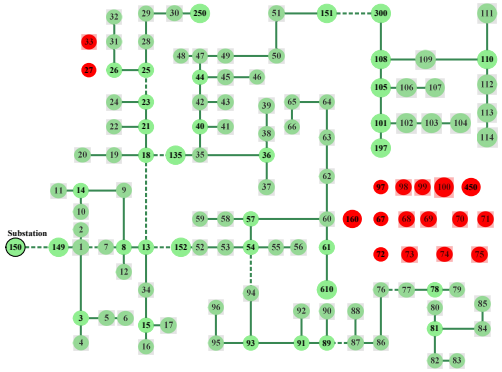

(e) Proactive topology showing loads that would be impacted by predicted outage

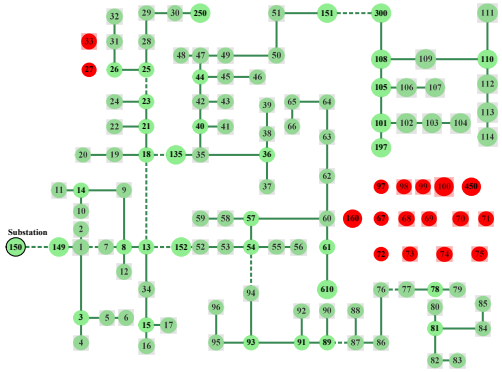

(f) New topology after the predicted outage locations are isolated

Figure B.4: Case C: One-line diagrams of modified IEEE 123-node test feeder showing network topology before and after implementing the proactive topology optimization and service restoration framework

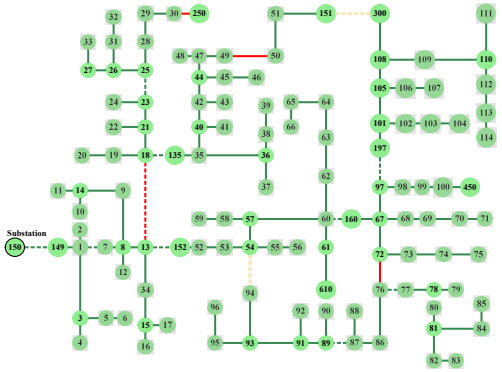

(a) Original topology with predicted outage locations 13–18, 30–250, 49–50 and 72–76 shown in red)

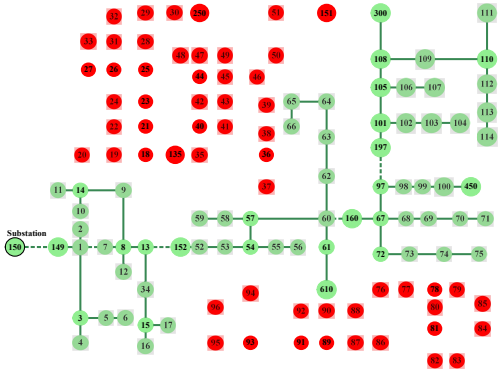

(b) Original topology showing loads that would be impacted by predicted outage

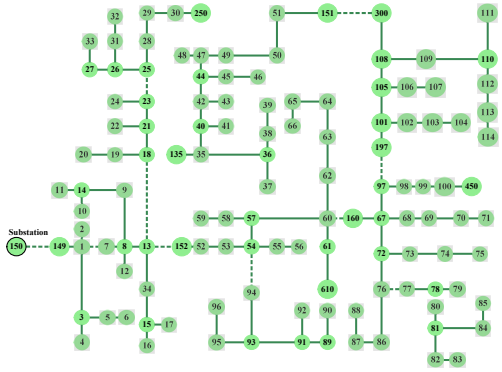

(c) Proactive topology

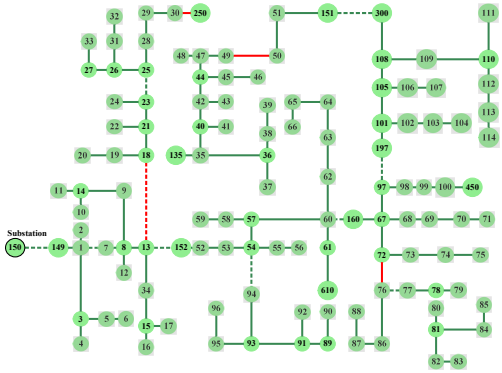

(d) Proactive topology with predicted outage locations shown in red

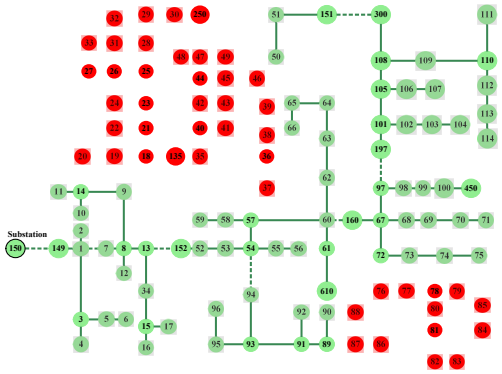

(e) Proactive topology showing loads that would be impacted by predicted outage

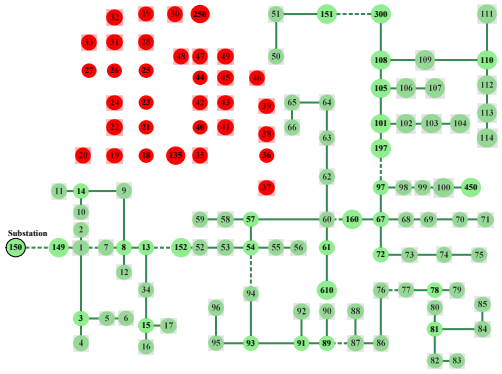

(f) New topology after the predicted outage locations are isolated

Figure B.5: Case D: One-line diagrams of modified IEEE 123-node test feeder showing network topology before and after implementing the proactive topology optimization and service restoration framework

APPENDIX C: WEIGHTED MULTIPLE OUTAGE CASE: DETAILED RESULTS OF SENSITIVITY ANALYSIS

C.1 Modified IEEE 13-bus Test Feeder

Table C.1: Weighted costs for weighted multiple outage case: IEEE 13-bus feeder cases A and B

Weights			**Case A**			**Case B**	
w_1	w_2	w_3	T_1	T_2	T_3	$T_1 = T_3$	T_2
0.0	0.0	1.0	130	130	0	0	130
0.0	0.1	0.9	145	117	28	13	117
0.0	0.2	0.8	160	104	56	26	104
0.0	0.3	0.7	175	91	84	39	91
0.0	0.4	0.6	190	78	112	52	78
0.0	0.5	0.5	205	65	140	65	65
0.0	0.6	0.4	220	52	168	78	52
0.0	0.7	0.3	235	39	196	91	39
0.0	0.8	0.2	250	26	224	104	26
0.0	0.9	0.1	265	13	252	117	13
0.0	1.0	0.0	280	0	280	130	0
0.1	0.0	0.9	117	117	13	0	117
0.1	0.1	0.8	132	104	41	13	104
0.1	0.2	0.7	147	91	69	26	91
0.1	0.3	0.6	162	78	97	39	78
0.1	0.4	0.5	177	65	125	52	65
0.1	0.5	0.4	192	52	153	65	52
0.1	0.6	0.3	207	39	181	78	39
0.1	0.7	0.2	222	26	209	91	26
0.1	0.8	0.1	237	13	237	104	13
0.1	0.9	0.0	252	0	265	117	0
0.2	0.0	0.8	104	104	26	0	104
0.2	0.1	0.7	119	91	54	13	91
0.2	0.2	0.6	134	78	82	26	78
0.2	0.3	0.5	149	65	110	39	65
0.2	0.4	0.4	164	52	138	52	52
0.2	0.5	0.3	179	39	166	65	39
0.2	0.6	0.2	194	26	194	78	26
0.2	0.7	0.1	209	13	222	91	13
0.2	0.8	0.0	224	0	250	104	0
0.3	0.0	0.7	91	91	39	0	91
0.3	0.1	0.6	106	78	67	13	78
0.3	0.2	0.5	121	65	95	26	65

Weights			**Case A**			**Case B**	
w_1	w_2	w_3	T_1	T_2	T_3	$T_1 = T_3$	T_2
0.3	0.3	0.4	136	52	123	39	52
0.333	0.333	0.333	136.667	43.333	136.667	43.329	43.329
0.3	0.4	0.3	151	39	151	52	39
0.3	0.5	0.2	166	26	179	65	26
0.3	0.6	0.1	181	13	207	78	13
0.3	0.7	0.0	196	0	235	91	0
0.4	0.0	0.6	78	78	52	0	78
0.4	0.1	0.5	93	65	80	13	65
0.4	0.2	0.4	108	52	108	26	52
0.4	0.3	0.3	123	39	136	39	39
0.4	0.4	0.2	138	26	164	52	26
0.4	0.5	0.1	153	13	192	65	13
0.4	0.6	0.0	168	0	220	78	0
0.5	0.0	0.5	65	65	65	0	65
0.5	0.1	0.4	80	52	93	13	52
0.5	0.2	0.3	95	39	121	26	39
0.5	0.3	0.2	110	26	149	39	26
0.5	0.4	0.1	125	13	177	52	13
0.5	0.5	0.0	140	0	205	65	0
0.6	0.0	0.4	52	52	78	0	52
0.6	0.1	0.3	67	39	106	13	39
0.6	0.2	0.2	82	26	134	26	26
0.6	0.3	0.1	97	13	162	39	13
0.6	0.4	0.0	112	0	190	52	0
0.7	0.0	0.3	39	39	91	0	39
0.7	0.1	0.2	54	26	119	13	26
0.7	0.2	0.1	69	13	147	26	13
0.7	0.3	0.0	84	0	175	39	0
0.8	0.0	0.2	26	26	104	0	26
0.8	0.1	0.1	41	13	132	13	13
0.8	0.2	0.0	56	0	160	26	0
0.9	0.0	0.1	13	13	117	0	13
0.9	0.1	0.0	28	0	145	13	0
1.0	0.0	0.0	0	0	130	0	0

C.2 Modified IEEE 123-bus Test Feeder

Table C.2: Weighted costs for weighted multiple outage case: IEEE 123-bus feeder cases A and B

Weights			**Case A**			**Case B**	
w_1	w_2	w_3	T_1	T_2	T_3	T_1	$T_2 = T_3$
0.0	0.0	1.0	465.0	465.0	0.0	245.0	0.0
0.0	0.1	0.9	429.5	418.5	49.5	276.0	0.0
0.0	0.2	0.8	394.0	372.0	99.0	307.0	0.0
0.0	0.3	0.7	358.5	325.5	148.5	338.0	0.0
0.0	0.4	0.6	323.0	279.0	198.0	369.0	0.0
0.0	0.5	0.5	287.5	232.5	247.5	400.0	0.0
0.0	0.6	0.4	252.0	186.0	297.0	431.0	0.0
0.0	0.7	0.3	216.5	139.5	346.5	462.0	0.0
0.0	0.8	0.2	181.0	93.0	396.0	493.0	0.0
0.0	0.9	0.1	145.5	46.5	445.5	524.0	0.0
0.0	1.0	0.0	110.0	0.0	495.0	555.0	0.0
0.1	0.0	0.9	418.5	429.5	37.0	220.5	6.0
0.1	0.1	0.8	383.0	383.0	86.5	251.5	6.0
0.1	0.2	0.7	347.5	336.5	136.0	282.5	6.0
0.1	0.3	0.6	312.0	290.0	185.5	313.5	6.0
0.1	0.4	0.5	276.5	243.5	235.0	344.5	6.0
0.1	0.5	0.4	241.0	197.0	284.5	375.5	6.0
0.1	0.6	0.3	205.5	150.5	334.0	406.5	6.0
0.1	0.7	0.2	170.0	104.0	383.5	437.5	6.0
0.1	0.8	0.1	134.5	57.5	433.0	468.5	6.0
0.1	0.9	0.0	99.0	11.0	482.5	499.5	6.0
0.2	0.0	0.8	372.0	394.0	74.0	196.0	12.0
0.2	0.1	0.7	336.5	347.5	123.5	227.0	12.0
0.2	0.2	0.6	301.0	301.0	173.0	258.0	12.0
0.2	0.3	0.5	265.5	254.5	222.5	289.0	12.0
0.2	0.4	0.4	230.0	208.0	272.0	320.0	12.0
0.2	0.5	0.3	194.5	161.5	321.5	351.0	12.0
0.2	0.6	0.2	159.0	115.0	371.0	382.0	12.0
0.2	0.7	0.1	123.5	68.5	420.5	413.0	12.0
0.2	0.8	0.0	88.0	22.0	470.0	444.0	12.0
0.3	0.0	0.7	325.5	358.5	111.0	171.5	18.0
0.3	0.1	0.6	290.0	312.0	160.5	202.5	18.0
0.3	0.2	0.5	254.5	265.5	210.0	233.5	18.0
0.3	0.3	0.4	219.0	219.0	259.5	264.5	18.0
0.333	0.333	0.333	191.667	191.667	288.33	266.667	20.0
0.3	0.4	0.3	183.5	172.5	309.0	295.5	18.0
0.3	0.5	0.2	148.0	126.0	358.5	326.5	18.0

Weights			**Case A**			**Case B**	
w_1	w_2	w_3	T_1	T_2	T_3	$T_1 = T_3$	T_2
0.3	0.6	0.1	112.5	79.5	408.0	357.5	18.0
0.3	0.7	0.0	77.0	33.0	457.5	388.5	18.0
0.4	0.0	0.6	279.0	323.0	148.0	147.0	24.0
0.4	0.1	0.5	243.5	276.5	197.5	178.0	24.0
0.4	0.2	0.4	208.0	230.0	247.0	209.0	24.0
0.4	0.3	0.3	172.5	183.5	296.5	240.0	24.0
0.4	0.4	0.2	137.0	137.0	346.0	271.0	24.0
0.4	0.5	0.1	101.5	90.5	395.5	302.0	24.0
0.4	0.6	0.0	66.0	44.0	445.0	333.0	24.0
0.5	0.0	0.5	232.5	287.5	185.0	122.5	30.0
0.5	0.1	0.4	197.0	241.0	234.5	153.5	30.0
0.5	0.2	0.3	161.5	194.5	284.0	184.5	30.0
0.5	0.3	0.2	126.0	148.0	333.5	215.5	30.0
0.5	0.4	0.1	90.5	101.5	383.0	246.5	30.0
0.5	0.5	0.0	55.0	55.0	432.5	277.5	30.0
0.6	0.0	0.4	186.0	252.0	222.0	98.0	36.0
0.6	0.1	0.3	150.5	205.5	271.5	129.0	36.0
0.6	0.2	0.2	115.0	159.0	321.0	160.0	36.0
0.6	0.3	0.1	79.5	112.5	370.5	191.0	36.0
0.6	0.4	0.0	44.0	66.0	420.0	222.0	36.0
0.7	0.0	0.3	139.5	216.5	259.0	73.5	42.0
0.7	0.1	0.2	104.0	170.0	308.5	104.5	42.0
0.7	0.2	0.1	68.5	123.5	358.0	135.5	42.0
0.7	0.3	0.0	33.0	77.0	407.5	166.5	42.0
0.8	0.0	0.2	93.0	181.0	296.0	49.0	48.0
0.8	0.1	0.1	57.5	134.5	345.5	80.0	48.0
0.8	0.2	0.0	22.0	88.0	395.0	111.0	48.0
0.9	0.0	0.1	46.5	145.5	333.0	24.5	54.0
0.9	0.1	0.0	11.0	99.0	382.5	55.5	54.0
1.0	0.0	0.0	0.0	110.0	370.0	0.0	60.0

APPENDIX D: COPYRIGHT STATEMENT

VITA

FULL NAME: Tumininu Ayotunde Mbanisi

EDUCATION:

Ph.D.	Electrical Engineering	UNC Charlotte, NC, USA	2023
M.S.	Electrical Engineering	UNC Charlotte, NC, USA	2017
B.Eng.	Electrical & Electronics Engineering	Covenant University, Nigeria	2013

PUBLICATIONS

[C1] **T. Lawanson***, V. Sharma, V. Cecchi, T. Hong, "Analysis of Outage Frequency and Duration in Distribution Systems using Machine Learning," *2020 52nd North American Power Symposium (NAPS)*, 2021, pp. 1-6.

[C2] D. Schulz, **T. Lawanson**, K. Ravikumar, V. Cecchi, "Loss Estimation and Visualization in Distribution Systems using AMI and Recloser Data," *2020 IEEE Transmission & Distribution Conference and Exposition (T&D)*, Chicago, IL, 2020, pp. 1-5.

[C3] R. Karandeh, **T. Lawanson** and V. Cecchi, "A Two-Stage Algorithm for Optimal Scheduling of Battery Energy Storage Systems for Peak-Shaving," *2019 North American Power Symposium (NAPS), Wichita*, KS, USA, 2019, pp. 1-6.

[C4] R. Karandeh, **T. Lawanson**, and V. Cecchi, "Impact of Operational Decisions and Size of Battery Energy Storage Systems on Demand Charge Reduction," *2019 IEEE Milan PowerTech*, Milan, Italy, 2019, pp. 1-6.

[C5] **T. Lawanson**, R. Karandeh, V. Cecchi, and A. Kling, "Impacts of Distributed Energy Resources and Load Models on Conservation Voltage Reduction," *2018 Clemson University Power Systems Conference (PSC)*, Charleston, SC, USA, 2018, pp. 1-6.

[C6] **T. Lawanson**, R. Karandeh, V. Cecchi, Z. Wartell and I. Cho, "Improving Power Distribution System Situational Awareness Using Visual Analytics," *SoutheastCon 2018*, St. Petersburg, FL, 2018, pp. 1-6.

*Last name changed from Lawanson to Mbanisi in 2021